

IDENTIFICATION AND CHARACTERISATION OF THE SPRED PROTEIN FAMILY

Dissertation zur Erlangung des
naturwissenschaftlichen Doktorgrades
der Bayerischen Julius-Maximilians-Universität Würzburg

Vorgelegt von

Catherine Marie Engelhardt,
geb. Bruel

aus

Aurillac, Frankreich

Würzburg 2004

Eingereicht am:.....

Mitglieder der Promotionskommission:

Vorsitzender:

Gutachter: Prof. Dr. U. Walter

Gutachter: Prof. Dr. G. Krohne

Betreuer: Dr. K. Schuh

Tag des Promotionskolloquiums:

Doktorurkunde ausgehändigt am:

Table of contents

TABLE OF CONTENTS	3
ZUSAMMENFASSUNG	5
SUMMARY	7
INTRODUCTION	9
FOUR FAMILIES OF EVH-1 DOMAIN CONTAINING PROTEINS AND THEIR FUNCTIONS.....	9
THE SPROUTY PROTEIN FAMILY.....	12
MAMMALIAN SPRED PROTEINS.....	13
AIM OF THE PRESENT WORK.....	14
INITIAL WORK	15
MATERIAL AND METHODS	17
MOLECULAR BIOLOGY TECHNIQUES.....	17
PROTEIN BIOCHEMISTRY TECHNIQUES.....	23
CELL CULTURE EXPERIMENTS.....	29
IMMUNOHISTOCHEMICAL EXPERIMENTS	31
BINDING EXPERIMENTS WITH THE EVH-1 DOMAIN OF SPRED-2.....	32
RESULTS	35
THE NOVEL HUMAN GENE FAMILY HOMOLOGOUS TO <i>DROSOPHILA</i> AE33.....	35
EXPRESSION PATTERN OF SPRED-1 AND SPRED-2 IN MOUSE AND HUMAN	40
THE ALTERNATIVE SPLICING OF <i>SPRED</i> GENES	48
SUBCELLULAR LOCALISATION OF SPRED-2 PROTEIN VARIANTS	61
EFFECT OF SPRED-2 SPLICING VARIANTS ON ERK ACTIVITY	65
BINDING PARTNERS OF THE SPRED-2 EVH-1 DOMAIN.....	66
DISCUSSION	72
DIFFERENTIAL EXPRESSION OF SPRED-1 AND -2 IN MICE	72
SPRED-2 EXPRESSION SUGGESTS A ROLE IN SECRETORY PATHWAYS.....	73
DISTRIBUTION OF SPRED-2 IN THE DECIDUA: A ROLE IN TROPHOBLAST INVASIVENESS	74
TWO STRUCTURALLY DISTINCT GROUPS OF HUMAN SPRED PROTEINS GENERATED BY EXTENSIVE ALTERNATIVE SPLICING.....	74
THE FUNCTION OF THE CYSTEINE-RICH DOMAIN	78
A NEW SUBCLASS OF EVH-1 DOMAINS.....	82
CONCLUDING REMARKS	84
REFERENCES	85
ABBREVIATIONS	92

ACKNOWLEDGEMENTS.....	94
DECLARATION	95
CURRICULUM VITAE	96
PUBLICATIONS	97

Zusammenfassung

Gegenstand der vorliegenden Arbeit war die Klonierung, sowie die biochemische und funktionelle Charakterisierung der neuen Spred Proteinfamilie, welche sich durch eine N-terminale EVH1-Domäne und C-terminal eine *Sprouty homology* Domäne (SPR) auszeichnet (Sprouty-related protein with an EVH-1 domain, Spred). Spred-1, -2, -3 sind membranassoziierte Substrate von Rezeptor-Tyrosin-Kinasen und hemmen den Wachstumsfaktor-stimulierten Ras Signalweg. Während für die drei Mitglieder der Spred-Familie ähnliche biochemische Funktionen beschrieben sind, ist bislang deren spezifische physiologische Funktion unbekannt.

Wir haben deshalb zunächst die mRNA- und Protein-Expression von Spred-1 und Spred-2 in verschiedenen Organen der Maus untersucht. Zudem haben wir die zelluläre und subzelluläre Lokalisation bestimmt. Dabei zeigte sich, daß sich die Expression der Spred-Isoformen deutlich voneinander unterscheidet. Während Spred-1 stark im Großhirn, Kleinhirn und in fetalen Geweben exprimiert wird, kommt Spred-2 verstärkt in adulten Geweben vor. Beim Menschen konnte zudem gezeigt werden, daß Spred-2 stark in Drüsenepithelien, in Zytotrophoblasten und auf subzellulärer Ebene mit sekretorischen Vesikeln assoziiert war.

Das Expressionsmuster der humanen Spred-Proteine wurde im Detail untersucht. Die Klonierung des humanen Spred-2 ergab eine 1254 bp lange kodierende Sequenz, die für ein Protein mit 418 Aminosäuren kodiert. Durch einen Immunoblot mit affinitätsgereinigten Antikörpern bestätigte sich die Expression eines 47 kD großen Proteins, gleichzeitig zeigten sich zusätzliche Varianten des Proteins mit abweichenden Größen. Daraufhin konnten vier kürzere mRNAs für Spred-2 kloniert werden, die durch alternatives Spleißen entstehen. Zudem konnten zwei neue Spred-Gene identifiziert werden, die auf unterschiedlichen Chromosomen lokalisiert sind und die jeweils für mehrere Proteine unterschiedlicher Größe kodieren. Alle Proteinisoformen und Spleißvarianten enthalten eine N-terminale EVH-1-Domäne, während nur die langen Isoformen ("a-Formen") zusätzlich eine C-terminale SPR-Domäne enthalten.

Die Untersuchung der Funktion der 5 klonierten Spleißvarianten von Spred-2 ergab eine differentielle subzelluläre Lokalisation. Zudem zeigte sich eine unterschiedliche Regulation der Serum- und EGF-induzierten ERK-Aktivierung durch die

verschiedenen Spred-2 Spleißvarianten.

Diese Ergebnisse zeigen, daß Spred-1 und Spred-2 ein hochspezifisches Expressionsmuster in verschiedenen Organen aufweisen, ein Befund, der auf eine spezifische funktionelle Rolle der einzelnen Isoformen hindeutet. Die vorliegenden Befunde weisen darauf hin, daß Spred-2 an der Regulation sekretorischer Vorgänge beteiligt ist. Die Mitglieder der humanen Spred Proteinfamilie werden von drei Genen kodiert, durch alternatives Spleißen resultieren hieraus mindestens 8 verschiedene mRNAs. Werden die korrespondierenden Proteine überexprimiert, zeigen sie differentielle subzelluläre Lokalisationen und unterschiedliche Regulation der MAP-Kinase Aktivität.

Summary

The subject of this thesis was the cloning and the initial biochemical and functional characterisation of novel human proteins with an N-terminal Ena-VASP homology (EVH)-1 domain and a C-terminal Sprouty homologous region (SPR), which are related to the *Drosophila* AE33 protein. During the course of this work, three mouse homologues of the AE33 fly protein have been reported and termed Sprouty-related protein with an EVH-1 domain 1, 2 and 3 (Spred-1, -2, -3)(Wakioka et al, 2001; Kato et al, 2003). Spred-1, -2 and -3 are membrane associated substrates of receptor tyrosine kinases and they act as negative regulators of the Ras pathway during growth factor stimulation. As the Spred-family members seem to exert similar functions, the specific function of each member remains enigmatic. Therefore, we investigated the mRNA and protein expression patterns of the two murine protein family members Spred-1 and Spred-2 on the whole organ level. Furthermore, we focussed on the cellular localisation and the role of human and murine Spred-2 in the organism. The expression patterns of Spred-1 and Spred-2 differed markedly among various tissues and cell types. In mouse, Spred-1 is abundantly expressed in adult brain, cerebellum, and fetal tissues, whereas Spred-2 was ubiquitously expressed. In humans, Spred-2 was found to be strongly expressed in glandular epithelia and in invasive cytotrophoblasts, and at the subcellular level its immunoreactivity was associated with secretory vesicles and was found to colocalise with Rab11 GTPase. The new human Spred gene family was investigated in detail. Cloning of the full-length form of human Spred-2 resulted in an 1254 bp coding sequence, corresponding to a 418 amino-acids protein. Immunoblotting with a set of affinity-purified antibodies confirmed the expression of a 47 kDa protein and suggested the presence of additional differently sized variants. Cloning of various shortened Spred-2 mRNAs and identification of 2 additional human Spred genes (localised on different chromosomes) with their respective EST (expressed sequence tag) revealed that the new human Spred gene family displays extensive splicing, leading to the generation of short and long Spred proteins. All protein isoforms and splicing variants contain an EVH1-domain located at the N-terminus of the protein. The full-length forms ("a" forms) comprised the SPR, another functional domain localised at the C-terminus whereas the short variants (Spred-1b, 2 c-e, 3 c) lack the entire C-terminal SPR

domain or part of it. The existence of short and long splicing variants of Spred-1, -2 and -3 revealed a common principle of organisation and splicing pattern in the Spred family.

Functional analyses of the 5 cloned Spred-2 splicing variants revealed differential subcellular localisation and differential regulation of serum- and EGF- mediated ERK activation in HEK-293 cells.

Taken together, these results indicate a highly specific expression pattern of Spred-1 and Spred-2 in various tissues suggesting a specific physiological role for the individual Spred isoform in these tissues. For example, Spred-2 appears to be involved in regulating secretory pathways. Furthermore, the human Spred family contains three genes, which are subject to extensive alternative splicing resulting in at least 8 different proteins with differential subcellular localisation and differential regulatory potential of the MAPK pathways during growth factor stimulation.

Introduction

Four families of EVH-1 domain containing proteins and their functions

A growing number of proteins involved in the maintenance of cytoskeletal integrity, actin-based cell motility, and signal transduction has been described to contain an Ena/VASP-homology domain 1 (EVH-1 domain) (Reinhard et al, 2002; Renfranz and Beckerle, 2002).

The EVH-1 domains represent protein interaction modules of 110 amino acids that specifically bind proline-rich sequences (PRS) (Reinhard et al, 1995; Reinhard et al, 1996; Niebuhr et al, 1997; Ball et al, 2002).

The interaction between the EVH-1 domain and its recognition sequences is responsible for targeting the actin assembly machinery to sites of cytoskeletal remodeling (Machesky and Way, 1998; Reinhard et al, 1995a), for regulating the actin cytoskeleton (Reinhard et al, 2001; Samarin et al, 2003), and for modulating synapse plasticity (Kato A. et al, 1997).

The structure of several EVH-1/PRS complexes have been solved with high resolution by NMR and X-ray crystallography (Ball et al, 2000; Fedorov et al, 1999; Prehoda et al, 1999; Barzik et al, 2001; Beneken et al, 2000). The overall structure of a compact parallel β -sandwich closed along one edge by a long α -helix revealed a close unexpected relationship to the membrane localisation module pleckstrin homology (PH), and the phosphotyrosine binding (PTB) domains (Fig. 1). Distinct from the SH3 domain, the EVH-1 peptide binding sites contain critical aromatic residues interacting with prolines through a V-shaped concave groove (Predoda et al, 1999).

EVH-1 domain containing proteins can be classified in 4 families (Renfranz et al, 2002; Ball et al, 2002): the Ena/VASP family of proteins, the Wiskott-Aldrich syndrome (WASP) protein family, the family of synaptic terminal proteins (Homer), and the newly described Spred family (Fig. 2).

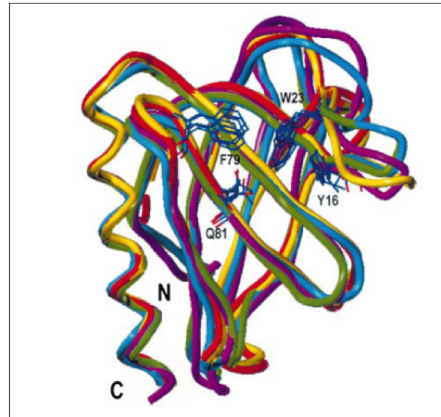


Figure 1: Schematic structure of the EVH-1 domain in which the backbone atoms (N, C α , and C') of five EVH-1 domains are superposed (from Ball et al, 2000).

The EVH-1 domain of Mena is represented in cyan, the EVH-1 domain of Evl in green, the Homer-1a EVH-1 domain in yellow, the EVH-1 domain of VASP in magenta, and the Vesl-2 EVH-1 domain in red. The aromatic triad is shown in blue: Y16, W23, F79 (human VASP numbering).

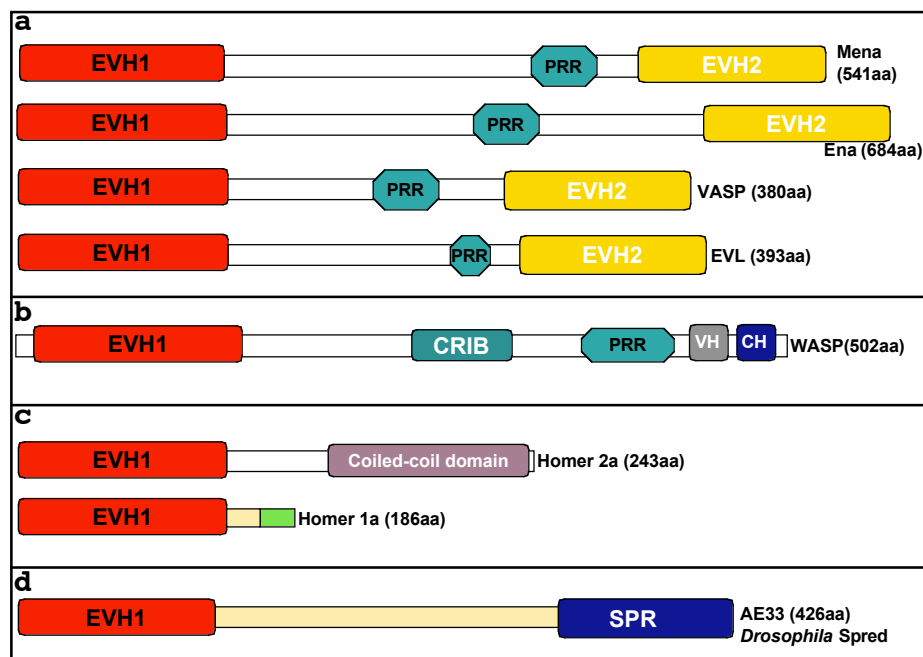


Figure 2: Scheme of members of the 4 EVH-1 domain containing protein families (adapted from Renfranz and Beckerle, 2002).

(a) Members of the Ena/VASP family share a conserved EVH-1 domain at the N-terminus, a central proline rich region (PRR) and a C-terminal EVH-2 domain. (b) Members of the WASP family share a conserved EVH-1 domain which is preceded by a leader of ca. 40 amino-acid in length. They display a cofilin homology domain (CH), a Cdc42/Rac interactive binding site (CRIB) and a Verprolin homology domain (VH). (c) Members of the Homer family have an EVH-1 domain at the N-terminus. Except for Homer 1a, other Homer proteins (typified here by Homer 2a) contain a coiled-coil domain, which facilitates multimerisation. Homer 1a contains a unique region at its C-terminus and is thought to act as dominant negative because of its inability to multimerise. (d) The *Drosophila* member of the Spred family has an N-terminal EVH-1 domain and a C-terminal cysteine-rich region typically found in Sprouty proteins (SPR).

VASP, a 46 kDa membrane associated protein being the first described member of

the Ena/VASP family of protein, was initially characterised as a prominent substrate for cAMP- and cGMP-dependent protein kinases and a component of inhibitory signal transduction pathways in human platelets and others cells (Halbruegge et al, 1989; Reinhard et al, 1999). The members of the Ena/VASP family (including the gene product of the *Drosophila enabled* gene (ena), its mammalian homologue Mena, and Enabled/Vasodilatator-stimulated phosphoprotein-like protein (Evl) share a similar overall domain organisation originally described for VASP including three regions of similarity: the N-terminal EVH-1 domain, a central proline-rich core which varies in size among family members, and the C-terminal EVH-2 which ranges in size from 151 amino-acids in VASP to 190 amino-acids in Ena (Haffner et al, 1995; Gertler et al, 1996).

VASP and Mena knockout mice show cryptic mild phenotypes (Hauser et al, 1999, Lanier et al, 1999, Aszodi et al, 1999) eventually due to the functional redundancy associated with the coexpression of VASP, Mena and EVL in certain tissues. However, in tissues where Mena is not expressed (i.e in platelets and in spleen) VASP^{-/-} mice exhibit a more obvious phenotype. The number of megakaryocytes is increased and the agonist-induced platelet activation is enhanced (Hauser et al, 1999). Furthermore, an enhanced Rac/p21-activated kinase activation has been reported in VASP^{-/-} cardiac fibroblasts, also displaying an increased spreading behaviour (García Arguinzonis et al, 2002).

The interaction between the Ena/VASP EVH-1 domain and its recognition sequence PRS is required for targeting the actin assembly machinery to sites of cytoskeletal remodeling. The EVH-1 domain is responsible for interaction with proteins associated with focal adhesion plaques, such as vinculin and zyxin (Brindle et al, 1996; Reinhard et al, 1996; Drees et al, 2000) and the proteins recruited by Ena/VASP family proteins are thought to directly promote actin filament elongation and nucleation (Reinhard et al, 1995; Machesky et al, 1998).

The N-terminal EVH-1 domain of the Ena/VASP family interacts also with FPPPP motifs of the ActA surface protein of *Listeria monocytogenes*. The multiple EVH-1 binding motifs are required to recruit the actin assembly machinery to the surface of the motile intracellular pathogen (Chakraborty et al, 1995) and essential to support its motility, its cell to cell spreading, and virulence (Niebuhr et al, 1997; Skoble et al, 2001).

Members of the WASP protein family harbour an EVH-1 domain near their N-termini

also termed WASP homology 1 domain (WH1). The human disease, “Wiskott-Aldrich syndrome”, characterised by immunodeficiency and autoimmune disorders, is caused by mutations in the gene encoding WASP. The WASP family proteins have a critical function in regulating the actin cytoskeleton; they are able to stimulate the nucleation of actin filament branches along existing filaments by activating the Arp2/3 complex (Zigmond et al, 2000).

The Homer family is the third EVH-1 containing protein family and interact via their EVH-1 domain with group I metabotropic glutamate receptors, IP3 (inositol 1,4,5 trisphosphate) receptors and ryanodine receptors (Brakeman et al, 1997; Tu et al, 1999; Naisbitt et al, 1999). Homer localises to the post-synaptic density region, a specialised actin structure found on the spines of neuronal dendrites. Proteins of the Homer family are thought to function in synaptic plasticity and in long term potentiation of excitatory synapses with implication for memory formation (Kato A. et al, 1997).

The fourth EVH-1 domain containing protein family is the recently described Spred (Sprouty-related protein with an EVH-1 domain) family, whose first identified member was the fly protein derived from AE33.

In *Drosophila*, AE33, a transcript encoding a novel EVH-1 domain containing protein, was identified as an insertion element bearing transcript in an enhancer-trap line. Its expression was found to be dependent on the transcription factors rough and glass during photoreceptor cell development (DeMille et al, 1996). The protein corresponding to AE33 contains - in addition to an EVH-1 domain at the N-terminus - a C-terminally located domain similar to the cysteine rich domain found in Sprouty family members.

The Sprouty protein family

In addition to an N-terminal EVH-1 domain, Spred proteins contain a C-terminal sprouty homology domain (SPR).

Sprouty was originally genetically identified as an antagonist of *Drosophila* FGF receptor signaling during tracheal development (Hacohen et al, 1998).

Reich et al (1999) showed that Sprouty can inhibit other receptor tyrosine kinase (RTK) signaling pathways, namely downstream of Heartless and the EGF receptor. Genetic interactions between Sprouty and several RTKs in multiple contexts have

been reported and it has become clear that Sprouty is a general inhibitor of RTK signaling during *Drosophila* development.

In mammals, four Sprouty homologs were identified as negative feedback regulators of fibroblast growth factor (FGF) signaling in angiogenesis (Minowada et al, 1999) and embryogenesis (de Maximy et al, 1999; Tefft et al, 1999).

Among fly and mammalian Sprouty family members, the C-terminal cysteine-rich region is the most conserved region (Impagnatiello et al, 2001).

Functional characterisation of mammalian Sprouty 1 and 2 has been initiated by Gross et al (2001). Mammalian Sprouty has been shown to regulate cell proliferation and differentiation by inhibiting events downstream of various RTKs (Kramer et al, 1999).

By specifically inhibiting Ras activation, they act on the Ras/Raf/MAP (mitogen-activated protein)-kinase pathway. Mammalian Sprouty is an important negative regulator of growth factor signaling and acts downstream of the GRB2-SOS complex where it selectively uncouples growth factor signals from Ras activation.

Mammalian Spred proteins

Using a yeast two-hybrid screen searching for growth factor receptor interacting proteins, Wakioka and co-workers recently discovered a mouse AE33 orthologue, named Spred-1 (Sprouty-related EVH-1 domain-containing protein). As well they reported the identification of murine Spred-2 which was found by homology search (Wakioka et al, 2001). Subsequently, Spred-3 was discovered through nucleic acid homology, thereby defining a novel class of EVH-1 domain containing proteins, the Spred protein family (Kato R. et al, 2003). In addition to the N-terminal EVH-1-domain, Spred-1 and -2 proteins contain a centrally located c-kit binding domain (c-KBD) which was shown to be responsible for the interaction with the receptor tyrosine kinases c-kit and c-fms which are required for growth factor-induced Spred phosphorylation and activation. All members of the Spred protein family contain a Sprouty-related C-terminal cysteine-rich SPR domain which is responsible for the translocation of Spred proteins to the membrane (Lim et al, 2000), for binding to PIP₂ (phosphatidylinositol 4,5-bisphosphate) (Lim et al, 2002), and for the interaction with Raf1 (Sasaki et al, 2003).

Spred-3 is characterised by the same tripartite domain structure as Spred-1 and -2

but its central c-KBD is not functional in terms of binding to c-kit and subsequent phosphorylation because of a substitution of a critical arginine amino acid residue (Kato R. et al, 2003).

Similar to Sprouty proteins, members of the Spred-protein family are negative feedback regulators of the extracellular signal regulated kinase (ERK) pathway (Wakioka et al, 2001) but they suppress ERK-signaling through a different mechanism (Sasaki et al, 2001).

Spred is an inhibitor of ERK-dependent differentiation in PC12 pheochromocytoma cells and C2C12 myoblastic cells (Sasaki et al, 2001). In contrast to Sprouty, Spred proteins bind constitutively to Ras and control both activation and translocation of Raf to the cell membrane (Wakioka et al, 2001).

Physiological functions of Spred-2 have been recently obtained from Spred-2 deficient mice (Nobuhisa et al, 2004). In vivo, Spred-2 is important for the regulation of hematopoiesis in the midgestation mouse embryo. Spred-2 functions as a negative regulator of aorta-gonad-mesonephros hematopoiesis by inhibiting hematopoietic cytokine signaling. Deficiency of Spred-2 causes hematopoietic abnormalities in adult mice, characterised by a marked increase in the number of megakaryocytes (elevated megakaryopoiesis) in spleen, and an increased colony forming potential of adult bone marrow derived hematopoietic progenitor cells but no quantitative abnormalities in peripheral blood composition was observed (Nobuhisa et al, 2004).

Recently, Spred 1 and 2 have been shown to control cell motility by suppressing activated RhoA- induced stress fiber formation (Miyoshi et al, 2004).

Aim of the present work

The purpose of the present study was to identify and characterise novel human EVH-1 containing proteins, which are potential human orthologues of *Drosophila* Spred (AE33) and gain insights into their tissue distribution and their putative function.

As the overall structure of Spred-1 and Spred-2 is very similar and because of the overlapping inhibitory activity of these protein family members, specificity might be gained through tissue specific expression pattern of the individual proteins. To date, very little information is available on the localisation of Spred-1 and -2 proteins in different organs and cell types. Comparison of the mRNA expression profile of Spred and Sprouty proteins in developing rat lung revealed expression of Spred RNA

messengers in mesenchymal cells whereas Sprouty RNA was found predominantly in epithelial cells (Hashimoto et al, 2002).

In the present study, the tissue distribution of Spred-1 and -2 was determined. Because of possible discrepancies between protein and mRNA expression patterns, the protein expression profile of Spred-1 and -2 in human and mouse tissues was also investigated systematically using two highly specific, affinity purified antibodies. Special attention was paid on the cellular distribution and subcellular localisation of the Spred-2 protein.

Furthermore, I demonstrated that the human Spred family, which contains three human genes, displays extensive alternative splicing leading to the generation of at least 8 different proteins. All protein isoforms and splicing variants contain an EVH-1 domain located at the N-terminus of the protein, the full-length forms ("a" forms) comprise a SPR domain, localised at the C-terminus whereas the short variants (Spred-1b, -2c-e, -3c) lack the C-terminal SPR domain. The existence of short and long splicing variants of Spred-1, -2 and -3 reveals a common principle of organisation and splicing pattern in the Spred family. I studied the function of these splicing variants in regulating growth factor induced ERK activation in HEK-293 cells. Additionally, I focussed on the putative ligands interacting with this a new class of EVH-1 domain.

Initial work

M. Messerschmitt initiated the project related to the characterisation of a new human EVH-1 containing protein related to *Drosophila* AE33.

She first identified the highly similar human protein in the human EST database. In order to search for novel EVH-1 domain containing proteins, the human EST (expressed sequence tags, NCBI-Genbank) database was queried with the EVH-1 domain of *Drosophila* AE33. From the blast results, four highly homologous partial sequences with the accession numbers T52235, D80468, AA251635 and AA069749, which were distinctly different from any known Ena/VASP family members, were selected.

The sequence corresponding to the EVH-1 domain was amplified by 5' RACE using a human fetal spleen cDNA library. The putative starting methionine and the subsequent amino acids of the EVH-1 domain were deduced from sequencing of the

5' RACE clone (Messerschmitt, 1998).

Based on the sequence information that M. Messerschmitt extracted from the sequencing of EST and 5' RACE clones, I started the cloning of the novel full length human protein with an AE33 type of EVH-1 protein and initiated its biochemical and functional characterisation.

Material and methods

Molecular biology techniques

Cloning of the Spred-2 coding region

The Spred-2a coding region was cloned from a human spleen cDNA library using the Marathon-ready cDNA Kit (Clontech) and from human brain, kidney and heart total RNA using the One Step RT-PCR kit (Qiagen) with the following primers:

Forward 5'-ggaattcgga**ATG**ACCGAAGAAACACACCCAGACGATGACAGCTAT-3'
(with an underlined EcoR1 at its 5' and the start codon ATG in bold)

and reverse: 5'-CTTGGAGTGGAAGGGAGCGGGGAGAAGATGAGAG-3'.

A touch-down PCR (table 1) was used to amplify the Spred-2a full length coding region.

Temperature	94 °C	94 °C	72 °C	94 °C	70 °C	94 °C	68 °C
Time	1 min	30 sec	3 min	30 sec	3 min	30 sec	3 min
		5 cycles		5 cycles		25 cycles	

Table 1: Thermocycle for the amplification of Spred-2 cDNA fragment.

The 1342 bp amplification product was gel-extracted and cloned into the pCR 2.1-TOPO^R vector (Invitrogen). This cloning strategy relies on the non template-dependent terminal transferase activity of the Taq polymerase that adds a single desoxyadenosine to the 3' end of PCR products. The linearised pCR 2.1-TOPO^R has a single overhanging 3' deoxythymidine residue. The topoisomerase covalently bound to the vector catalyses the ligation reaction. After transformation and culture of *E.coli*, individual clones were screened for the presence of an insert and sequenced.

Isolation of total RNA

Human placenta samples were snap-frozen in liquid nitrogen immediately after excision and stored at -80°C until use. The homogenisation was performed with an Ultra Turrax device (Ika) in Trizol^R Reagent (Gibco) (1 ml of Trizol was used for 30 mg of tissue). The homogenate was incubated for 10 min at room temperature and the remaining unsolubilized tissue particles were pelleted by centrifugation (3.000 g, 10 min, 4°C). For a phase separation of the solution, chloroforme (0.2 ml/ml Trizol)

was added to the supernatant. After vigorous mixing, the sample was subjected to centrifugation (10000 g, 15 min, 4°C). The upper watery phase was collected, transferred to a new tube, and mixed with isopropanol (0.5 ml isopropanol/ml Trizol). After incubation at room temperature for 2 min, the RNA was precipitated by centrifugation (10000 g, 10 min, 4°C). The precipitate was washed with ice-cold ethanol and resuspended in RNase-free water. The total RNA was treated with DNase I (Ambion) according to the manufacturer's instructions and stored at -80°C.

Cloning of Spred-2 splicing variants

Total RNA was reverse transcribed and subsequently amplified using Spred-2 specific primers (Fig. 3).

Spred-2a and -2e coding regions were cloned from human placenta using the QIAGEN® One Step RT-PCR Kit according to the manufacturer's instruction with the following forward and reverse primers (Fig. 3, primer 1: 5'-ggaattcgga**ATG**ACCGAAGAAACACACCCAGACGATGACAGCTAT-3' and primer 4: 5'-CTTGGAGTGGAAGGGAGCGGGGAGAAAGATGAGAG-3' using 2 µg of total RNA per reaction.

The Spred-2c, -2d coding region were cloned by RT-PCR from total RNA isolated from the human choriocarcinoma cell line JEG, human placenta, human brain, human kidney, human heart with forward primer, 5'-ggaattcgga**ATG**ACCGAAGAAACACACCCAGACGATGACAGCTAT-3' and reverse primer 5'-atgctcgag**TTAC**AGGAGGACAGTGGGTAGGCCAGGAGCCTTCT-3' (Fig. 3, primer 1 and 3). A thermocycle including the reverse transcription reaction steps and followed by a touch-down PCR for the first 8 cycles was programmed as follows: 55 °C for 30 min, 95 °C for 15 min, 94 °C for 30 sec, 8 "touch-down" cycles of 94 °C for 30 sec, 72 °C for 1.30 min (the annealing temperature decreased by 0.5 °C each cycle) and followed by 25 cycles 94°C for 30 sec, 68 °C for 30 sec, 72 °C for 1 min and a final extension at 72°C for 10 min.

Spred-2b full-length coding sequence was cloned from a brain cDNA library (gene Pool™ normal human brain cDNA, Invitrogen) by PCR using the Advantage^R Polymerase Mix (Clontech) and the following forward and reverse primers (Fig. 3, primers 1 and 5):

5'-ggaattcgga**ATG**ACCGAAGAAACACACCCAGACGATGACAGCTAT-3',
5'-GAAAGAGAGTCTTCGACGCTCTTGGAAAAATCAA-3'.

The amplified products were gel-purified and cloned into the pCR2.1-TOPO[®] vector (Invitrogen). Sequencing of the amplified DNAs was carried out using an ABI-PRISM automated DNA sequencing system according to the manufacturer's instructions.

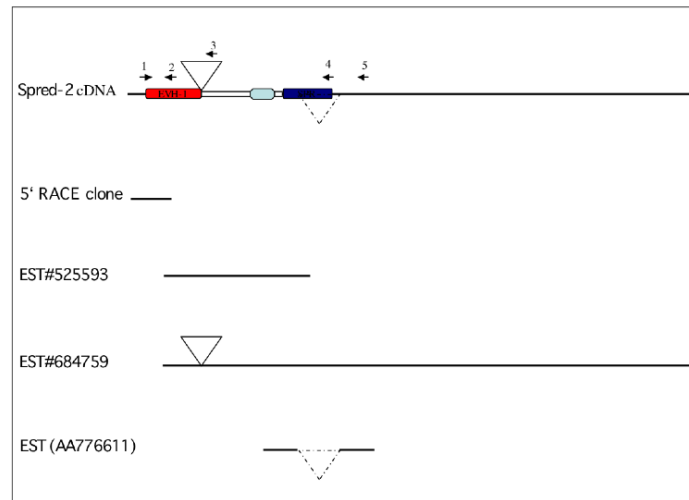


Figure 3: Overlapping clones assembled to deduce the full-length cDNA of the AE33 human homologue.

On the upper part, the Spred-2 cDNA is represented with its three corresponding domains: in red the EVH-1 domain, in light blue the c-KBD domain and in dark blue the SPR domain.

The three ESTs which have been initially used to deduce the sequence of Spred-2 and to design primers for the cloning of the 5' by RACE and subsequently for the cloning of the full-length coding region of human Spred-2a are shown in the lower part. The insert found in the EST#684759 is depicted as a triangle in the Spred-2 cDNA. This inserted sequence is located right after the sequence encoding the EVH-1 domain. The missing sequence found in the EST AA776611, depicted as a dotted triangle is reported in the Spred-2 cDNA. This deleted sequence is located within the SPR domain at the C-terminus of Spred-2. Arrow 1 represents the forward primer used for the cloning of Spred-2, the arrow 2 represents the primer used for 5' RACE, the arrow 3 the reverse primer used for the cloning of Spred-2c, -2d annealing in exon 4, the arrow 4 shows the reverse primer annealing in exon 8 (part B) and the arrow 5 represents the reverse primer annealing to exon 8 (part C) which was used for the amplification of the Spred-2b coding region.

Tagging of the Spred protein

N-terminal Flag tagging and C-terminal c-myc antigen tagging, plasmid construction:

The Spred-2a coding region was amplified with the following primer pair:

Flag-Edi-5' 5'-ATGGATCCCAGGAATGACCGAAGAAACACACCCAGACGA-3' and
 Flag-Edi-3': 5'-ATGCTCGAGTGGTCCCGCGGCCGCTTTGTGCTTCCCGCCAC-3'

(the underlined sequences are BamHI and XhoI restriction sites, respectively) and subcloned into the Flag and c-myc tags containing mammalian expression vectors (p-CMV-tag1) (Stratagene). The encoded Spred-2a product contains an N-terminal flag tag and a C-terminal c-myc tag (Fig. 4).

N-terminal VSV-tagging of Spred-2, plasmid construction:

For expression studies, the full-length coding sequences for the 418 amino-acids of Spred-2a, for the 348 amino-acids of Spred-2b, for the 144 amino-acids of Spred-2c, for the 165 amino-acids of Spred-2d and for the 148 amino-acids of Spred-2e were cloned into an eukaryotic expression vector pCMV-tag1 (Stratagene).

All cDNAs were amplified using the proof-reading Advantage[®] polymerase mix (Clontech) and as forward primer the 5'VSVSac1 primer (comprising the underlined Sac1 restriction site, the Kozak sequence and the sequence coding for the VSV-G tag: MEYTDIEMNRLGKP followed by the Spred-2 5' sequence: 5'-GGAATTCGGAATGACCGAAGAAACACACCCAGACGATGACAGCTATGAAGAAA CACACCCAGACGA-3'. The reverse primer used for subcloning of Spred-2a and -2e was 5'-ATGCTCGAGCTTGGAGTGAAGGGAGCGGGGAGA-3', for the subcloning for Spred-2b: 5'-ATGCTCGAGTTAGAAAGAGAGTCTTTCGACGCTCTT-3', for the subcloning of Spred-2c, and -2d, 5'-ATGCTCGAGTTACAGGAGGACAGTGGGTAGGCCAGGAGCCTTCT-3' and for the subcloning of the SPR truncated variant 2a(SPR): 5'-ATGCTCGAGTTACGAGCGCTCTCCGTCCTCCTTCCG-3'.

All the reverse primers contain a XhoI restriction site at their 5' end (which is underlined in the primer sequence). The endogenous stop codon of each cDNA was used. Amplification conditions were one step of 1 min at 95 °C and 28 cycles of 30 sec at 95 °C followed by 2 min at 68 °C.

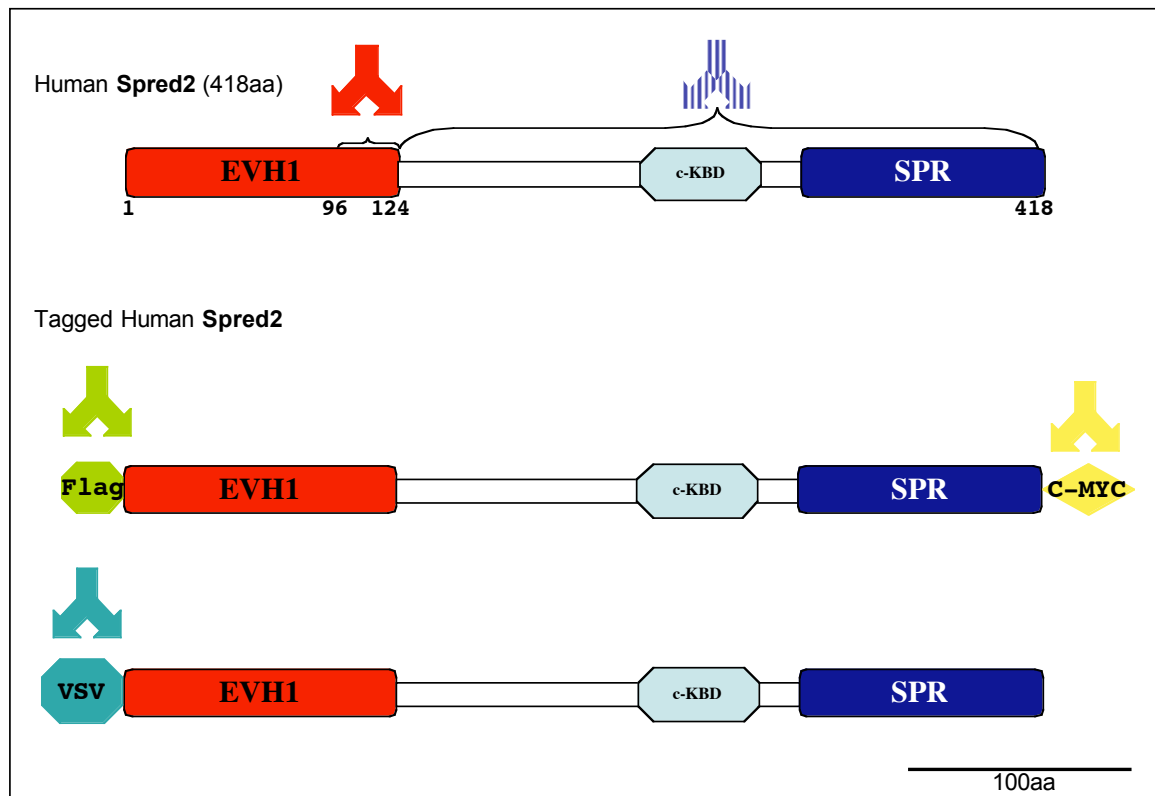


Figure 4: Antibodies to detect endogenous and recombinant Spred-2a.

The N- and C-terminal artificial tags allowed the detection of the recombinant proteins with commercially available antibodies. The endogenous Spred proteins were detected with 2 polyclonal antibodies.

RNase protection assay

Cloning and generation of the antisense probe (Fig. 5):

The probe 2A with a length of 261 bp was amplified with the forward primer in exon 8 (part B): 5'-CCCTTGCTCGTGCGATACTAGCGA-3' and the reverse primer in exon 8 (part B): 5'-CTCATCTTCTCCCCCGCTCCCTTCCACTCCAAG-3'.

The probe 2B with a length of 507 bp was amplified with the forward primer in exon 8 (part A): 5'-CCGATGCCAAGGCCCTACCGCCAG-3' and the reverse primer in exon 8 (part C): 5'-TTGATTTTTCCAAGAGCGTCGAAGACTCT-3'.

The probe 2D with a length of 304 bp was amplified with the forward primer in exon 3: 5'-TTGGAATGCTATGTAAGAAAGGACTTGG-3' and the reverse primer in exon 3a: 5'-CCAGGTCAGTAGATGCCAAACTTTTTGG-3'.

The probe 2E with a length of 243 bp was amplified with the forward primer in exon 2: 5'-TGACAGCTATATTGTGCGTGTCAAGGC-3' and the reverse in exon 6: 5'-

GAGCTTGGCGATGATGACGTTTTTACA-3'. The four resulting probes are depicted in Fig. 5.

The four probes were subcloned into the pDrive^R cloning vector (Qiagen) according to the manufacturer's instructions. As the cloning vector contains 2 promoters (for T7 or SP6 polymerase) on each side on the insert, it allows unoriented cloning. The orientation of the inserted fragment was determined by sequencing. The ³²P-labelled antisense 2A and 2D probes were generated by T7 polymerase (Ambion), the antisense 2B and 2E probes were generated by SP6 polymerase (Ambion).

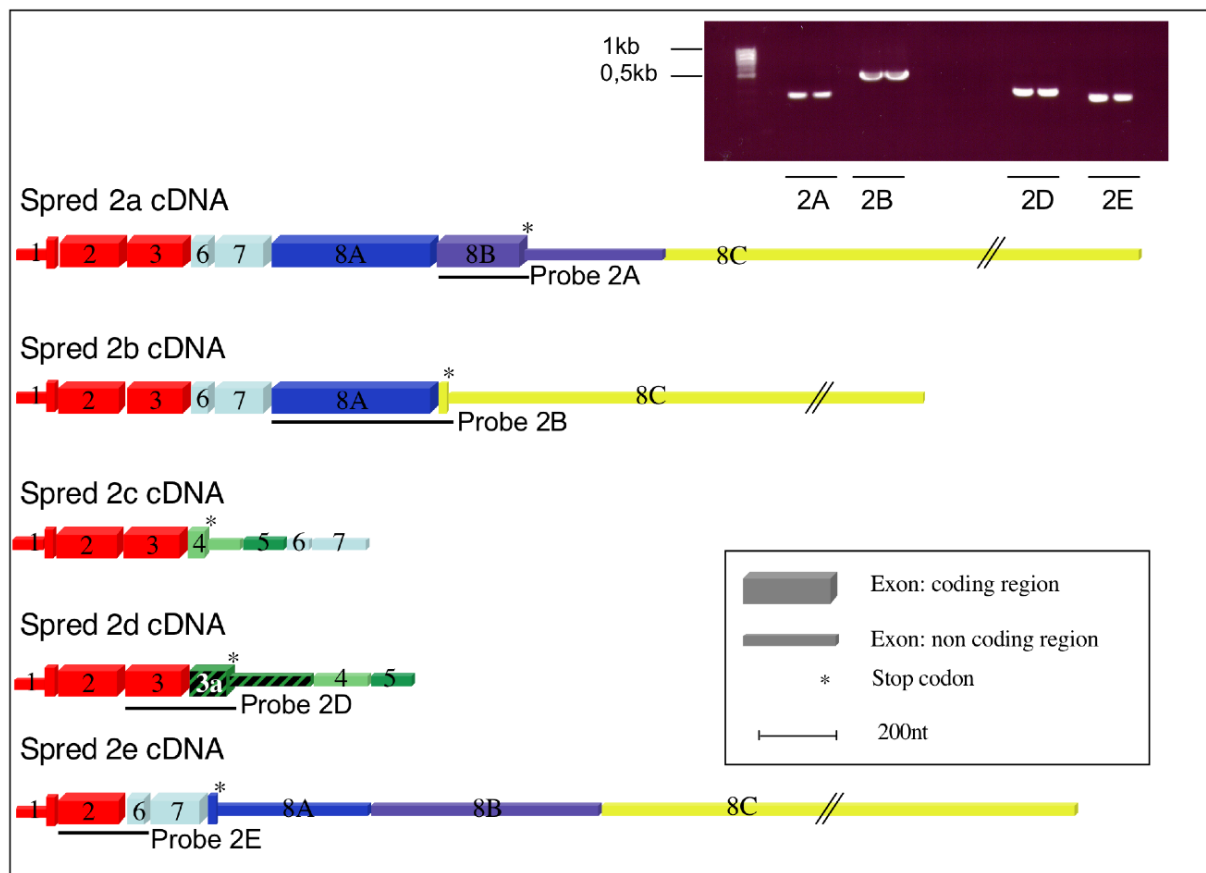


Figure 5: Spred-2 variant specific probes used for RNase protection analysis

The 261 bp long probe 2A anneals in exon 8 (part C). The 507 bp long probe 2B anneals in exon 8 and covers the boundaries between part B and C of exon 8. The 304 bp long probe 2D anneals apart and over the splicing boundary exon 3-exon 3a. The 243 bp long probe 2E anneals apart and over the splicing boundary exon 2-exon 6.

Labelling and hybridisation

After fractionation by polyacrylamide gel electrophoresis, the antisense probes were eluted and mixed with 8 µg of total human RNA per reaction. As negative control, yeast RNA was used instead of human total RNA. From this solution the antisense

probe and the RNA were precipitated with 1/10 volume NH_4OAc and 2.5 volumes ethanol. After 30 minutes incubation at -80°C , the precipitate was spun down (20000g) and air-dried.

The pellet was solubilised in 10 μl hybridisation buffer (Ambion), incubated 3 min at 95°C and hybridisation was allowed to occur overnight at 45°C . Single-stranded RNA was digested by treatment with RNase A and T1 (Ambion) for 30 min at 37°C . Samples containing the RNA-hybrids were precipitated and the pellet was recovered in 6 μl loading buffer, incubated briefly at 95°C , and electrophoresed on 20 X 40 cm 5% polyacrylamide/ 8 M urea gels for 2 to 4 hours at 25 W. The gels were transferred to a paper filter (Whatman) and dried before phosphoimager analyses. The size of the unprotected fragment was approx. 60 nucleotides longer than that of the protected fragment, thus excluding the contribution of undigested probe to the signal.

In vitro transcription-translation

The 6 pCMV-VSV-Spred-2 constructs (corresponding to the splicing variants) contain a T7 RNA polymerase promoter upstream of the insert; therefore they have been used as templates for *in vitro* transcription-translation using the TNT[®] coupled reticulocyte lysate system (Promega).

One μg circular plasmid template of each pCMV-VSV-Spred-2 construct was added to 25 μl of TNT[®] rabbit reticulocyte lysate, 2 μl of TNT[®] reaction buffer, 1 μl of TNT[®] T7 RNA polymerase, 1 μl of amino acid mixture (1mM), and 40 U of RNasin^R ribonuclease inhibitor. Nuclease-free water was added to a final volume of 50 μl . The reactions were incubated at 30°C for 90 min under constant agitation. After addition of 3-fold concentrated SDS sample buffer, the translation products were fractionated on a 15% SDS-PAGE gel and subjected to Western blotting. The membrane was probed with the monoclonal anti-VSV antibody at a dilution of 1: 500 in PBS/4% milk.

Protein biochemistry techniques

Generation of Spred-2-specific antibodies

To perform biochemical and immunocytochemical analyses of Spred-2, polyclonal sera were raised against an immunogenic fragment covering the Spred-2a protein from amino acid 95 to amino-acid residue 415. This sequence (from clone EST 251635 which misses the first 95 aa of the N-terminal EVH-1 and the last three

alanine residues of the Spred-2a protein) was cloned into a prokaryotic expression vector in frame and downstream of the sequence encoding GST protein. The resulting fusion protein GST-Spred-2a (96-415) was purified from inclusion bodies, and used to immunize two rabbits.

After immunisation, antibodies raised against the GST-Spred-2a (96-415) fusion protein were affinity purified using the immobilised antigen or immobilised antigenic fragments.

As the anti-EVH-1 antibody recognises epitopes located at the second half of the EVH-1 domain (between amino acids 95-148), it cannot be used for the detection of Spred-2e, which only comprises the first 69 N-terminal amino acids of the EVH-1 domain. In order to specifically visualise the Spred-2e variant, an immunogenic fragment derived from the Spred-2e C-terminal domain, was used to raise polyclonal antibodies. This sequence, encoding the eighty C-terminal amino acids of Spred-2e, (showing no homology to other Spred-2 variants) was cloned into the prokaryotic expression vector pGEX-4T2 in frame and downstream of the sequence encoding GST. The fusion protein GST-Spred-2e (69-148) was purified from inclusion bodies and was used to immunize a rabbit.

GST pre-absorption and affinity purification of the anti-serum on immobilized Spred-2e antigenic fragment were performed.

GST fusion protein expression and purification

The sequence corresponding to the Spred-2 EVH-1 domain was cloned into PGEX-4T-2 (Pharmacia) with help of the following primers: 5'-CGGGATCCATGACCGAAGAAACACACCCA-3' and 5'-GGAATTCATTCTATAAGGTCTTCGATTGC-3' using BamH1 and EcoR1.

For the production of the Spred-2a antigen as a GST fusion protein, the EST clone 251635 was digested with EcoR1 and Not1 and the insert was subcloned into pGEX-4T-1 (Pharmacia) (Messerschmitt, 1998), thus allowing prokaryotic expression of the GST-Spred-2a (96-415) protein.

For the production of the Spred-2e antigen, the fragment amplified with the following forward primer 5'-AATGGATCCCCGCAACAACGTCATCTTCCACCATCC-3' and the reverse primer: 5'-ATGGCTCGAGTCACCTGGCGGTAGGGCCTTGCA-3' was digested with BamH1 and Xho1 and the insert was subcloned into pGEX-4T-2 (Pharmacia), thus allowing prokaryotic expression of the GST-Spred-2e (95-148)

protein.

For the production of the Spred-1 antigen, the corresponding coding region to mouse Spred-1 (124-233) was cloned into pGEX-4T-2 (this construct and the protein production has been done by Dr. Karin Bundschu).

Overnight cultures of transformed *E.coli* BL21 were diluted by 1:40 in fresh shaking 2xYT medium supplemented with ampicillin (100 µg/ml) and incubated at 37 °C under continuous agitation. In the late exponential growth phase, at OD₆₀₀=0.8 the expression of the fusion protein was induced with IPTG (1 mM final concentration). After 4 h of expression, the bacteria were harvested (5000 g, 15 min), lysed by osmotic shock and the pellet resuspended with ice-cold lysis buffer (50 mM Tris-Cl, pH 8, 5 mM EDTA, 10 mM NaCl, supplemented with 1 mg/ml lysozyme).

Because the fusion proteins, derived from the constructs pGEX-Spred-2a (96-415) and pGEX-Spred-2e (95-148), accumulated in insoluble aggregates, isolation of the inclusion bodies was necessary to recover the expressed protein (Nagai et al, 1987).

In case of soluble protein (like GST-EVH-1) the lysis occurred during 30 min of incubation on ice. Subsequently, Triton X-100 was added to the final concentration of 1% (v/v). The lysate was vigorously mixed and sonified for 10 min (Branson sonifier 250) (parameters: 50% duty cycle, 50% power output). After centrifugation for 10 min at 14.000 rpm (microfuge Eppendorf, 5415), the supernatant was used for glutathione (GSH) affinity chromatography according to the manufacturer's instructions. The GSH beads were pre-equilibrated with lysis buffer and 1% Triton X-100 and after addition of the supernatant to the beads, the reaction was incubated for 1 h at 4°C under constant rotation. The bound GST fusion proteins were recovered through elution with 10 mM GSH, pH 8.0. After dialysis in PBS or carbonate buffer, the protein preparations were stored at 4 °C up to one week or at -80°C for long-term storage.

Isolation of inclusion bodies from *E.coli*

The constructs pGEX-Spred-2a (96-415) and pGEX-Spred-2e (95-148) generated to produce the antigen for immunisation were tested for expression in *E.coli*. The two fusion proteins accumulated in insoluble aggregates. The expressed recombinant proteins could only be recovered in inclusion bodies (Nagai et al, 1987). After standard IPTG induction and expression, the inclusion bodies were isolated and washed according to the following protocol: cells were pelleted (3000 g for 5 min) and

completely suspended in lysis buffer (50 mM Tris-Cl, pH 8.0, 25% sucrose (w/v), 1 mM EDTA, 1 ml of lysis buffer/g wet cell pellet) at 4 °C. The cells were lysed by addition of 2 mg/ml lysozyme dissolved in lysis buffer and incubated for 30 min on ice. In order to shear the DNA and to decrease viscosity, sonification of the viscous solution for 10 min (50% duty cycle, 20% power output) was performed. After 30 min of incubation on ice, the detergent buffer (0.2 M NaCl, 1% deoxycholic acid (w/v), 1% Nonidet P-40 (v/v), 20 mM Tris-Cl (pH 7.5), 2 mM EDTA) was added to the lysate (2 ml of buffer per 1 ml of lysate) and after stirring at 4°C for at least 30 min, the homogenate was centrifuged at 5000 g for 10 min. The slightly orange coloured supernatant was carefully removed and the pellet completely suspended in the washing solution (0.5 % Triton X-100 (v/v), 1 mM EDTA) and centrifuged at 8000g for 5 min. The milky supernatant was carefully removed and the pellet resuspended in washing solution and centrifuged. This washing procedure was repeated to solubilise the membrane fraction completely until a tight pellet was obtained. The final pellet, which contains the fusion protein, was finally washed with 70 % ethanol.

Immunisation of rabbits

The inclusion bodies were weighted (wet weight) and resuspended with sterile PBS to a final concentration of 10 mg/ml. After sonification, the resuspended inclusion bodies were aliquoted to 250 µl. Each aliquot was emulsified in a sonification bath with one volume of incomplete Freund's adjuvant. 250 µl of the emulsion (1.25 mg of protein) were used for each intradermal injection. The rabbits were boosted three times every two weeks and the blood was sampled two weeks following the last injection from the peripheral ear vein. The blood samples were incubated for 30 min at 37°C for proper cloth formation and then centrifuged at low speed (1000 g, 5 min) to purify sera.

Electroelution of proteins from polyacrylamide gels

A 20 x16 cm gel was stained with Coomassie-Brilliant-Blue (0.2% R-250, 0.5% acetic acid, 20% methanol) for 10 min and subsequently destained in 30% methanol for 1 hour. The band of interest was cut out and neutralized 3 times in 1 M Tris/HCl (pH 7.5). The gel piece was introduced into the electroelution device (Biotrap BT 1000 from Schleicher & Schuell) according to the manufacturer's instructions. The electroelution buffer was composed of 25 mM Tris-HCl, 192 mM glycine, 0.025%

SDS. After electroelution at 6V/cm for 14h, the polarity was inverted for 1 min and the sample was collected between the two membranes.

Coupling of proteins for preparative affinity chromatography

The protein preparations to be coupled were dialysed against coupling buffer at 4 °C (0.2 M NaHCO₃, 0.5 M NaCl, pH 8.3). In case of proteins isolated from inclusion bodies and purified by electroelution (which are insoluble in the standard coupling buffer), the buffer was supplemented with 0.025% SDS.

Hi-Trap NHS-activated 1 ml columns (Amersham Pharmacia Biotech) were prepared for the coupling of the ligand by injecting ice-cold HCl solution (1 mM) to remove the isopropanol containing buffer used for storage.

One ml volume of protein sample (1-5 mg/ml) was immediately injected in the column with a syringe and the column was sealed and incubated for 30 min at 25 °C.

In order to inactivate remaining active groups that had not reacted with the ligand and to wash out unbound ligands, the column was washed subsequently with 6 ml ethanolamine buffer (0.5 M ethanolamine, 0.5 M NaCl, pH 8.3) and with 6 ml acetate buffer (0.1 M acetate, 0.5 M NaCl, pH 4.0). Once more, 6 ml of ethanolamine-based buffer was injected and the column was incubated 30 min at room temperature in order to inactivate the free reactive groups. After three more injections alternating between ethanolamine and acetate based buffers, PBS was injected in order to neutralise the pH. The column was stored in PBS with 0.1 % NaN₃ at 4 °C.

Affinity purification of antisera

Affinity-purified anti-Spred antibodies were prepared by adsorption and elution of antibodies using protein antigens immobilized on Hi-Trap^R Sepharose columns (Amersham Pharmacia Biotech).

Before coupling, the protein preparations were dialysed against coupling buffer at 4°C : (0.2 M NaHCO₃, 0.5 M NaCl, pH 8.3). In case of proteins which were isolated from inclusion bodies and subsequently purified by electroelution, the buffer was supplemented with 0.025 % SDS.

One to five mg/ml of purified protein was coupled to the Hi-Trap NHS-activated 1 ml column (Amersham Pharmacia Biotech) according to the manufacturer's instructions. In order to remove any molecules that might co-elute later, the column was first stripped with elution buffer (100 mM glycine pH 3.0) and the column was equilibrated

with PBS.

The post-immune serum was diluted 1:10 in PBS and run through Hi-Trap columns connected in series at a flow rate not exceeding 0.1 ml/min at 4 °C.

The diluted serum was run through either two Hi-Trap columns, containing GST and the antigen (either GST-Spred-1 (124-233) or GST-Spred-2 (96-415)) or through 3 serial columns containing GST, GST-Spred-2 EVH-1, and the immobilized antigen: GST-Spred-2 (96-415). After reaching the baseline upon washing with PBS supplemented with 350 mM NaCl, the bound antibodies on each column were eluted separately with 100 mM glycine, pH 3.0 (5 column volumes) at a flow rate of 1 ml/min. One ml fractions were added to 40 µl of 1 M Tris-Cl, pH 8.9 per tube in order to neutralize the eluted samples immediately and to avoid protein denaturation.

Each of the elution fractions was analysed on a 12% SDS-PAGE gel. The fractions containing the affinity-purified antibodies were pooled and concentrated using a Centricon 30K device (Amicon, USA). The GST-preabsorbed antibody eluted from the second column, named anti Spred-1, -2 or Anti-EVH-1, recognised epitopes between aa 96 and 124 of Spred-2 and the antibody eluted from the third column named Anti-C.TER recognised epitopes between aa 125 and 415 of Spred-2a.

Glycerol was added to the concentrated antibody pools to a final concentration of 40 %. The antibodies were stored in aliquots at -20°C. Protein concentrations were estimated from the OD_{280nm} (1 mg/ml of antibody yields an OD₂₈₀ of 1.3) and as well using the Lowry reagent (Sigma Diagnostics).

Gel electrophoresis and immunoblotting

SDS-polyacrylamide gel electrophoresis (SDS-PAGE) was performed using 15 to 10% (w/v) polyacrylamide gels (Laemmli, 1970) and proteins were immunoblotted to nitrocellulose (Schleicher und Schuell) using a semi-dry transfer system (Fast Blot B33, Biometra). After blocking with 0.025 % (v/v) Tween 20, 0.15 % (v/v) Triton X-100 ("PBS-TT") and 4% milk for 1 hour at room temperature, the membranes were washed with PBS-TT (3 times, for 10 min each) and incubated overnight with the affinity purified anti-Spred antibodies at concentrations of 0.2 µg/ml to 0.6 µg/ml in PBS-TT-Milk. First antibodies were detected with goat anti-rabbit HRP-conjugated secondary antibody (at a dilution 1:4.000) (Dianova) and the blots were developed using the enhanced chemiluminescence detection kit (ECL, Amersham).

Antibodies

The primary antibodies were:

polyclonal anti-Flag epitope/fusion tag (Alpha Diagnostic International) stock 1 mg/ml,
monoclonal anti-cytokeratin large spectrum (Dako), stock 2 mg/ml,
monoclonal anti-caveolin-1 (BD Transduction Laboratories), stock 250 µg/ml,
monoclonal mouse anti-vimentin (Dako), stock 60 µg/ml,
monoclonal mouse anti-desmin (Dako), stock 170 µg/ml,
monoclonal anti-GST (NanoTools), stock 0.1 mg/ml,
monoclonal anti-VSV glycoprotein clone P4D5 (Sigma), stock 6.5 mg/ml,
polyclonal M4 anti-VASP serum (Halbruegge et al, 1989),
monoclonal anti-c-myc (Roche Diagnostics), stock 0.4 mg/ml
polyclonal anti-phospho ERK (p44/42 MAPK T202-Y204) clone 9101S (Cell Signaling)
polyclonal anti-ERK (p44/42 MAPkinase) clone 9102S (Cell Signaling).

The secondary antibodies used for Western blot were:

affinity purified donkey anti-mouse IgG, (H+L) HRP-conjugated (Dianova)
affinity purified goat anti-rabbit IgG (H+L) HRP-conjugated (Dianova) (0.8 mg/ml).

For indirect immunofluorescence, the following fluorescent dye-conjugated antibodies were used:

CyTM3 (Biotrend) or Alexa 555 Fluor (Molecular Probes) goat anti rabbit IgG+IgM

CyTM2 (Biotrend) or Alexa 488 Flour (Molecular Probes) goat anti-mouse IgG+IgM.

Cell culture experiments

Mammalian cell culture and transient transfections

PTK2 and HEK-293 cells were cultured in DMEM supplemented with 10% (v/v) fetal calf serum (FCS), 100 units/ml penicillin/streptomycin in a humidified incubator with 5% CO₂ at 37 °C. The cells were passaged after reaching 80-90% confluency. For cell starvation experiments at 80% confluency, the cells were washed with pre-warmed PBS and cultivated in serum-free medium for 24 hours.

PTK2 cells at 50-80% confluency were transfected with the indicated mammalian expression plasmid, using the FuGENE[®] 6 system (Roche Molecular Biochemicals)

or the Effectene[®] reagent (Qiagen) according to the manufacturer's instructions.

The reagent/DNA complex was not removed from the epithelial cells prior to the assay. For testing the level of gene expression, the cells were harvested or fixed 48 hours after transfection.

Serum-induced ERK activation in HEK-293 cells

HEK-293 cells were cultured in DMEM supplemented with 10% fetal calf serum until they reached 20 % confluency in 10 cm diameter dishes. They were transfected with the pCMV-VSV-Spred-2a, pCMV-VSV-Spred-2b, pCMV-VSV-Spred-2c, pCMV-VSV-Spred-2a(SPR)⁻ using the FuGENE[®] 6 transfection reagent. The cells were starved in serum-free DMEM for 24h and then stimulated with 10% serum. The optimal stimulation time was determined with help of time-course experiments performed with the following points: 3, 4, 5, 6, 10, 13, 15 and 20 min. A 13 min stimulation period resulted in the strongest ERK activation.

Cells were solubilised in 1 ml modified double concentrated RIPA buffer (20 mM Tris, pH 7.5, 4°C, 75 mM NaCl, 1% (w/v) Na-deoxycholate, 2% (v/v) Triton X-100, 0.1% SDS, 100 U/ml aprotinin, 10 mM EDTA, 2 g/ml leupeptin, 5 mM benzamidin supplemented with phosphatase inhibitors) for 10 min on ice and were collected with a cell scraper. The homogenates were centrifuged (13000 rpm, 20 min at 4 °C) and stored at - 80°C. SDS samples were prepared for electrophoresis. 45 µl were loaded on 8% or 12.5% gels. After immunoblotting, the membranes were incubated with the polyclonal anti-phospho ERK antibody at a dilution 1:1000 or with the polyclonal anti-ERK antibody at a dilution 1:1000 or with the monoclonal anti-VSV antibody at a dilution of 1:500.

EGF-induced ERK activation in HEK-293 cells

HEK-293 cells were cultured in DMEM supplemented with 10% fetal calf serum until 40 % confluency in 6-well plates. They were transfected with the pCMV-VSV-Spred-2a, pCMV-VSV-Spred-2b, pCMV-VSV-Spred-2c, pCMV-VSV-Spred-2a(SPR)⁻, pCMV-VSV-Spred-2d, pCMV-VSV-Spred-2e, using the Effectene[®] transfection reagent (Qiagen). The cells were starved in DMEM for 24 hours and subsequently stimulated for 2 min with 25 ng/ml recombinant human EGF (Invitrogen). The optimal stimulation time was determined with help of a time course experiment performed with the following time points: 1, 2, 2.5, 5, 7.5, 10, 15 min. After 24 h expression, the

cells were washed with 2.5 ml PBS, and starved in serum-free DMEM for 24 h. After EGF-stimulation, the cells were immediately recovered and lysed in SDS sample buffer (200 µl/well). The samples were boiled 5 min and subjected to electrophoresis. The 10% gels were immunoblotted and the corresponding membranes were probed with the anti-phospho ERK, the anti-ERK, and the anti-VSV antibodies.

Immunohistochemical experiments

Tissues from PBS/ 4% paraformaldehyde-perfused mice or rats were prepared and analysed as described (Gambaryan et al, 1996). Human placental and decidual tissues from the first trimester (10 weeks gestation) of normal pregnancies and human skin biopsies were cryoprotected, snap-frozen in liquid nitrogen (a generous gift from Dr. U. Kammerer, Würzburg). Sections of 7 µm width were cut and fixed with ice-cold acetone for 10 min. Human thymus and tonsils were fixed with paraformaldehyde (4 %) 20 min on ice. Non-specific binding sites were blocked using 10 % human immunoglobulin (Beriglobin^R, Chiron Behring) in PBS for 30 min at room temperature. The slides were incubated overnight at 4 °C in a moist chamber with primary antibodies at a concentration of 2 µg/ml, washed 3 times with PBS and incubated with a 200-fold dilution of the fluorescently labelled anti-rabbit/anti-mouse immunoglobulins for 1 hour at room temperature. After three times washing and a brief dipping into H₂O, the slides were mounted in Moviol[®].

For tissue culture, cells seeded at low density and grown on cover slips were fixed and permeabilized by sequential incubation with 3.7 % paraformaldehyde in PBS for 20 min on ice, and 0.2 % Triton X-100 in PBS for 10 min at room temperature with PBS washing between incubation. After fixation, covers slips were incubated for 1 hour at 37 °C with the primary antibody in a moist chamber. Subsequently cells were washed 3 times with PBS and incubated with the fluorescently conjugated secondary antibodies.

The specimens were examined with Leitz Aristophan/Zeiss Axiophot microscopes equipped with epifluorescence optics.

Binding experiments with the EVH-1 domain of Spred-2

Peptide overlay

³²P-labelling of the GST-EVH-1 protein probe:

-20 μ l of GST-EVH-1 (Spred-2) Cc: 0,7 mg/ml ($3.5 \cdot 10^{-11}$ mol protein)

-1 μ l γ cGKinase Cc 1,2 μ g/ μ l ($1.57 \cdot 10^{-12}$ mol enzyme)

-5 μ l cGMP 50 μ M

-5 μ l 10X Buffer: 100 mM HEPES, pH 7.4, 50 mM MgCl₂, 10 mM DTE, 2 mM EDTA

-1 μ l (cAMP dependant kinase) C-Subunit 340 μ g/ml ($0,08110^{-11}$ mol)

-5 μ l H₂O (up to 37 μ l)

-13 μ l ATP Mix (3 μ l 32 - γ ATP 40 μ Ci, 0,666 μ M and 10 μ l ATP (500 μ M))

After one hour incubation of the 50 μ l reaction in a water bath at 30 °C, the unincorporated ATP was removed by gel filtration. The reaction was applied on a gel filtration microspin G25 column (Pharmacia) previously equilibrated with 1X blocking buffer (PBS (10 mM NaPi, pH 7.4, 150 mM NaCl), 0.05 % Tween 20, 0.3 % Triton X-100, 1 % hemoglobin (0.01 % NaN₃), 0.5 mM DTT. After centrifugation in the microfuge (2 min at 3000 rpm), the flow-through containing the labelled protein was collected and a fraction of it was analysed by electrophoresis on a 15% gel and by autoradiography of the gel.

Overlay:

The membranes with the N-terminally acetylated peptides (produced and spotted by JERINI Peptide Technologies) was rinsed in a small volume of ethanol 100% for 1 min and washed three times with an appropriate volume of PBS for 10 min and blocked 30 min at room temperature on a shaker. The membrane was incubated for 1 h 30 min at room temperature with the purified probe in 1.5 ml blocking buffer (5 μ g of ³²P protein /ml) or with 5 μ g of unlabelled protein/ml.

In case of the radioactive probe, the membrane was washed 3 times with 4 ml of PBSTT1/2 (PBS, 0.025 % Tween 20, 0.15 % Triton X-100) and put into a plastic bag and an X-Omat (Kodak) film was exposed for 14 h at -80°C for autoradiography.

In case of incubation with the unlabelled protein, the membrane was washed 3 times with PBSTT1/2 and incubated with the anti-EVH-1 (described above) antibody for 1 h

(at a final concentration of 0.5 µg/ml in PBS-4% Milk). The membrane was then washed and developed with the goat anti-rabbit IgG (H+L) HRP-conjugated secondary antibody (diluted 1:2.000) (Dianova) using the enhanced chemiluminescence detection kit (ECL, Amersham).

Regeneration of the membrane:

The membranes were stripped according to the manufacturer's instructions with serial incubations in various regeneration buffers: SDS buffer (62.5 mM TRIS, 2 % SDS, 100 mM 2-mercaptoethanol), urea buffer (8 M urea, 1 % SDS, 0,1 % 2-mercaptoethanol), acetic acid based buffer (10 % acetic acid, 50 % ethanol).

Affinity chromatography

Preparation of the tissue homogenate:

Tissues were freshly collected and weighed. Homogenisation of tissues was performed in 2X RIPA buffer (20 mM Tris, pH 7.5, 4 °C, 75 mM NaCl, 1 % (w/v) Na-deoxycholate, 2 % (v/v) Triton X-100, 0.1 % SDS, 100 U/ml aprotinin, 10 mM EDTA, 2 g/ml leupeptin, 5 mM benzamidin) in a ratio of 10 ml of buffer per gram of tissue using the Ultra Turrax device (Ika) and the douncer. The samples were centrifuged at 14.000 g for 15 min and the supernatant was loaded with a peristaltic pump onto the column (with the immobilised GST-EVH1 or GST) at a maximal speed of 0.3 ml/min. The column was washed with 1X RIPA until the baseline was reached and then subsequently washed with PBS supplemented with 350 mM NaCl. The bound proteins were eluted in 2 steps: 100 mM glycine, pH 3.0 and 8 M Urea, 50 mM Tris, pH 8.0, 0.5 M NaCl. The elution fractions were visualized on 8-15% SDS-PAGE upon staining with Silver (Biorad) or with Coomassie G-250.

Sedimentation experiments with intermediate filaments

50 µg of lyophilised recombinant Syrian hamster vimentin (TEBU) was reconstituted in 10 µl H₂O, 0.5 mM DTT and 90 µl subunit buffer (5 mM PIPES, pH 7.0, 1 mM DTT). Then recombinant vimentin was polymerised *in vitro* by adding 5.25 µl 20X polymerisation buffer (5 mM PIPES, pH 7.0, 5M NaCl). After mixing thoroughly, the reaction was incubated 60 min at 35 °C. Purified protein: GST-EVH-1 (Spred-2) or BSA (bovine serum albumin) (50 µl of 2 mg/ml solution) and 250 µl of H₂O were

added to the polymerised vimentin and after mixing carefully, the proteins were incubated for 2 hours at room temperature. 400 µl protein mixture was put on top of 200 µl sucrose solution (5% sucrose in 50 mM KCl) in a ultracentrifugation tube and the samples were subjected to an ultracentrifugation at 100000 g for 30 minutes at 25 °C. The supernatant (300 µl of the upper phase) and the pellet were collected and the protein content was analysed by electrophoresis on a 14 % SDS-PAGE, stained with Coomassie G-250.

Results

The novel human gene family homologous to *Drosophila* AE33

Identification and cloning of the human Spred gene family

In order to search for novel EVH-1 domain containing proteins, the human EST (expressed sequence tag) database (NCBI) was queried with the sequence of the EVH-1 containing *Drosophila* protein AE33. Four highly homologous partial sequences (accession numbers T52235, D80468, AA251635 and AA069749), previously not recognized as members of the EVH-1 domain containing protein family, were identified. From the compiled sequence information available from the sequencing of overlapping EST clones #684759 and #525593 (EST accession numbers AA251635 and AA069749 respectively) and the sequencing of a 5' RACE clone, the cDNA sequence was deduced (Messerschmitt, 1998).

Various sets of primers were designed (as shown in Fig. 3, primers 1 and 4) to clone the 1352 bp full-length coding region from reverse transcribed total RNA isolated from human spleen, human brain, and human heart. The 1254 ORF of the cloned cDNA encodes a protein of 418 aa.

During the progress of this work, the mouse orthologue of this gene was described and has been termed Spred-2 (Wakioka et al, 2001). Through a sequence similarity search with the full-length human Spred-2 coding sequence, I identified two additional very closely related human proteins: Spred-1 (whose mouse homologue was described by Wakioka et al, 2001) and Spred-3. Cloning of the *spred3* cDNA was reported later by (Kato R. et al, 2003). The mammalian Spred family members and the *Drosophila* orthologue AE33 share 2 domains: the N-terminal EVH-1 domains and the C-terminal cysteine-rich domain related to Sprouty, termed SPR domain.

These 2 domains are found independently in other protein families: the EVH-1 domain is the N-terminal domain of each of the Ena/VASP and Homer family members whereas the SPR is highly similar to the Sprouty cysteine-rich region. The amino acid alignment of EVH-1 domains of Spred family members and other EVH-1 containing proteins is represented in Fig. 6, panel A. As well, at the amino-acid level, alignments of Spred SPRs and Sprouty cysteine-rich regions are depicted in Fig. 6.

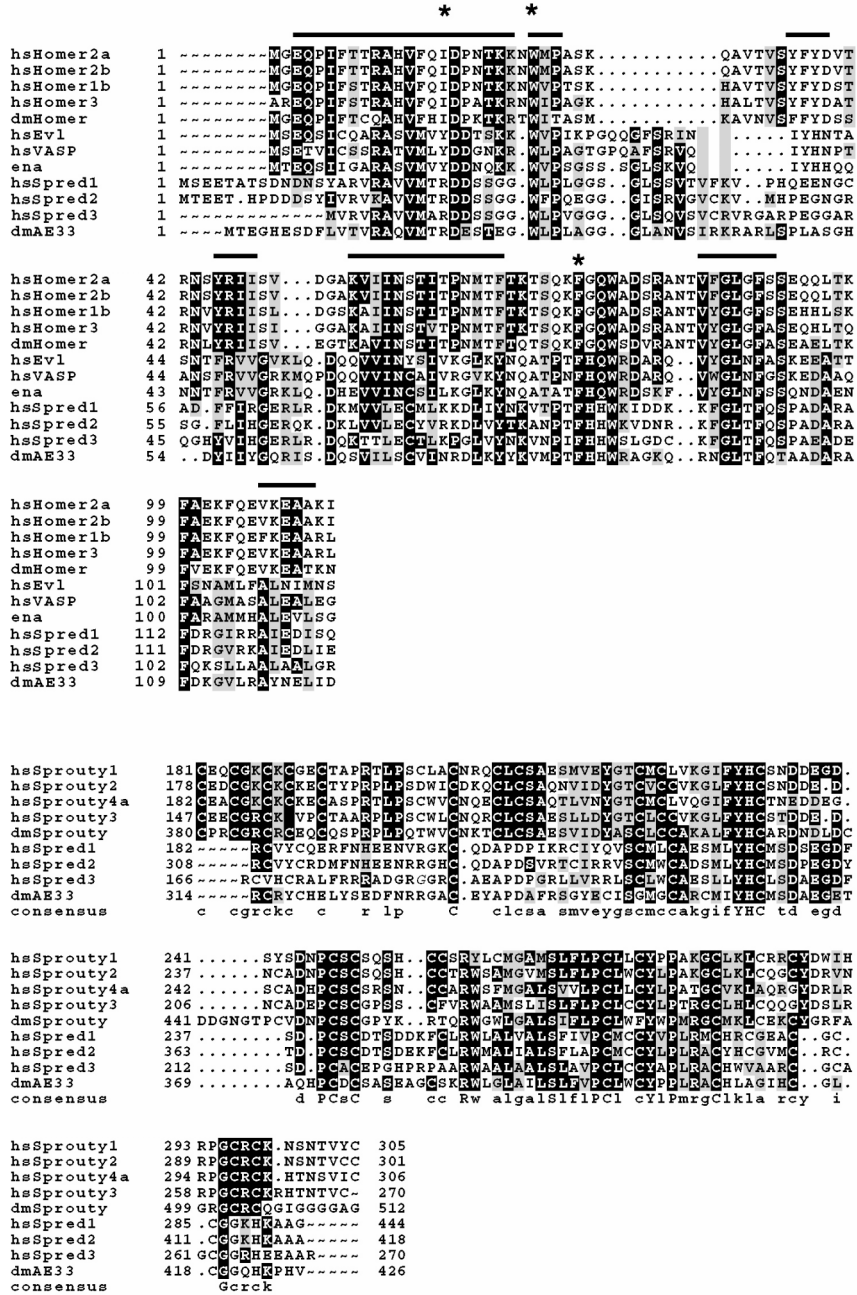


Figure 6: Comparison (identities/similarities) of the EVH-1 domains of the different EVH-1 domain containing family members (upper panel) and comparison of the cysteine-rich domain of the Sprouty family members and the cysteine-rich domain related to Sprouty (the SPR domain) of the Sprayed family members (lower panel).

The Ena /VASP family members are: *Homo sapiens* VASP (hsVASP), *Homo sapiens* Evl (hsEvl), *Drosophila melanogaster* Ena, the homer family members are: *Homo sapiens* Homer 2a (hsHomer2a), *Homo sapiens* Homer 2b (hsHomer2b), *Homo sapiens* Homer 1b (hsHomer1b) and *Homo sapiens* Homer 3 (hsHomer3) and the Sprayed family members are: *Drosophila melanogaster* AE33 (dmAE33), *Homo sapiens* Sprayed-1 (hsSprayed1), *Homo sapiens* Sprayed-2 (hsSprayed2), *Homo sapiens* Sprayed-3 (hsSprayed3). The Sprouty family members are *Drosophila melanogaster* Sprouty (dmSprouty), *Homo sapiens* Sprouty 1 (hsSprouty1), *Homo sapiens* Sprouty 2 (hsSprouty2), *Homo sapiens* Sprouty 3 (hsSprouty3), *Homo sapiens* Sprouty 4a (hsSprouty4a) and the Sprayed family counterparts are: *Drosophila melanogaster* AE33 (dmAE33), *Homo sapiens* Sprayed-1 (hsSprayed1), *Homo sapiens* Sprayed-2 (hsSprayed2), *Homo sapiens* Sprayed-3 (hsSprayed3). Identical amino-acid residues are shown in back box and similar amino-acid residues are shown in gray box.

Comparison of the Spred domains with related domains

The EVH-1 domain

The so-called aromatic triad in all EVH-1 domains is a highly conserved cluster of three aromatic residues known to be structurally exposed to the surface (Ball et al, 2002). It forms in the known EVH-1 domain/ligand complexes the ligand binding interface. The residues belonging to this triad are labelled with an asterisk in Fig. 6, panel A. In all Spred EVH-1 domains (like in others EVH-1 domains), the W23 (VASP numbering) is invariant. The triad Y16, W23, F79 of class I EVH-1 domain (hsVASP numbering, labelled with an asterisk) is different from the triad of the class II EVH-1 domain (Ball et al, 2002). A substitution of the Y16 to an aliphatic residue is observed among the Homer family members. In case of the Spred EVH-1 domain the Y16 is substituted to a basic amino acid (R24, hsSpred1 numbering). This substitution implies that the binding cleft between W31 and R24 (hsSpred1 numbering) is different from the different classes of EVH-1. Such substitution could suggest a possible mechanism for selective binding. Differences in the consensus sequence of the PRS target can be expected and this substitution in the recognition site suggests the existence of another class of ligands interacting with the Spred EVH-1 domain.

The most highly conserved regions essential for hydrophobic core packing and therefore crucial for the proper folding of domains have been reported (Ball et al, 2002). They are depicted with bars in Fig. 6, panel A.

The conservation of residues within the Sprouty cysteine-rich domains and the Spred SPR domains

The C-terminal domains of Sprouty and Spred are cysteine-rich. The C-termini of human Sprouty 1, 2, and 3 consist of more than 20 % cysteine. Human Spred-1 and -2 contain slightly more than 16 % cysteine residues within their SPR. The alignment of the cysteine-rich region of Sprouty and the SPR of Spred proteins reveals a conservation of 52 % of the cysteine residues. Human Sprouty 2 has 27 cysteines, 23 are conserved among the Sprouty family members and 12 (out of 18 cysteine residues) are conserved in human Spred-2. Homology between the two domains is especially high in the last two thirds of the SPR (region defined from S341 to K415, hsSpred2 numbering): 40.5 % homology and 56 % identity between human Spred-1

and human Sprouty1. Within the last 2 thirds of these cysteine-rich regions, a conservation of 71 % of the cysteine residues is observed and most prolines: P246, P269, and P276, (numbers referred to hsSprouty1) which are known to markedly influence protein architecture are conserved. As well, serines and tyrosines (Y231, S248, S265, Y274, numbers referred to hsSprouty1) are conserved in Spred and Sprouty C-terminal regions.

Chromosomal assignment and exon/intron organisation of the 3 human genes belonging to the Spred family

I next sought to determine the genomic organisation of the three Spred family members. Searching genomic sequence databases (GenBank, EMBL, unfinished high throughput genomic sequences) with the Spred cDNA fragments helped to isolate some clones comprising the various human *spred* genes. For each of the clone cytogenetical information, available in the databases allowed a detailed chromosomal assignment of the *spred* genes.

The clone RP11-604N3 and the working draft sequence segment NT_024645 (gi 18698849) comprise the *spred1* gene. The NT_024645 sequence maps to chromosome 15q13.2. The BAC clones RP-11-568D19 (gi 15668165) and RP-11-356P4, (gi 19033993), localising to chromosome 2, covered the human *spred2* gene. Two sequence tagged sites (STS) SHGC-64931 and SHGC-31078, respectively, one overlapping the *spred2* exon 8/exon 9 junction and the other mapping within exon 9 provide some more detailed cytogenetical information. The two STS within human *spred2* gene map to chromosome 2p13.3. The working draft sequence segment NT_011233 (gi 3702281) comprising the *spred3* gene suggested a cytogenetical location on chromosome 19q13.13. The alignment of the corresponding genomic sequences to their respective cDNAs of Spred-1, -2, and -3 led to the identification of coding regions within the human genomic sequence and enabled the assignment of the exon/intron organisation to the different genes. The exon-intron structure and exon boundaries of the 3 human *spred* genes have been summarised in table 2.

<i>spred1</i>	Exon	Intron – exon boundaries		Exon Size (bp)	Exon – intron boundaries		Intron
	1	caccccagtg	GCTGGAGGAG	363	CTGACAACGA	<u>g</u> taagcgcct	46.1
	2	tctatttt <u>ag</u>	TAATAGTTAT	169	GGACAAAATG	<u>g</u> taatgaata	22.7
	3	cttttgtc <u>ag</u>	GTGGTTTTGG	169	ATTCTCAAG	<u>g</u> taggtattc	2.3
	4	attttctt <u>ag</u>	GATGCCCCGA	47	TGACTTACAA	<u>g</u> taagtaatg	14.9
	5	ttcccaat <u>ag</u>	GCAAATGAAG	159	AGCCAATCAG	<u>g</u> taagaagat	9.5
	6	tgtatttt <u>ag</u>	ATAACATTTG	102	CCAAAATAGG	<u>g</u> taagtaatg	1.5
	7	tctttttt <u>ag</u>	GTCCCTTTGA	1525	AAACATTATA	gaaaaaaaaagt	4.4
	7'			219	TGAGACTAAG	ttaagttcac	5.7
	8	ttattttc <u>ag</u>	GTTTTTCAGA	49	ATACCCACAA	<u>g</u> taagtagaa	1.2
9	ttttttgt <u>ag</u>	AGACAAGGTG	ND	ND	ND	-	

<i>spred2</i>	Exon	Intron - exon boundaries		Exon size (bp)	Exon – intron boundaries		Intron
	1	tccccaaatc	AGGCGATCTC	125	ACCCAGACGA	<u>g</u> taagtttgg	87
	2	gtcgtttt <u>ag</u>	TGACAGCTAT	178	AGACAAACTG	<u>g</u> taatggcag	9.9
	3	catccttc <u>ag</u>	GTGGTATTGG	169	CTTATAGAAG	<u>g</u> tattgaact	0.339
	3a	cttataga <u>ag</u>	GTATTGAACT	339	CTTGGCTCAG	aagtagagaa	-
	4	Cttggctc <u>ag</u>	AAGTAGAGAA	151	TGGTCTATGG	<u>g</u> taagtgagt	1.8
	5	tattctct <u>ag</u>	CAGCGAGTGC	117	CAATTCCCAG	<u>g</u> taacttgtt	0.132
	6	gtcttttt <u>ag</u>	GTTCAACAAC	65	CGTTTTTACA	<u>g</u> taagtttcc	11.5
	7	ctctacac <u>ag</u>	ACAGCTACAG	150	CCTCGATCAG	<u>g</u> tgagcagca	2.6
	8 8 _A 8 _C	tacgggac <u>ag</u>	CCGATGCCAA	3334 439	ATCCTATCAG CATCCGCCGG	atcgcgtggct <u>g</u> tgagctgca	- 0.578

<i>spred3</i>	Exon	Intron - exon boundaries		Exon Size (bp)	Exon – intron boundaries		Intron
	1	ND	ND		ND	ND	ND
	2	ttccccccac	CTCCTGCAGG	190	GGACCAGAAA	<u>g</u> tgagccacc	1.4
	2'			97	CCTCAGCCAG	<u>g</u> tgagcgtgt	1.5
	3	tgccccctc <u>ag</u>	ACAACCTTGG	169	CTGGGTCGAG	<u>g</u> tgagcagcc	0.098
	4	cctgcccc <u>ag</u>	GCTCACTCAC	213	AACTATGAGT	<u>g</u> tcaattcaa	2.9
	4'			78	CCCTCTGACG	<u>g</u> tgagtgtcc	2.01
	5	ccattttcc <u>ag</u>	CTCTCCAGT	116	GCTCAAAGAG	<u>g</u> tgagctcac	0.165
6	tctcctcc <u>ag</u>	TCCCACGTGG	144	CTCCGCTCAG	<u>g</u> tgcgacctg	1.04	
7	tccgtcgc <u>ag</u>	AGCAGACGGG	508	CTTCATTGGG	<u>g</u> tgtctgtct	-	
7'			309	AGGCTGCGCG	<u>g</u> tgaggacgg		

Table 2: Exon-intron structures and boundary sequences of the human *spred1*, *spred2* and *spred3* genes.

Intron sequences are given in lower case and the exons sequences in uppercase letters. Intron sizes are given in kb. The underlined letter pairs ag and gt are the conventional donor and acceptor splicing sites. The exon 7 of *spred1* is found to be alternatively internally spliced; the alternative exon is called exon 7'. An internal splicing event occurs within exon 8 of *spred2*. In some transcripts, the fragment of 578 nucleotides termed exon 8, part B (8_B) is excluded and exon 8, part A (8_A) associates with exon 8, part C (8_C). The exons 2, 4 and 7 of *spred3* are found to be alternatively spliced. The alternative exons are called exons 2', 4', 7', respectively.

Expression pattern of Spred-1 and Spred-2 in mouse and human

Generation of Spred-1- and Spred-2-specific antibodies

In order to investigate the protein expression profile of the Spred proteins, two polyclonal rabbit antibodies specific for Spred-1 and Spred-2 were raised.

Because of the high homology between Spred-1 and Spred-2, especially between their EVH-1 (62 % homology), SPR (76 %) and the c-KBD (45 %) domains, the Spred-1 specific antibody was raised and affinity-purified against the intermediate region of Spred-1, a region between the C-terminal boundary of the EVH-1 domain and the N-terminal boundary of the c-KBD, which shows the lowest similarity between the 2 Spred family members (aa 124-233). The generation of the fusion protein GST-mouse Spred-1 (124-233) and the column has been made by my colleague Dr. Karin Bundschu.

The Spred-2-specific antibody was raised and affinity-purified against the region comprised between the amino acids 96-415 of Spred-2.

The cross-reactivity and the specificity of the 2 antibodies were tested by Western blotting and by immunofluorescence staining of transfected cells. The two affinity purified antibodies raised against Spred-1 and Spred-2 recognised specifically the corresponding antigen without cross-reacting with the other family member and they detected a 49 kDa protein band for murine Spred-1 and a 47 kDa protein band for murine Spred-2, respectively (Engelhardt et al, 2004). Positive controls were made with overexpressed Spred proteins in the eukaryotic HEK 293 cells (a non-tagged full-length version and a 6xHis/c-myc-tagged version of mouse Spred-1 and Spred-2). The affinity-purified anti-Spred-1 antibody recognised the overexpressed Spred-1 protein and the 6xHis/c-myc-tagged Spred-1 protein expressed upon transfection in HEK 293 cells, but did not detect the overexpressed Spred-2 protein or the tagged version of Spred-2. In parallel, expression of tagged proteins was checked with a anti-6xHis specific antibody.

The Spred-2 specific antibody recognised the Spred-2 protein, but no crossreactivity with the overexpressed Spred-1 proteins was observed.

Distribution of Spred-1 and Spred-2 mRNA and protein in mouse tissues

In mouse, expression of Spred-1 and Spred-2 mRNAs and proteins were analysed by RT-PCR and Western blotting (Engelhardt et al, 2004). Spred-1 transcript was found in large amount in mouse brain. A weak signal for Spred-1 transcript was also observed in mouse testis. RT-PCR analyses demonstrated the presence of the Spred-2 transcript in almost all tissues except in mouse kidney and skeletal muscle. These results are in accordance with the Northern hybridization data reported recently in the literature (Kato R. et al, 2003). At the protein level (Fig. 7), the strongest Spred-1 immunoreactivity, was found in brain and cerebellum of adult mice (Fig. 7, panel A) whereas Spred-2 immunoreactivity was observed predominantly in mouse lung, liver, and testis (Fig. 7, panel B). In contrast to Spred-1, Spred-2 was clearly detectable as a 47 kDa band in all investigated tissues. The anti-Spred-2 antibody recognised a second band of approximately 42 kDa, which is thought to be a short alternative splicing product of the Spred-2 gene.

In order to test whether the expression patterns of the Spred proteins change during development, the immunoreactivity of mouse fetal tissues was investigated.

Spred-2 immunoreactivity was absent in the 16 day-old fetus whereas Spred-1 was expressed in mouse fetal liver and fetal brain (Fig. 7, panel C).

To define the cellular localisation of Spred-2 in testicular tissue, immunohistochemical stainings were made with the anti-Spred-2 antibody in adult mouse testis sections. Strong staining of Spred-2 was especially found in the mature spermatids projecting into the lumen of the seminiferous tubules (Fig. 8, panels A, B and control panels C, D). Near the basal membrane, cells were slightly stained as well (these cells could be spermatogonia or the interstitial endocrine Leydig cells).

As the late spermatids and the sperm in the *ductuli seminiferi* showed a strong staining of Spred-2, the subcellular localisation of Spred proteins in mature spermatozoon collected from the *cauda epididymidis* was examined. A very prominent staining of Spred-2 was seen in the acrosomal region of the head and the principal piece of the tail, in a form of dotted pattern along the axoneme within the fibrous sheath (Fig. 8, panels E-F).

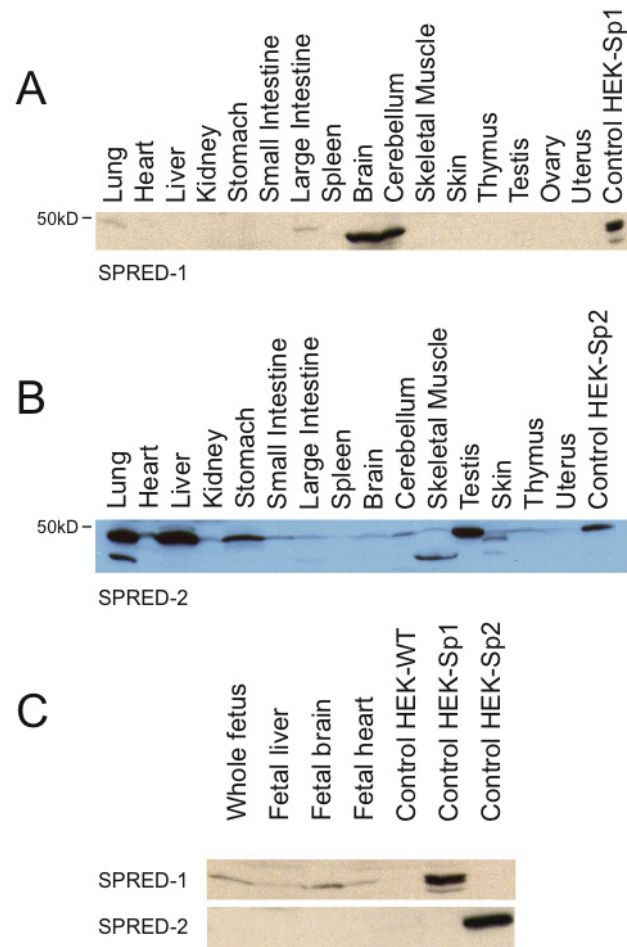


Figure 7: Analysis of Spred-1 and Spred-2 protein expression in various mouse tissues

(A) Western blot analysis using the affinity purified anti-Spred-1 antibody and tissue extracts from adult mice (30 μ g total protein/lane). Expression of Spred-1 was observed in total brain extracts as well as in cerebellum extracts. Positive control (last lane): Extract from transfected cells overexpressing full-length murine Spred-1.

(B) Western blot analysis using the affinity purified anti-Spred-2 antibody and tissue extracts from adult mice (30 μ g total protein/lane). Expression of Spred-2 was observed in various organs, the most prominent signals were observed in lung, liver, stomach, testis, and skin, a weaker signal was detected in nearly all organs tested. Positive control (last lane): Extract from transfected cells overexpressing full-length murine Spred-2.

(C) Western blots demonstrating expression of Spred-1 in whole fetus, fetal liver, fetal brain, fetal heart at day 16 of gestation (upper panel) and - in contrast - lack of expression of Spred-2 in corresponding fetal tissues (lower panel).

The following controls were performed: lysate of HEK 293 cells, WT (wild type, untransfected), lysate of HEK 293 cells transfected with the construct pcDNA-mouse Spred-1 and lysate of HEK 293 cells transfected with the construct pcDNA-mouse Spred-2. Tissue homogenates were prepared as described and 30 μ g total protein/lane were separated by SDS-PAGE, blotted and Spred-1 and 2 proteins detected with the isoform specific antibodies. Equal protein loading was verified by Ponceau staining (not shown).

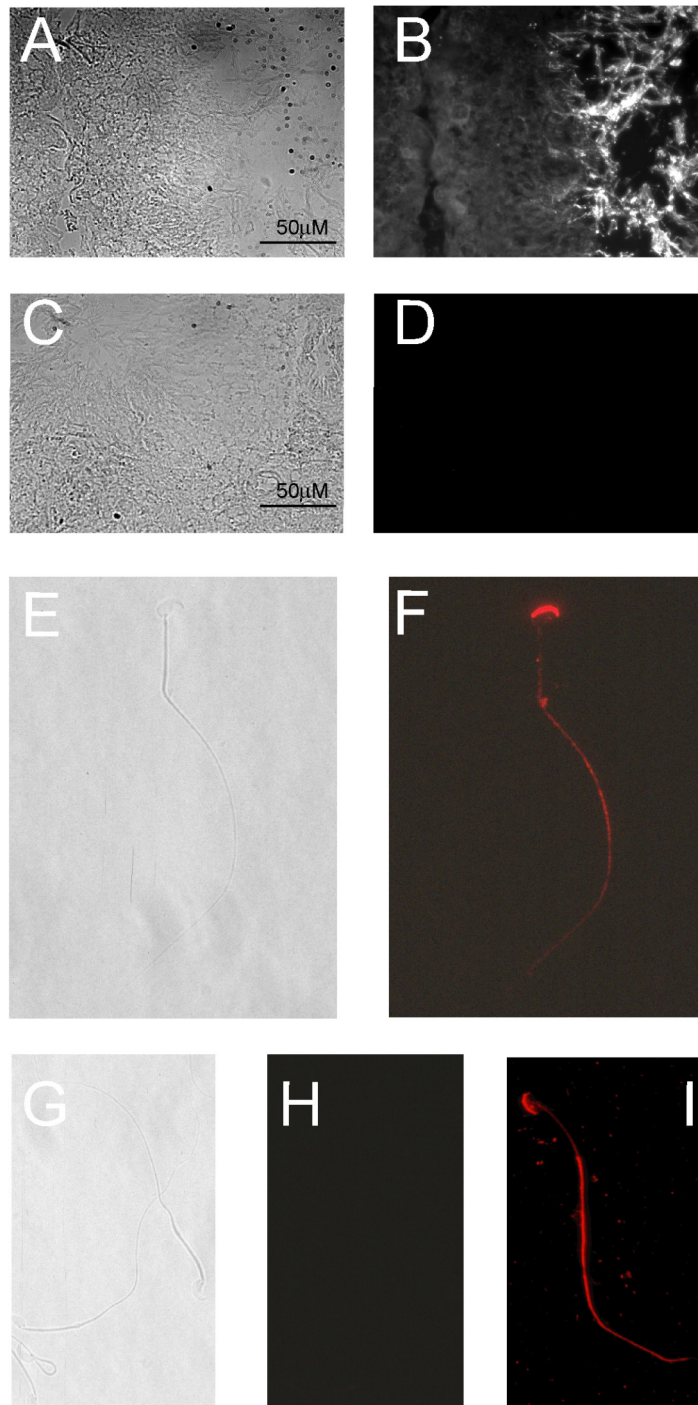


Figure 8: Spred-2 expression and localisation in mouse testis and sperm

(A) Phase contrast micrograph of mouse testis, corresponding to panel B, original magnification 40 X. (B) Immunohistochemical staining of mouse testis with the anti-Spred-2 antibody, detected with a goat anti-rabbit Alexa Fluor[®] 555-labeled antibody, revealed strong staining of mature spermatids projecting into the lumen of seminiferous tubules and a weak staining of endocrine Leydig cells. (C) Phase contrast picture of testis section, corresponding to control panel (D, original magnification 40 X). (D) Immunohistochemical control staining with secondary antibody alone showed no unspecific staining. (E) Phase contrast micrograph of mouse sperm isolated from the cauda epididymidis, corresponding to panel (F). (F) Staining of a single spermatozoon with the Spred-2 specific antibody in the acrosomal vesicle and sperm tail (F, red, original magnification 63 X, oil immersion). (G) Phase contrast micrograph of mouse sperm, corresponding to control staining with secondary antibody alone in panel (H). (I) Immunohistochemical staining of a single mouse sperm with the anti-PMCA4 antibody, serving as positive control (Schuh et al, 2004) (63 X, oil immersion).

Spred-2 immunoreactivity in human tissues

In order to evaluate the expression profile of Spred-1 and -2 in various human tissues, we determined the immunoreactivity of a panel of human tissues using a multi-tissue array (work done together with Dr. Kai Schuh).

As also observed in mouse tissue preparations, strong staining of Spred-2 in human hepatocytes suggested a high content of Spred-2 in this tissue.

In human skin, the *stratum granulosum* and the *stratum spinosum* showed a strong Spred-2 immunoreactivity, and the *stratum basale* was weakly stained. Spred-2 was also present in the cytoplasm of the *stratum spinosum* cells, especially in some vesicle-like structures that are thought to be the secretory granules called membrane-coating granules.

In human small intestine, like in other organs of the gastrointestinal tract, the most prominent staining was found in the mucosal layer. The mucus secreting Goblet cells were negative whereas epithelial absorptive cells in the intestinal mucosa were immunoreactive for Spred-2. The apical pole of the cells was strongly stained; a dotted pattern close to the luminal membrane characterised this staining.

Spred-2 immunoreactivity in human glandular tissues

By screening a large panel of human tissues, the strongest immunoreactivity of Spred-2 was observed in glandular epithelia. High levels of Spred-2 were found in the salivary glands (Fig. 9, panel B), the prostate (Fig. 9 panel J), the thyroid gland (especially the colloid filling the lumen of the active epithelia was strongly stained)(Fig. 9 panel F), the duct of sweat glands (the secretory cuboidal cells but not the myoepithelial cells were strongly stained) in the reticular layer of the dermis (Fig. 9, panels M, N) and the endometrial glands of the first term pregnant uterus (Fig. 10 panel A). As well, a strong reactivity was observed in the peripheral myoepithelial submucosal glands close to the tonsils (Fig. 9, panels O, P). Immunostaining was observed predominantly in epithelial cell membrane and appeared to be more intense at the apical cell pole, where the secretory granules are located.

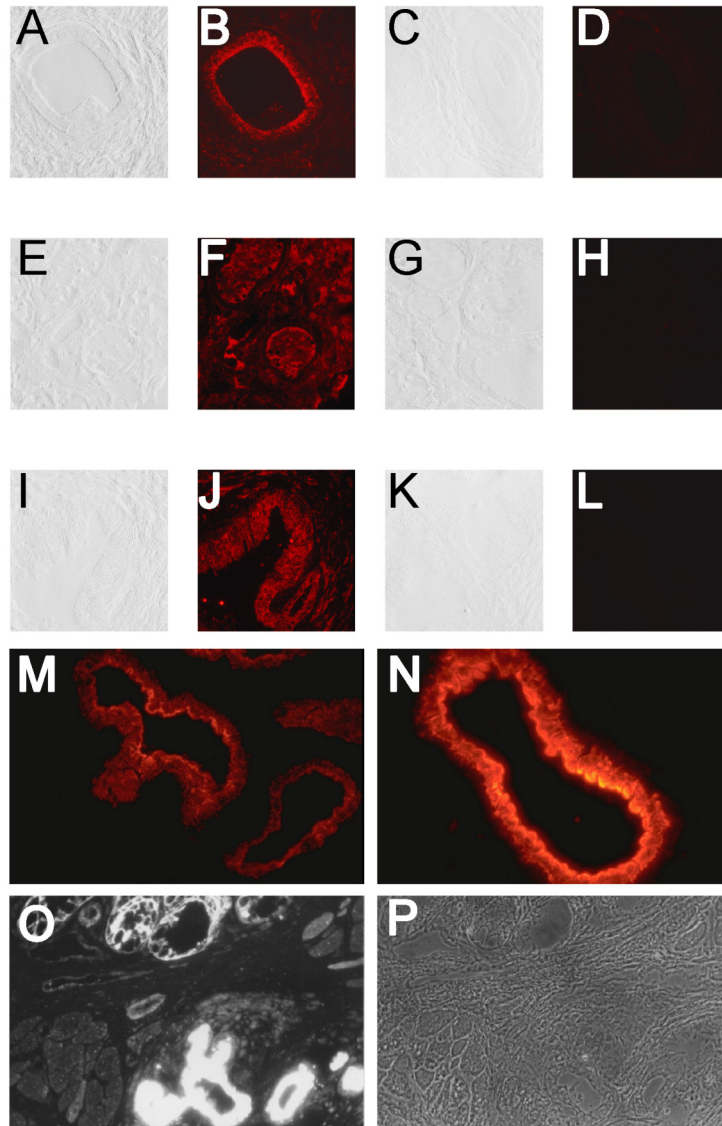


Figure 9: Spred-2 immunoreactivity in adult salivary glands, in the thyroid gland, in the prostate, in sweat glands, and in the submucosal peripheral glands near the tonsils
 (A) Phase contrast of human salivary gland section, corresponding to staining in panel (B). (B) Immunohistochemical staining of Spred-2 in adult human salivary gland (original magnification 40 X). (C) Phase contrast of control staining (of salivary gland) with secondary antibody alone (D). (E) Phase contrast of human thyroid gland section, corresponding to staining in panel (F). (F) Immunohistochemical staining of Spred-2 in adult human thyroid gland (original magnification 40 X). (G) Phase contrast of control staining (H) of thyroid gland. (I) Phase contrast of human prostate section, corresponding to staining in panel (J). (J) Immunohistochemical staining of Spred-2 in adult human prostate (40 X). (K) Phase contrast of control staining (L) of prostate. (M, N) Immunohistochemical staining of Spred-2 in sweat glands of the adult human skin (orig. magn. 25 X for C and 40 X for D). (O) Immunohistochemical staining of adult human tonsils/ submucosal peripheral glands with the anti-Spred-2 antibody and CyTM3 anti-rabbit (40 X) and corresponding phase contrast (P).

Spred- 2 immunoreactivity at the feto-maternal interface

Stainings of sections of the first term decidua covering the feto-maternal border from

the placenta to the myometrium, where the implantation of the fetus occurs, were performed. In order to characterise the immunoreactive cells, double-staining experiments were performed on the same sections with the anti-pancytokeratins antibody, which is a marker for cells from ectodermal origin such as trophoblasts and glandular epithelium.

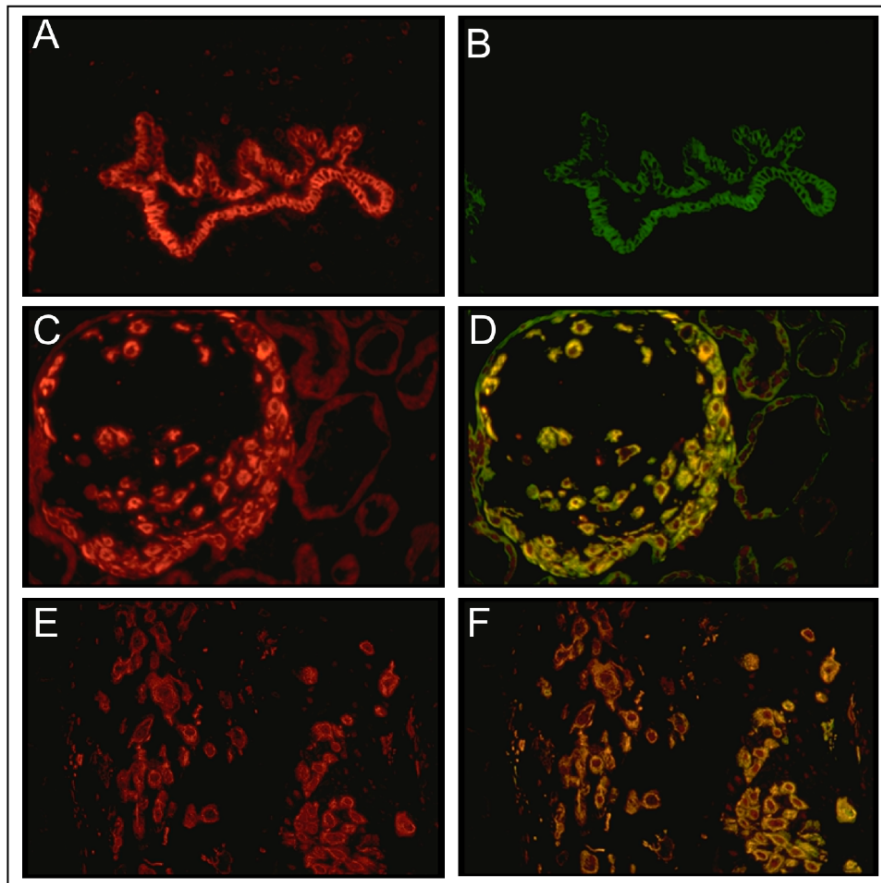


Figure 10: Spred-2 expression in the endometrial glands of the early pregnant uterus (A,B), in the anchoring villous of the placenta (C,D) and in trophoblasts invading the decidua during the first term of the pregnancy (10 weeks of gestation) (E,F).

(A,C,E): Immunohistochemical staining with the anti-Spred-2 and Cy3 anti-rabbit Ig (red fluorescence). Panel (B/D/F): Immunohistochemical staining with the epithelial and trophoblast marker: the monoclonal anti-cytokeratins antibody and Cy2 anti-mouse Ig (green fluorescence). The panels D/F are merged pictures from the double staining (anti-Spred-2 in red and anti-cytokeratins in green).

In placenta tissues of the first trimester, villous cytotrophoblast cells showed prominent staining for Spred-2 (Fig. 10, panel C). Most interestingly, distal cells of the extravillous trophoblast cell column showed the strongest Spred-2 immunoreactivity. Staining of Spred-2 on cytotrophoblast cells of the column was observed, whereas the syncytiotrophoblasts were always negative.

Expression of Spred-2 was maintained by the invasive interstitial trophoblasts (Fig.

10, panel E) and was not lost deeper in the placental bed. The trophoblasts differentiate into sessile multinucleated giant cells in the deep placental bed (Loke and King, 1995).

However, the staining intensity of the invasive trophoblasts decreased from the proximal extravillous trophoblasts (localised close to the villi) to the myometrium.

Therefore these findings, suggest that Spred-2 expression correlates with the invasive phenotype of the trophoblasts. Interstitial and endovascular trophoblastic cells (displacing endothelial cells and disrupting vessels walls) showed strong Spred-2 immunoreactivity in the first trimester decidual tissues. The non-invaded vessels were negative.

Spred-2 immunoreactivity in rat heart

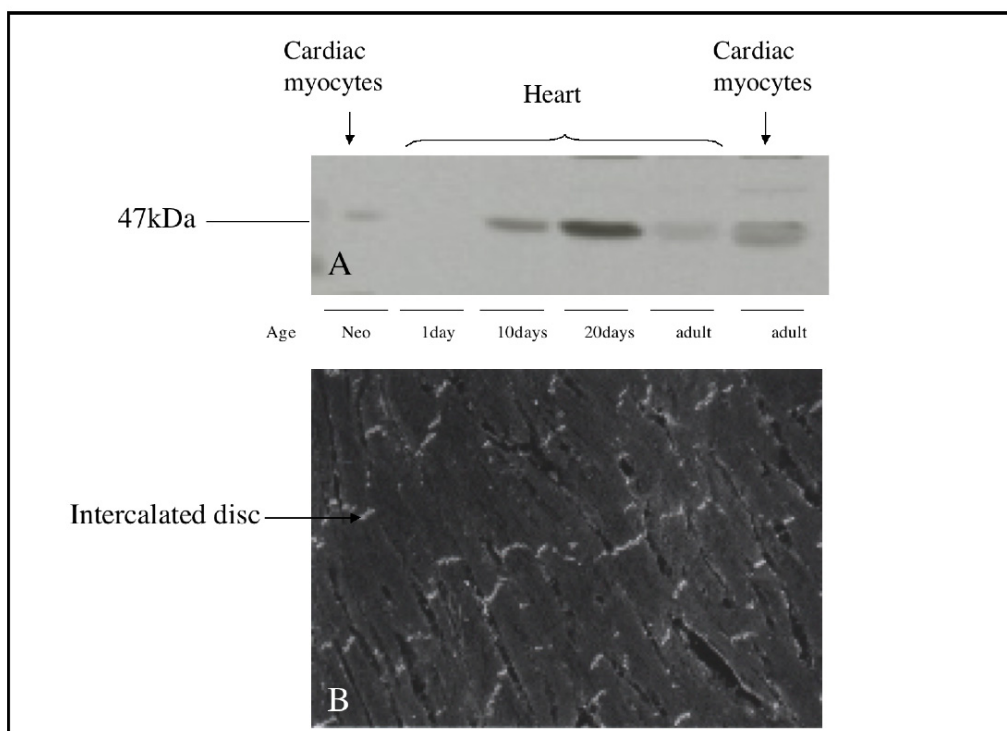


Figure 11: Spred-2 expression in cardiac myocytes (A) and localisation of Spred-2 in the intercalated discs (B).

(A) Western blot of rat heart homogenates prepared from animals of the indicated age and probed with the anti-C.TER (Spred-2) antibody. The Spred-2 immunoreactivities of isolated cardiac myocytes are shown in lane 1 for a new born and in lane 6 for an adult rat. (B) Immunohistochemical staining with the anti-C.TER (Spred-2) of an adult rat heart. The myocytes and heart homogenates have been prepared by Dr. Stepan Gambaryan.

The expression of Spred-2 in the heart was checked during the development (Fig. 11). The expression of Spred-2 at birth was almost undetectable, then it progressively increased to reach a high expression level at day 20. The expression

was very low in adult rat heart. The signal found in cardiac myocytes was stronger than the one obtained with crude heart homogenates. Myocytes samples were found to be enriched with the Spred-2 protein. Immunohistochemical staining revealed that Spred-2 localises in the intercalated discs of the heart like the other EVH-1 family member VASP does (Eigenthaler et al, 2003).

The alternative splicing of *spred* genes

Evidence for the existence of alternatively splicing products derived from the *spred2* gene.

Spred-2 Western blots of mouse tissues lysates revealed the existence of a 42 kDa Spred-2-related product (Fig. 7, B).

Further analyses of the *spred2*-related clones available in the human EST databases, revealed the presence of heterogenous cDNAs, which seemed to be produced by differential splicing of the *spred2* gene.

Sequencing of the clones #684759 (EST accession number AA251635) and #525593 (EST accession number AA069749) indicates that they were partially identical: the nucleotides from 1 to 86 of clone #684759 were found to be identical to the sequence from nucleotides 164 to 250 of clone #525593 and the sequence downstream of nucleotide 87 of #684759 was identical to sequence from nucleotide 518 of clone #525593. Indeed, the clone #525593 between nucleotides 250 and 518 contained extra sequence of 268 bp in length. The Spred-2 cDNA which was first cloned, did not comprise this "insert".

The human EST clone aa776611 missed the last 578 nucleotides of the 3' end of the Spred-2 coding region. The corresponding protein lacked the C-terminal region of full length Spred-2.

Taken together, sequencing information of those clones indicated that the *spred2* gene generates at least 3 forms of transcripts.

Cloning of 4 splicing variants of human *spred2* gene

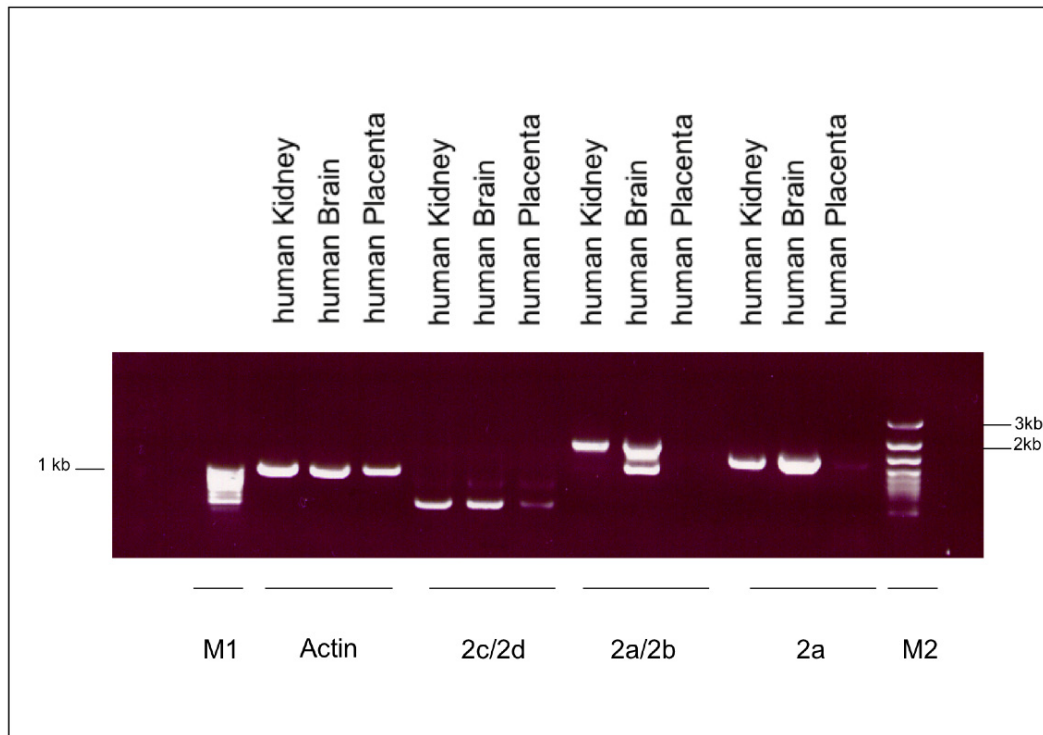


Figure 12: RT-PCR from total RNA extracted from human placenta, human brain, human kidney.

Four reactions were performed on each tissue. The reaction 2a amplified the full-length coding region of Spred-2a (called Spred-2a) with the primer sets: 1 and 4 (Fig. 3), the reaction 2a/2b amplified the full-length coding region of Spred-2b (1100 pb) and -2a (1678 pb) with the primer sets 1 and 5 (Fig. 3), the reaction 2c/2d amplified the full-length coding region of Spred-2c (436 bp) and -2d (775 bp) with the primer sets 1 and 3. The reaction „actin“ was a control reaction to check the integrity of the mRNA.

Cloning of the human splicing variant: Spred-2b

The human EST clone aa776611 encodes a partial sequence missing some of the Spred-2a cDNA. This sequence lacks part of the exon 8: part B so the 3' part of exon 8 (part A) is directly joined to the 5' part of exon 8 (part C) via an unusual splicing site. The exon 8 (part C) encodes part of the cysteine-rich region related to Sprouty (SPR) at the C-terminal. This splicing variant was named Spred-2b.

The coding region of Spred-2b, comprising exons 1, 2, 3, 6, 7, 8, 10, was amplified as a 1100 bp RT-PCR product from human brain total RNA (Fig. 12). The PCR performed from brain RNA with the primers 1 and 5 (Fig. 3) (which anneal in exon 1 and in exon 8, part C respectively), gave 2 products: the Spred-2b cDNA coding region of 1100 bp and a product of 1678 bp corresponding to the Spred-2a cDNA fragment containing part of the untranslated region. The protein product derived from

the transcript Spred-2b is composed of 378 amino acid residues.

Cloning of the human splicing variant: Spred-2c

The clone #525593 (accession number AA069749) comprises an insert sequence composed of 2 exons: exon 4 and 5, which are normally spliced out in Spred-2a cDNA. Another 3' primer (arrow 3 in Fig. 3) located on exon 4 was designed for the cloning of the variant containing exon 4. From the PCR performed with the primer sets 1 and 3, one differentially spliced product of 436 bp containing exons 1, 2, 3, 4 was isolated from whole human brain and human heart and placenta total RNA. This novel alternatively spliced variant, named Spred-2c, was recovered from total RNA isolated from human kidney, brain and placenta (Fig. 12). According to the sequencing of the clone #525593, the cDNA of Spred-2c includes exons 4 and 5 between exons 3 and 6. Due to an in-frame stop codon in exon 4, Spred-2c cDNA encodes a protein of 144 amino acids in length comprising the 124 amino acids of the EVH-1 domain joined to 20 additional amino acids at the C-terminus.

Cloning of the human splicing variant: Spred-2d

An unexpected second product of 775 bp was co-amplified under the conditions used to clone Spred-2c (Fig. 12). This new product, which was named Spred-2d cDNA, contains an additional sequence corresponding to the intronic sequence between exons 3 and 4. This unspliced sequence, located on the gene between exons 3 and 4, assigned as "exon 3a" has to be considered as preliminary because it could be only present in a pre-messenger RNA form of Spred-2c (cf. Discussion).

As the "exon 3a" sequence contains a premature in-frame stop codon, the cDNA encodes a 165 amino-acids protein containing the 124 amino acids of the EVH-1 domain and 41 extra amino acids at the C-terminus.

Cloning of the human splicing variant: Spred-2e

While amplifying Spred-2a cDNA from two mature human placenta RNAs by One-Step RT-PCR (performed with the sets of primers 1 and 4 used for the cloning of Spred-2a) together with the expected 1352 bp band, another slightly smaller band appeared (Fig. 13). The sequencing of this product, termed Spred-2e, revealed that it lacked the exon 3. In the Spred-2e transcript, the exon 2 is directly spliced to exon 6.

Spred-2e messenger RNA is produced by differential splicing based on exon skipping (excluding the exon 3 which normally encodes the last 56 amino acids of the EVH-1 domain). This splicing variant encodes a 148 amino acids product which contains only the first 69 amino acids of the EVH-1 domain followed by 79 amino acids. The last 79 C-terminal amino acids of the Spred-2e polypeptide sequence are encoded by exons 6, 7 and 8 and are derived from a different frame than the one used for the translation of Spred-2a-d. In this frame, the part A of exon 8 contains a premature stop codon. The Spred-2e messenger yields a protein that has only the first 69 amino acids in common with the other Spred-2 proteins.

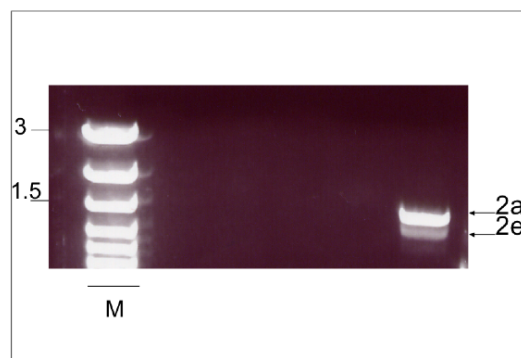


Figure 13: Cloning of the Spred-2e splicing variants by RT-PCR from total RNA extracted from human placenta.

Discovering of the Spred-2e variant by amplification of Spred-2a by RT-PCR from human placenta total RNA with the primers 1 and 4. The large slower migrating band is the 1352 pb band corresponding to the full length coding region of Spred-2a and the small faster migrating band is the variant termed Spred-2e. The size of the marker bands is given in kb.

A summary of the alternative splicing of the *spred2* gene is shown in Fig. 14.

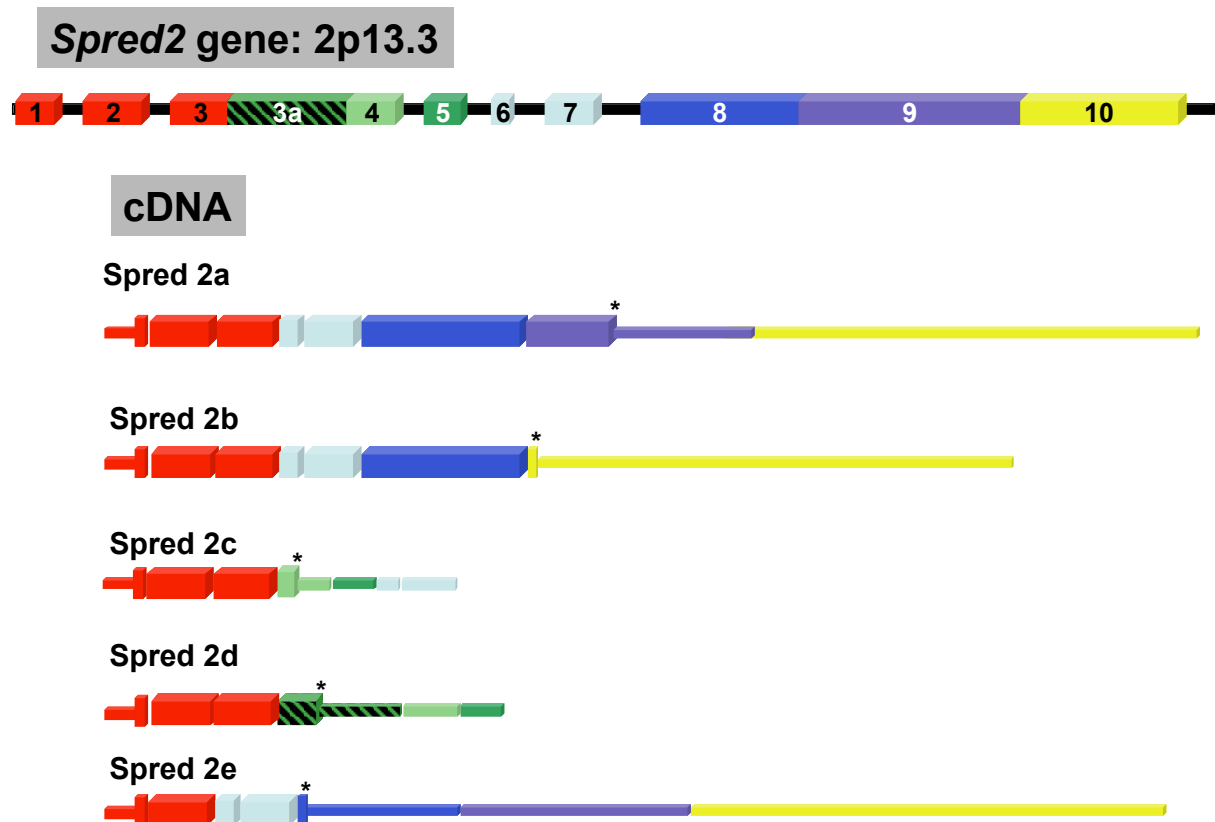


Figure 14: The alternative splicing of the *spred2* gene.

Analyses of the Spred-2-specific transcripts revealed the existence of at least 5 splicing variants of Spred-2. The *spred2* gene is depicted (in the upper scheme) and the 5 cDNAs (with their exons composition) generated by its alternative splicing are shown below.

Confirmation of the existence of the Spred-2 splicing variants by RNase protection assay.

Because of the possible amplification artefacts generated by RT-PCR, the presence of 4 of the Spred-2 transcripts was confirmed with an RNase protection assay, which allows specific and quantitative determination of specific transcripts and which circumvents the problem linked to amplification artefacts.

The probes were overlapping the exon boundaries (see material and methods, Fig. 5), to allow identification of the various splicing products.

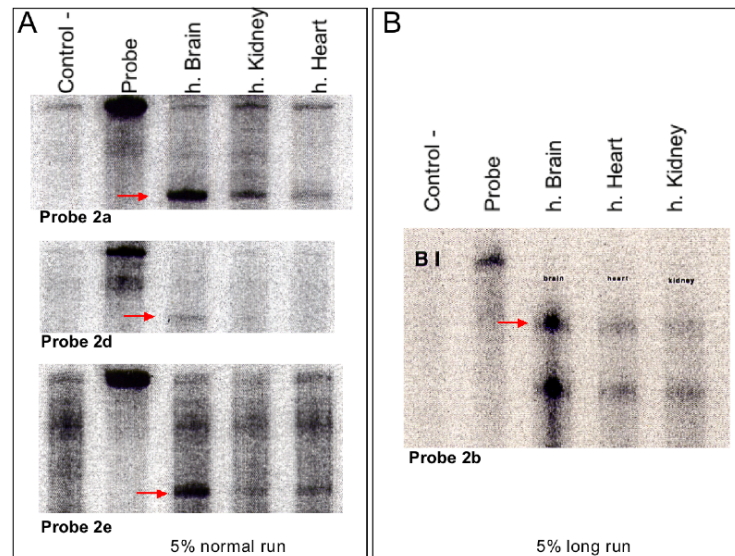


Figure 15: Detection of the Spred-2a, -2b, -2d, 2e messenger RNAs in human brain, human kidney, human heart by RNase protection analysis.

The larger product which hybridised with the 261 bp probe 2a represents the Spred-2a transcript (A, upper panel). The larger product, which hybridized with the 507 bp probe 2b represents the Spred-2b transcript, a stronger signal showing a smaller hybridizing product is given by the Spred-2a transcript (panel B). The larger product, which hybridized with the 304 bp long probe 2d represents the Spred-2d transcript (A, middle panel). The product pointed with a red arrow, which hybridized with the probe 2e represents the Spred-2e transcript (A, lower panel). As negative control, the probe was mixed with total RNA extracted from yeast (panels A and B).

The transcript Spred-2a was strongly expressed in human brain and to a lesser extent in human kidney (Fig. 15). The transcript Spred-2b was found predominantly in human brain. These results are in accordance with the RT-PCR results performed with the same RNA pools. A weak signal corresponding to transcripts Spred-2d was detected in human brain. The transcript Spred-2e was detected in human brain and to a lesser extent in human heart.

The alternative splicing of spread1 primary transcript

A further database search revealed that publicly available EST (T52235, AI026771) and THC sequences (THC539777, THC562043, THC491401) represent two differentially spliced Spred-1 cDNA sequences.

A scheme of the 2 alternatively spliced products derived from the *spread1* gene is shown in Fig. 16.

The Spred-1a transcript

T52235, THC562043, THC491401, and part of THC479791 (reverse orientation)

cover exons 2 to 7 of Spred-1 (Spred-1a). The recently published clone BC018015 (gi 17390018) comprises the exon 1 containing the initiation site. This product encodes a complete EVH-1 domain, followed by a central part related in sequence to the Spred-2 middle piece, and a C-terminal Sprouty homologous region. The Stop codon is present in the exon 7 (Fig. 16). The full-length coding region of Spred-1a was amplified by RT-PCR from human placenta, human brain, human heart and human kidney (data not shown). These results revealed differences in the expression profile of Spred-1 in mouse and human.

The Spred-1b transcript

The EST sequence AI026771 corresponds to the reverse and complement sequence of a different *spred1* splicing product. It varies from the previously described Spred-1a transcript in its 3' sequence, which is characterised by a direct fusion of the 219 most 5' nucleotides of exon 7 to exon 8 and 9.

The transcript organisation in terms of exon composition is very similar to the Spred-2b splicing product, so I termed it, in analogy to the "2b form", Spred-1b.

This transcript is special in that the splice junction found in the transcribed sequence does not follow the usual splicing rules (table 2). This junction leads to an in-frame stop codon close to the 5' end of exon 9, introducing a pre-mature stop, 194 amino-acids after the EVH-1 domain.

The variant Spred-1b, like in case of Spred-2b, lacks part of the C-terminus found in the "a" form. The cysteine-rich region related to sprouty is completely missing in the case of Spred-1b protein, a region which is likely responsible for the membrane association (cf. Discussion).

The alternative splicing of spred3 transcript

Analyses of the 2 EST sequences (D80468, AI028379) and the exons predicted from genomic sequence segment NT_011233 (gi 3702281) by the grail 3.2 program gave information about the putative *spred3* gene products.

Spred3 gene products depicted on Fig. 16 are partial sequences: one corresponding to a short Spred-3 form: "c", which encodes an essentially complete splice variant. It comprises the N-terminal EVH-1 domain followed by 44 additional amino acids and 2 partial ORFs covering these 2 important functional domains of the large "a" form i.e. the EVH-1 and SPR domain. As the Spred-3 transcripts were found to be similarly

organised as the transcripts encoding the long Spred-2a and the small Spred-2c, they were then termed in analogy Spred-3a and -3c, respectively.

According to the little amount of EST sequences available in the databases, the expression level of the product of the *spred3* gene seems to be low and specific to certain tissues.

The exons 1 and 2 of *spred3* like the exons 2 and 3 of the *spred1* and *spred2* genes, encode for the EVH-1 domain.

The exon 7 of the *spred3* gene (like the exon 7 of *spred1* and 8 of *spred2*) encodes a cysteine-rich region similar to the Sprouty C-terminus (SPR).

The intermediate region, normally bridging the two main domains, the N-terminal EVH-1 and the C-terminal SPR in the large Spred proteins within the Spred-3a protein has been recently published (Kato R. et al, 2003).

In line with the alternative splicing of the *spred2* gene, the exon 4, found in the Spred-3c transcript (which contains an in-frame stop codon), can be spliced out resulting in a product in which the exon 3 is directly spliced to exon 5 or 6, and the last exon of the coding region is the exon 7 so the encoded product could exhibit a typical organisation of a “Spred a” form comprising the EVH-1 domain, an intermediate region and the SPR.



Figure 16: Spred transcripts generated by alternative splicing of the genes *spred1* and *spred3*.

Two products are derived by alternative splicing from the human *spred1* gene. The exons 1, 2, 3 colored in red encode for the EVH-1 domain, the exon 4, 5, 6 for the intermediate region

and the exon 7 for the c-Kit binding domain and the SPR. The exon 7 is internally spliced in case of Spred-1b cDNA. The corresponding protein product comprises the c-Kit binding domain but lacks the SPR. Two products are derived by alternative splicing from the human *spred3* gene. The exons 2, 3 colored in red encode for the EVH-1 domain, and the exon 7 for the c-Kit binding domain and the SPR. The black star shows a stop codon.

The domain organisation of the human Spred protein isoforms and variants

Five messenger RNAs derived from the *spred2* gene have been reported here and searching the database revealed at least 2 variants for each of the other *spred* human genes. All corresponding proteins share the N-terminal EVH-1 domain and differ in length and sequence of their C-terminus (table 3)(cf. Discussion, Fig. 28).

The Spred proteins can be classified in 2 groups: the large (“a and b”) and the short forms (“c, d”). The “e” form has been found only in the case of *spred2* gene.

Among the large variants, the “a” form comprises the EVH-1 domain, an intermediate region where the c-Kit binding domain is localised and the C- terminal SPR domain.

The form “b” comprises the EVH-1 domain, the intermediate region with the c-Kit binding domain but lacks the complete SPR (in case of Spred-1b) or part of it (the last 70 amino acids in case of Spred-2b).

Among the short *spred* gene products, the “c and d” forms encompass the EVH-1 domain at the N-terminal and a small C-terminal tail of 20 to 44 amino-acids which does not share homology with any of the large forms.

Interestingly, the C-terminal parts of the variants Spred-2c and Spred-2d, although encoded by intron 3-4 (also called exon “3a”) and by exon 4 of the *spred2* gene respectively, share sequence homology (data not shown).

Spred-2e protein variant is unconventional: it comprises a truncated EVH-1 domain, which may not fold properly and be functional (cf. Discussion).

The molecular characteristics of the human *Spred* proteins

The characteristics of each of the human *Spred* proteins are summarised in table 3.

Name of the Splicing variant	Exons *: Stop codon	Predicted molecular Mass (kDa)	Length (Amino Acids)	N-terminal EVH-1 Spred1:125aa Spred2:124aa Spred3:116aa	C-terminal SPR 111aa	C-Kit/ C-Fms binding domain (CKB) Spred1:52aa Spred2:56aa
1a	1+2+3+4+5 +6+7*	ca 51	444	+ M1-Q125	+ R234-G444	+
1b	1+2+3+4+5+ 6+7'+8*+9	ca. 33	300	+ M1-Q125	-	+
2a	1+2+3+6+7 +8 (A+B+C)*	47.9	418	+ M1-E124	+ R308 –A418	+
2b	1+2+3+6+7 +8' (A+C)*	39.8	348	+ M1-E124	R308-C348 (41 aa only)	+
2c	1+2+3+4*+ 5+6+7	16.3	144	+ M1-E124	-	-
2d	1+2+3a*+4 +5.....	18.6	165	+ M1-E124	-	-
2e	1+2+6+7+8*	16.6	148	M1-V69 (69 aa only)	-	-
3a	1+2+3+4*	29.7	270	+ M1-R112	+ R294-R408	
3c	1+2+3+.....+7*	18.5	161	+ M1-R116	-	-

Table 3: Summary of the mRNA exon composition, the length, the calculated molecular weight and the domains of the proteins encoded by the 3 human *spred* genes.

The exons 1, 2 and 3 of the *spred1* and -2 genes and the exon 1 and 2 of the *spred3* gene encode the EVH-1 domain. The exon 4 and “exon 3a” of *spred2* encode the C-terminal tail of the short *Spred* forms (“c/d”). The exon 4 of *spred1* is not yet identified. The exons 6 and 7 of *spred* genes encode the intermediate region in case of *Spred*-2a and -2b whereas in case of *spred1*, exon 5 encodes as well part of the intermediate region. The exon 7 of *spred1*/ -3 and exon 8 of *spred2* encode the part of the intermediate region comprising the c-Kit binding domain and the cysteine-rich region related to Sprouty (SPR) and constitute the 3' untranslated region. This last exon can be alternatively spliced in case of *spred1* and *spred2* generating transcripts which encode truncated forms lacking the SPR: “b” variants.

In vitro transcription/ translation of the *Spred*-2 splicing variant

The five splicing variants and a truncated variant missing the SPR domain were cloned in a pCMV vector. Each variant was N-terminally tagged with a VSV-G

polypeptide, which allows detection due to its immunoreactivity.

The constructs were used as template for *in vitro* translation/ transcription as the vector contains a T3 promoter sequence upstream of the cloned sequence. The generated proteins were visualised by immunodetection using an antibody directed against the VSV polypeptide (Fig. 17).

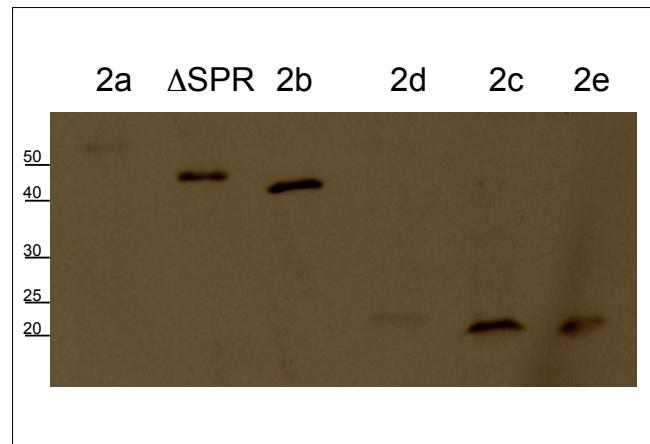


Figure 17: Western blot of the rabbit reticulocytes lysates after *in vitro* translation/transcription of the VSV tagged Spred-2 splicing variants.

The VSV-Spred-2a has an expected molecular weight of 49.5 kDa, VSV-Spred-2b of 41.5 kDa, VSV-Spred-2d of 20 kDa, VSV-Spred-2c of 17.8 kDa, VSV-Spred-2e of 18 kDa. The encoded protein migrated slightly slower as the calculated size, indicating that the human Spred-2 proteins may be subjected in this system to significant post-transcriptional modifications which affect slightly their molecular weight.

According to this experiment, the apparent molecular weight upon electrophoresis of the products were used as a reference for the detection of the Spred-2 variant in tissue lysates. Subsequently, the constructs were used for transfection of eukaryotic cells.

The anti-EVH-1 and anti-C.TER antibodies

After immunisation, antibodies raised against the GST-Spred-2a (96-415) fragment fusion protein were affinity-purified with the immobilised antigen (“Anti-Spred2” antibody used for the determination of the mouse expression profile) or with different parts of the antigen. A series of three affinity columns was set up; the first column contained covalently coupled GST protein, the middle column covalently coupled GST-Spred-2 EVH-1 domain (1-124), and the last column contained coupled GST-Spred-2a (96-415) antigen.

Thus, antibodies directed against different parts of the original antigen could be affinity-purified and preadsorbed, respectively. The two polyclonal antibody pools

were named: anti-EVH-1 (Spred-2) and anti-C.TER (Spred-2) and are schematically depicted in Fig. 18.

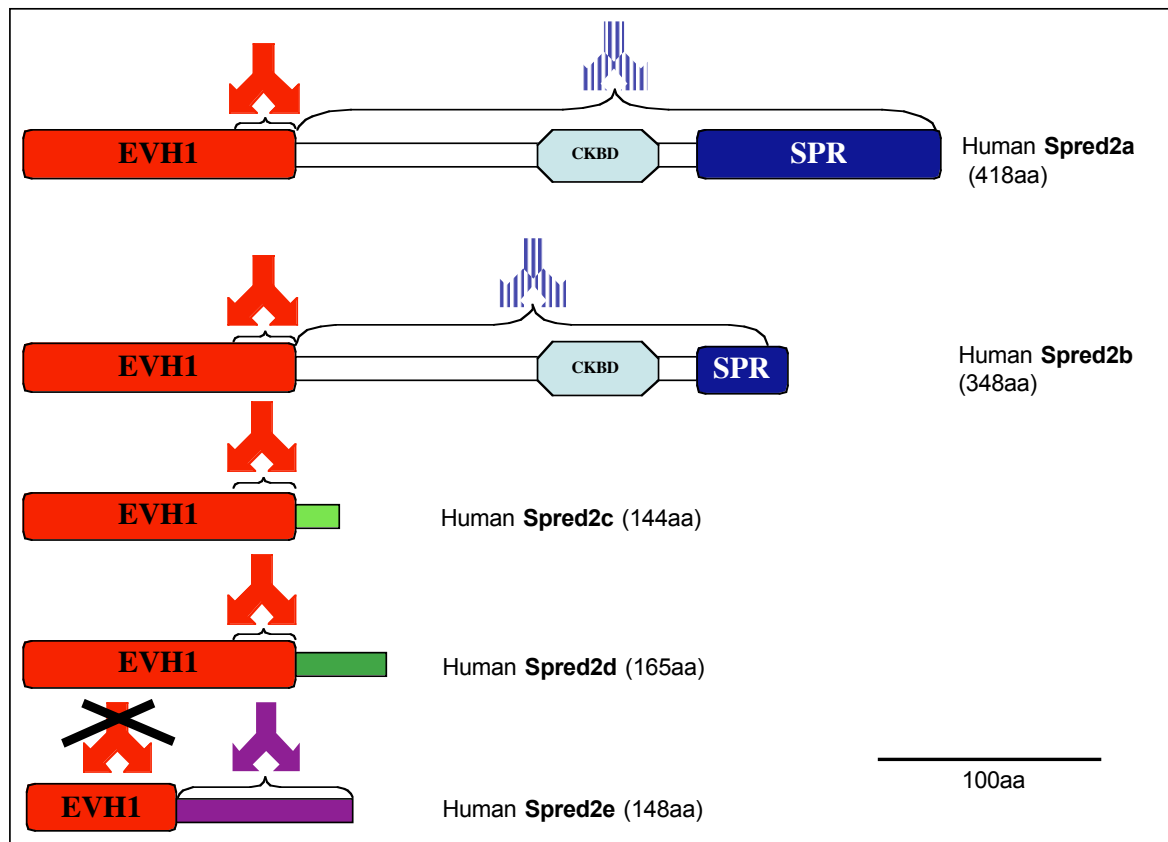


Figure 18: Scheme of the three Spred-2 specific antibodies raised for the detection of the Spred-2 splicing variants.

The antibody shown in red recognised specifically the EVH-1 domain of Spred-2, the blue/white antibody is specific for the C-terminal domain and the detection of Spred-2a/-2b. The purple antibody has been raised to detect specifically the Spred-2e variant. The anti-EVH-1 antibody should be able to recognise epitopes located within the EVH-1 domain between amino-acid residues 96 and 124 of Spred-2a, Spred-2b, Spred-2c, Spred-2d and the anti-C.TER antibody should recognise epitopes located between amino-acid residues 124 and 415 of Spred-2a and between amino-acid residues 124 and 339 of Spred-2b.

Characterisation of the antibodies

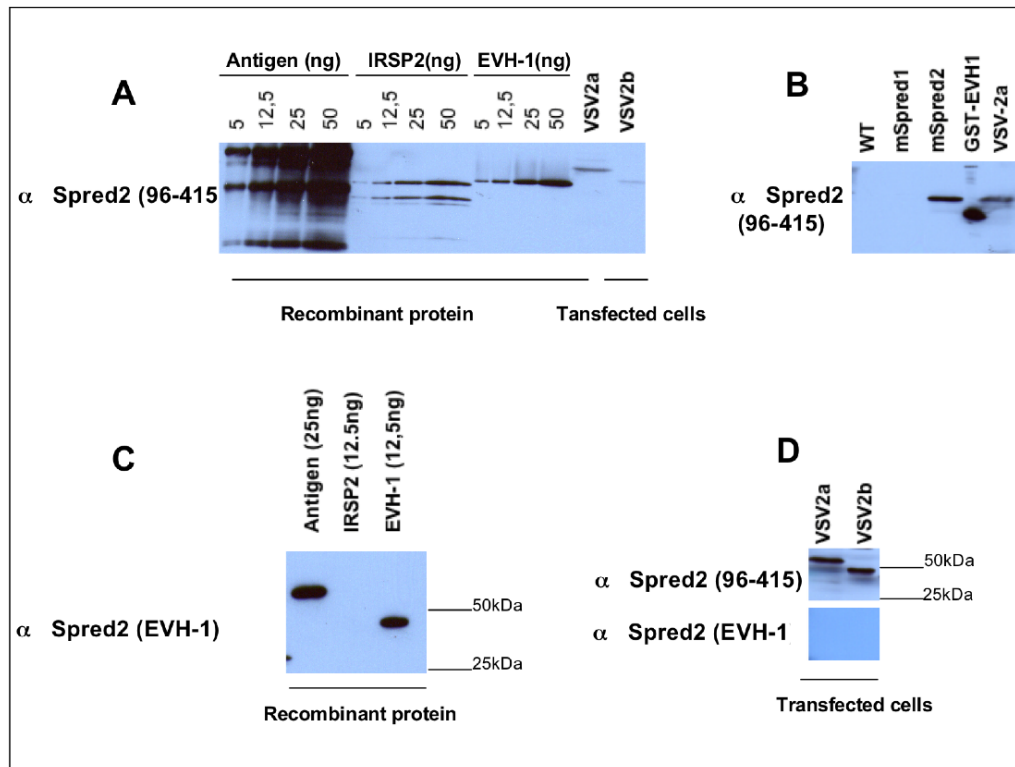


Figure 19: Characterisation of Spred-2 antibodies.

(A): Western blot analysis using the affinity-purified anti-Spred-2 (96-415) and Spred-2 recombinant protein or overexpressed protein in transfected cells. 5, 12.5, 25 and 50 ng of the antigen (GST-Spred-2 (96-415), of the intermediate region of Spred-2 (GST-Spred-2(124-233), and of the N- terminal domain of Spred-2 (GST-EVH-1(1-124) were loaded on a 10 % gel. Extracts from transfected cells overexpressing human VSV-Spred-2a and VSV-Spred-2b were applied. Recognition of various Spred-2 regions was obtained for 5 ng protein of recombinant protein and in cells transfected with the VSV-Spred-2a and -2b.

(B): Western blot analysis using the affinity purified anti-Spred-2 (96-415) antibody and lysate of cells transfected with murine Spred-1 and Spred-2, human VSV-Spred-2a. (The mouse Spred-1 and -2 constructs have been cloned by Dr. Karin Bundschu). The Spred-2 antibodies did not recognise the overexpressed mouse Spred-1 protein whereas it recognised the murine Spred-2 as well as the human Spred-2 (VSV-2a). As negative control, lysate of wild type recipient cells (WT), in this case the PtK2 cells were applied. As positive control, 10 ng of recombinant purified GST-EVH-1 protein expressed in *E. coli* were used.

(C): Western blot analysis using the affinity-purified anti-Spred-2 (EVH-1) antibody and Spred-2 recombinant protein and overexpressed protein in transfected cells. 25 ng of the antigen (GST-Spred-2(96-415), 12.5 ng of the intermediate region of Spred-2 (GST-Spred-2(124-233), and 12.5 ng of N-terminal domain of Spred-2 (GST-EVH-1(1-124) were applied on a 10 % gel. The EVH-1 antibody recognised the antigen and the EVH-1 domain of Spred-2 but not its intermediate region.

(D): Western blot analysis using the affinity-purified anti-Spred-2 (96-415) or anti-Spred2 (EVH-1) antibodies and lysates of cells transfected with human VSV-Spred-2a, -2b. The EVH-1 antibody could not detect under these conditions the overexpressed VSV-2a and VSV-2b.

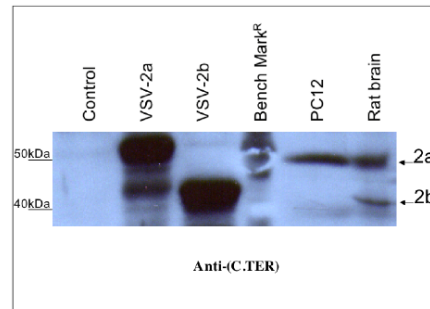


Figure 20: Western blotting analysis with the anti-C.TER antibody and tissue or cell lysates (30 μ g/lane).

Transfected cells (PtK2) expressing the VSV-Spred-2a and -2b, or untransfected cells were used as control. Spred-2a was identified in the rat pheochromocytoma cell line (PC12) and rat brain homogenate whereas the Spred-2b form was only detected in rat brain.

The affinity-purified anti-Spred-2 (96-415) antibody recognised the antigen and the recombinant proteins corresponding to the Spred-2 N-terminus or the intermediate region of Spred-2 (Fig. 19, panel A). It recognised the human VSV-Spred-2a and -2b form as well as the murine Spred-2 expressed in PtK2 cells but did not show any cross-reactivity with the murine Spred-1. Therefore, the antibody fraction was used for determination of the Spred-2 expression pattern in mice.

The affinity-purified anti-Spred2 (EVH-1) antibody recognised the antigen and the recombinant EVH-1 domain very well but was unable to detect the VSV-Spred-2a and -2b variants expressed in PtK2 cells. This antibody was not further used for the detection of the Spred-2 variants in tissue lysates. The affinity-purified anti-C.TER antibody recognised the VSV-Spred-2a and -2b form in transfected PtK2 cells. This antibody was used for the detection of the Spred-2a and -2b forms in rat pheochromocytoma cells and in rat brain lysate (Fig. 20). The affinity-purified antibody anti-Spred-2e was tested with recombinant protein (electroeluted fragment) and the *in vitro* transcribed and translated protein or the overexpressed VSV-Spred-2e in eukaryotic cells (data not shown). It was able to recognise the recombinant protein but not the *in vitro* translated product. This antibody could not be further used to test the expression of Spred-2e in tissue lysates.

Subcellular localisation of Spred-2 protein variants

Immunofluorescence staining of transfected cells with five different VSV-tagged Spred-2 variants and with a truncated derivative missing the SPR domain was performed in order to determine the subcellular localisation of each *spred2* variant

and the role of the SPR in directing Spred-2 to distinct subcellular localisation. To investigate the subcellular distribution of individual splice variants in more detail, VSV-tagged versions of the Spred isoforms have been expressed in the rat kangaroo kidney epithelial cell line: PtK2.

Subcellular localisation of Spred-2a

VSV-tagged Spred-2a transfected into PtK2 cells localised at the membrane and all over the cytoplasm with a homogenous staining. However, some cytoplasmic brightly stained vesicles were found organised like beads on a string (as if they were associated with filament like structures) concentrated around the nucleus while the nucleus itself did not show staining for VSV-Spred-2a (Fig. 21).

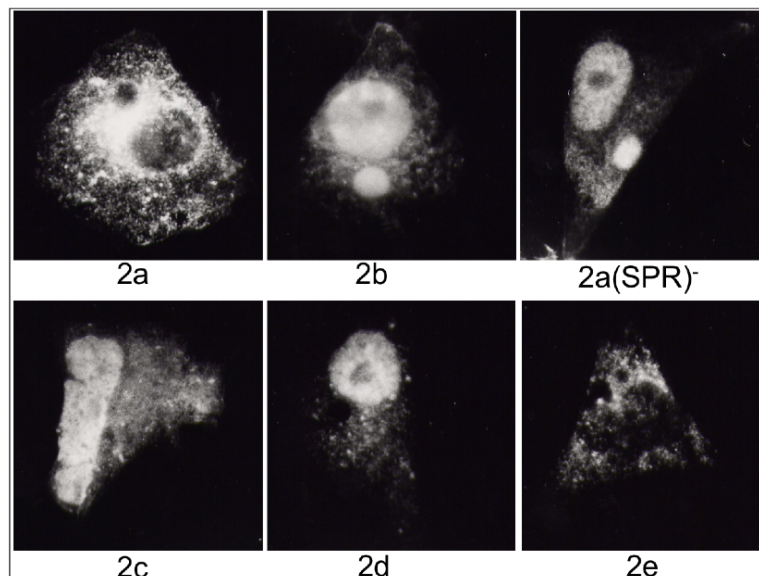


Figure 21: Immunofluorescence pictures of the transiently transfected PtK2 with the VSV-tagged Spred-2 constructs.

The cells expressed VSV-tagged Spred-2a, VSV-tagged Spred-2a lacking the SPR domain: 2a(SPR)⁻ with VSV-tagged Spred-2b, with VSV-tagged Spred-2c, with VSV-tagged Spred-2d, with VSV-tagged Spred-2e. 48 hours after transfection, the cells were fixed and stained with the monoclonal anti-VSV antibody and the CyTM3-conjugated anti-mouse Ig.

This typical localisation pattern of Spred-2a to vesicular structures predominantly found in perinuclear regions of the Golgi region and at the membrane, raised the question whether Spred-2a localises to membrane invaginations called caveolae. Therefore, I performed costaining of Spred-2a and caveolin-1, a cholesterol-binding protein in lipid rafts and a principal component of cell membrane invaginations forming the caveolae (Galbiati et al, 2001). No costaining of Spred-2 and Caveolin was observed.

Stainings of endogenous Spred-2 in HEK 293 cells with the anti-Spred-2 antibody showed a similar dotted pattern, suggesting labeling of vesicle-like structures and localisation of endogenous human Spred-2a to these vesicles.

In order to further define the vesicle-like staining pattern, costaining experiments of endogenous Spred-2a with ER- (anti-SERCA), Golgi- (anti-58K) specific markers, and with eNOS (a caveolin-interacting protein) were performed using HEK 293 cells, which express Spred-2a. Because Spred-2 did not colocalise with any of the above listed organelles, we asked whether the staining pattern may be linked to vesicles involved in endocytosis or secretion, which are characterised by the presence of certain Rab GTPases. Rab GTPases regulate vesicle transport processes of the endocytotic and exocytotic pathways (Novick et Zerial, 1997; Sönnichsen et al, 2000).

To test our hypothesis whether Spred-2a protein colocalise with specific Rab GTPases, we costained endogenous Spred-2 protein and the green fluorescent protein (GFP)-tagged Rab5 and Rab11 GTPases in HEK cells. These experiments revealed that Spred-2 specifically colocalised with the Rab11 GTPase. The proteins had a congruent localisation pattern characterised by an accumulation in perinuclear regions and a punctate cytoplasmic distribution (Engelhardt et al, 2004).

Rab11 localises to the trans-Golgi network (TGN), post-Golgi vesicles and the recycling endosomes (Sönnichsen et al, 2000) (Ullrich et al, 1996) (Urbé et al, 1993). In contrast, Rab5a GTPase, mostly in the perinuclear region (overlapping with the *trans*-Golgi marker), was found to be colocalised with Spred-2 to a much lesser extent than Rab11 (Engelhardt et al, 2004).

Subcellular localisation of Spred-2b

Spred-2b showed a dual cellular localisation pattern present in the cytoplasm and in the nucleus. VSV-Spred-2b localised predominantly to uniformly shaped vesicles distributed all over the cell (including the nucleus except the nucleoli). The cytoplasmic small vesicles were different from the structures observed in the Spred-2a-transfected cells with respect to shape, size, and localisation.

Subcellular localisation of Spred-2c

The overexpressed protein VSV-Spred-2c displayed an intranuclear localisation. It was diffusely distributed in the nucleoplasm but highly concentrated in defined

subnuclear structures termed “speckles” (on average 4 to 5 per cell irregularly shaped structures per nucleus). In order to characterise these speckles, preliminary co-staining experiments with the SC-35 speckles marker (specific for a subnuclear compartment enriched in small ribonucleoprotein particles and various splicing factors) were performed. Spred-2c did not colocalise with SC-35 containing speckles (data not shown). In addition, a weak fine homogenous cytoplasmic staining with some very weakly stained filament like structures could be noticed.

Subcellular localisation of Spred-2d

The cells overexpressing Spred-2d showed strongly staining nuclear aggregates or dots whose shape was inhomogenous.

Subcellular localisation of Spred-2e

After transfection, only very few cells expressed VSV-Spred-2e. The limited number of expressing cells was consistent with the low expression level observed on the Western blots (data not shown). Many cells presenting inhomogeneous DNA/nuclear staining with Hoescht 256 dye (which may be apoptotic) were present in the transfected cell monolayers. Therefore, it was conceivable that this product is toxic for the cells.

In cells showing clear expression of Spred-2e, the membrane was not stained, the signal in the cytoplasm was very faint (slightly above background) at the periphery. Spred-2e was distributed all over the cell including the nucleus and it was concentrated especially in cytosolic structures possibly representing protein aggregates. These structures were irregular bright dots distributed all over the cytoplasm.

The Sprouty homology region is required for membrane localisation

Because of the dramatic difference in the subcellular localisation of Spred-2a and -2b, the role of the C-terminal domain of Spred-2a in terms of subcellular localisation was investigated. Therefore, a VSV construct with a truncated form of Spred-2a which lacks the SPR was transfected in PtK2 and an indirect staining of Spred-2a was performed.

As seen in Fig. 22, the SPR-lacking variant localised essentially to the nucleus, and lost its typical membrane and vesicular localisation.

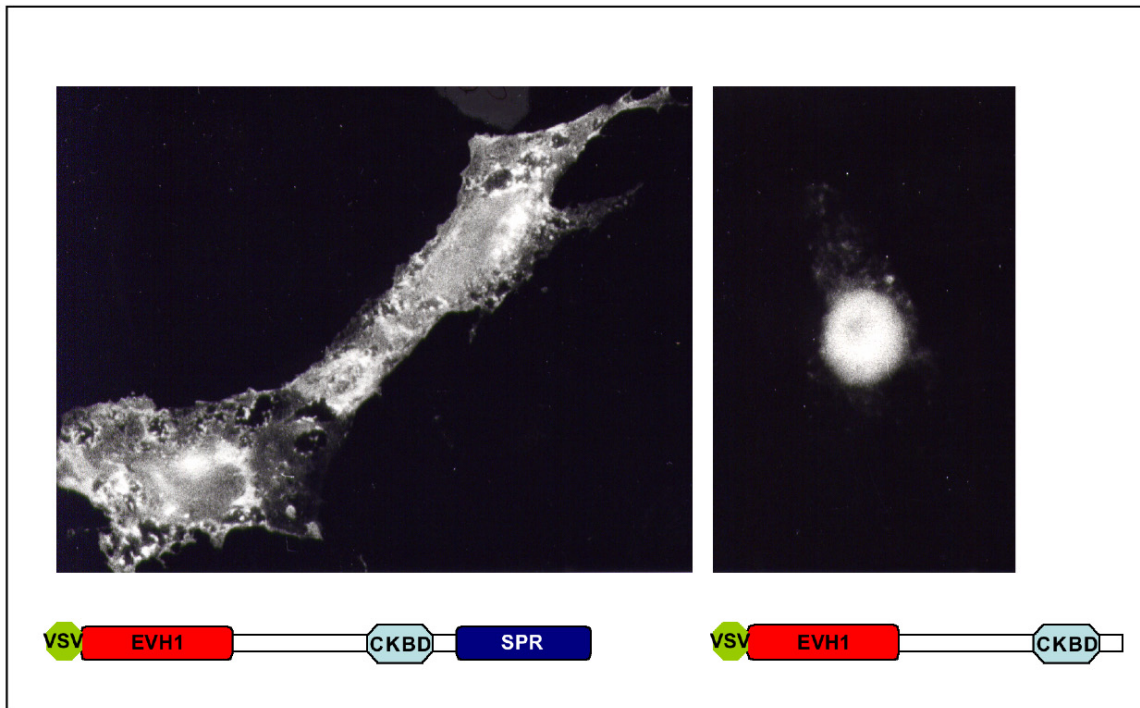


Figure 22: The truncation of the SPR leads to the localisation of the protein to the nucleus. The SPR seems to be responsible for membrane localisation of Spred-2a. PtK2 cells were either transfected with VSV-Spred-2a (left) or with the SPR-lacking variant VSV-Spred-2a(SPR⁻) and immunostained with the primary anti-VSV antibody and a fluorescently labelled CyTM3 anti-mouse Ig.

Effect of Spred-2 splicing variants on ERK activity

As reported by Wakioka et al (2001), Spred proteins act as inhibitors of the ERK signaling by controlling the activation of Raf-1 and by binding constitutively to Ras.

They performed all their experiments with the Spred-1a and -2a isoforms and could show in their system the inhibition of the ERK pathway upon growth factor stimulation. Very little information is known about the functional domain involved in the inhibition of MAPK signaling. Recently, Sasaki et al (2003) reported the interaction of the SPR with Raf-1. An open question remained whether all the Spred-2 isoforms are able to inhibit the MAP-kinase signaling upon growth factor stimulation. Upon starvation and 13 min serum stimulation, ERK was significantly activated. In cells transfected with Spred-2a and -2b the activation was significantly lower (Fig. 23).

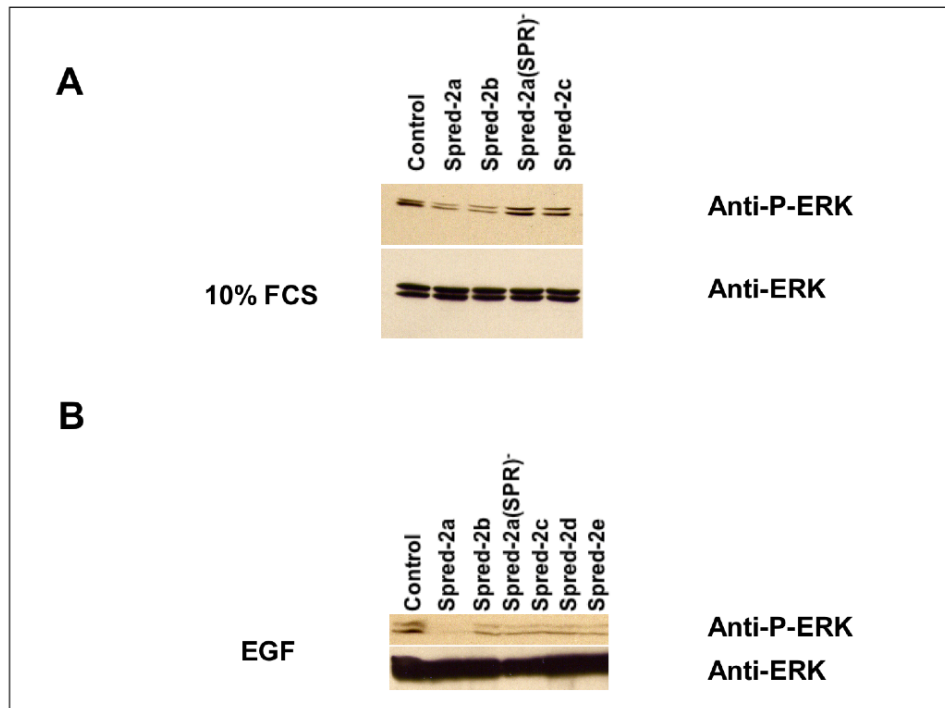


Figure 23: Effect of the Spred-2 variants on serum- und EGF- mediated ERK activation. HEK 293 cells were transiently transfected with the various VSV constructs, starved for 24 h and stimulated with serum (FCS, 10%) for 13 min (panel A) or treated with EGF (25 ng/ml) for 2 min (panel B). Phosphorylation of ERK in its activating loop was monitored with the anti-Phospho-ERK antibody and regarded as parameter for ERK activation. The phosphorylation status was compared to the total amount of ERK in the sample detected with the anti-ERK antibody.

A construct lacking the complete SPR or the variant Spred-2c lacking the intermediate region and the SPR did not inhibit the serum-mediated ERK activation whereas the constructs Spred-2a and -2b showed significant inhibition. A similar experiment was performed with a more specific stimulation using EGF. After 24 h starvation and subsequent EGF treatment the following results were found: the variants missing part of the SPR (Spred-2b) or the full SPR (Spred-2a(SPR)⁻, Spred-2c, Spred-2d, Spred-2e), could not inhibit the EGF mediated MAP-kinase activation in the same extent as the Spred-2a form did (Fig. 23). Only the full-length Spred-2a has an inhibitory function on the MAPK pathway.

Binding partners of the Spred-2 EVH-1 domain

Isolation of ligands for the Spred-2 EVH-1 by affinity chromatography

In order to isolate ligands of the Spred-2 EVH-1 domain, the Spred-2 EVH-1 domain was expressed as a recombinant protein (fused to GST) (Fig. 24, panel A). The

purified fusion protein was covalently coupled to NHS-activated sepharose beads in order to perform a preparative affinity chromatography with bound GST-EVH-1 domain. Because tonsils express high levels of Spred-2, this tissue was chosen as the ligand source. The lysate prepared from fresh porcine tonsils was passed through the column. After extensive washing, elution with an urea based buffer yielded a major double band of 53/55kDa (Fig. 24, panel C) which was subjected to mass spectrometry (MALDI-MS-PSD). Analyses of the digested fragments led to the identification of porcine vimentin and desmin.

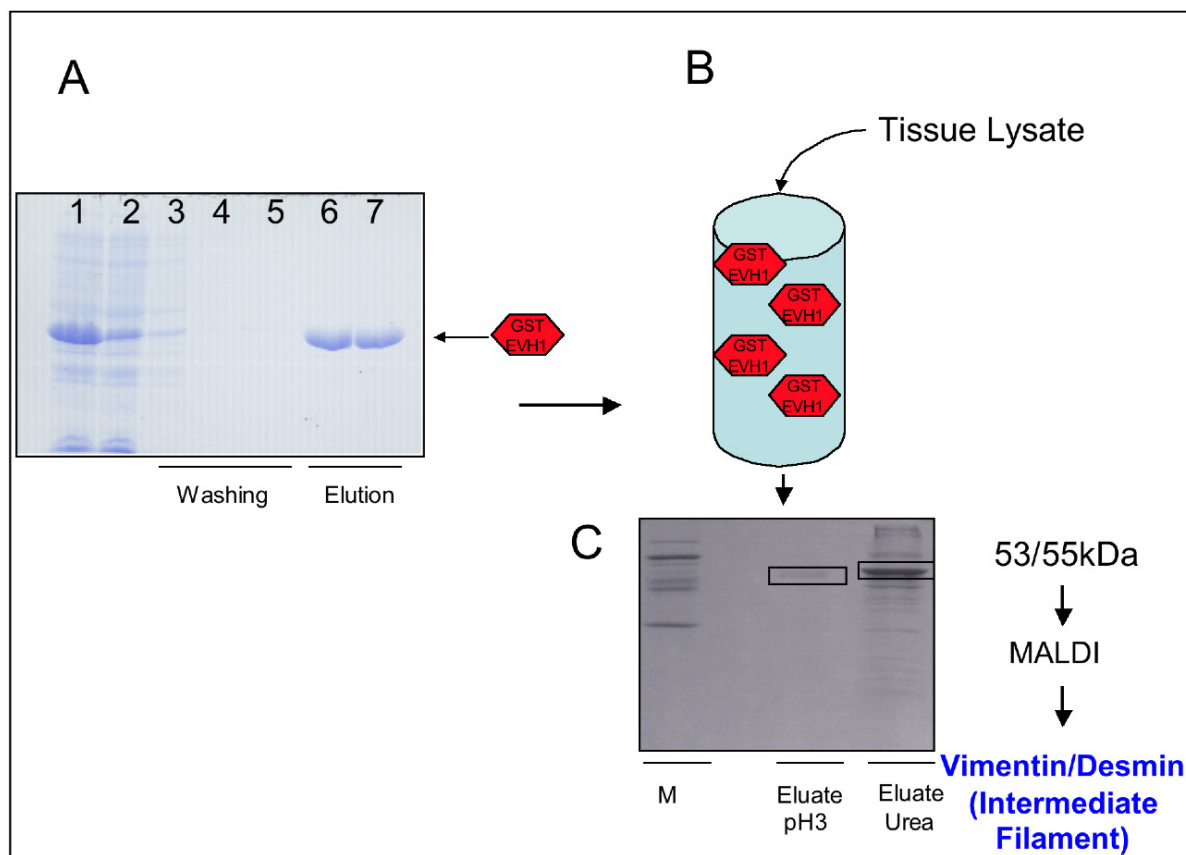


Figure 24: Isolation of ligands of the Spred-2 EVH-1 domain.

(A): Expression of the Spred-2 EVH-1 domain in *E. coli* as a GST fusion protein

Lane 1: Bacterial lysate after 3 h of expression, lane 2: depleted lysate after incubation with GSH beads, lanes 3 to 5: washing of the beads, lanes 6-7: elution of the fusion protein from the GSH beads with 10 mM GSH yielding the purified GST-EVH-1 used for covalent coupling to the activated matrix.

(B): The tissue homogenate was run through a column containing the immobilised GST-EVH-1 domain and after thorough washing, the proteins bound to the GST-EVH-1 column were eluted with 2 types of buffer. Lane 1: Marker. Lane 2: eluate of the GST-EVH-1 column with a glycine based buffer, pH 3.0, Lane 3: eluate of the GST-EVH1 column with an urea based buffer.

Vimentin is a type III intermediate filament protein expressed predominantly in cells of

mesenchymal origin (Kreis and Vale, 1999). In order to verify the hypothesis that vimentin could interact with Spred-2 EVH-1 domain, I performed sedimentation experiments with the polymerised protein after incubation with the EVH-1 domain (Fig. 25) and pull down experiments with monomeric vimentin and EVH-1 beads (data not shown).

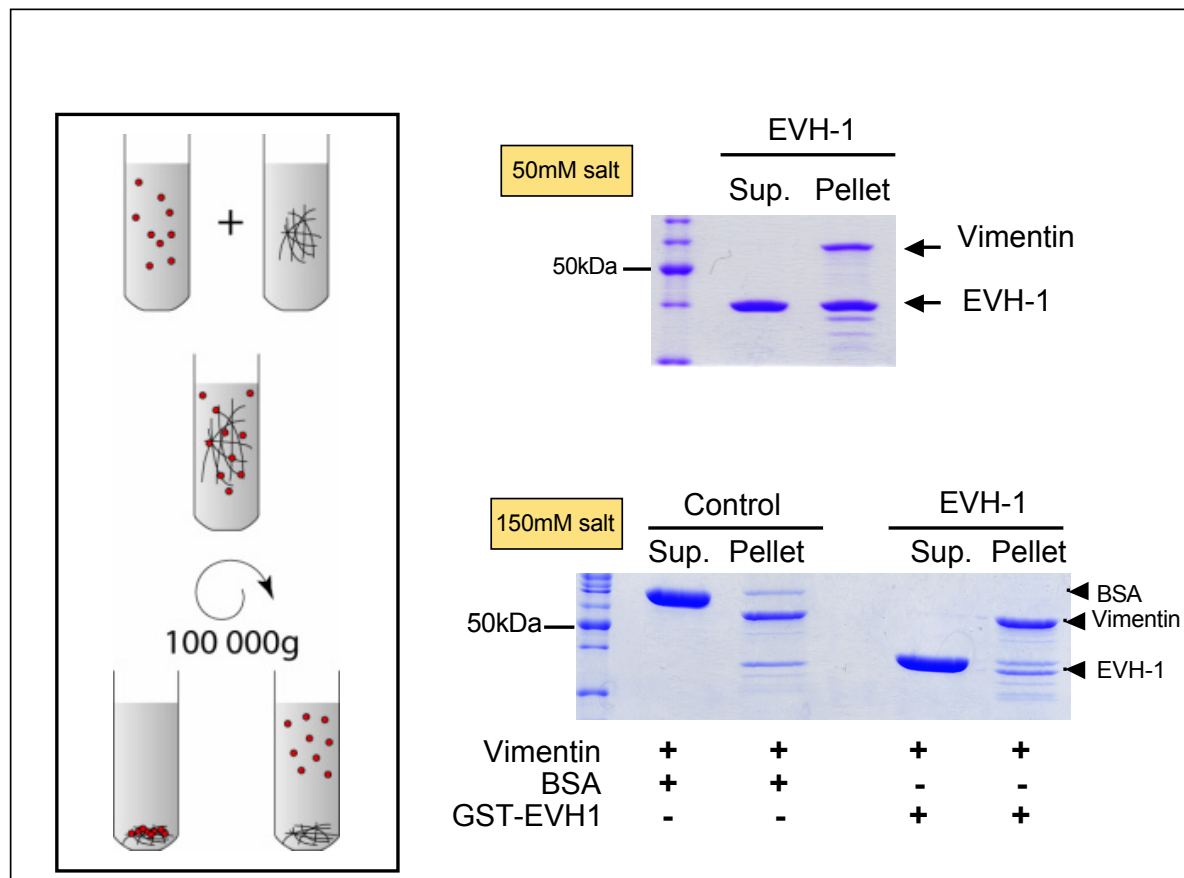


Figure 25: Sedimentation experiments to test *in vitro* the interaction of Spred-2 EVH-1 and the vimentin intermediate filaments.

Polymers of recombinant vimentin were incubated with the purified EVH-1 domain in a low ionic strength buffer (50 mM NaCl) or in 150 mM NaCl. The samples were subjected to ultracentrifugation at 100.000 g. After centrifugation the protein contents of the pellet and the supernatant were analysed on a 14% SDS-PAGE.

The EVH-1 domain could be recovered partially in the pellet together with the vimentin filament when the assay was performed under low salt concentration. However, in a standard salt concentration (150 mM), the EVH-1 domain did not cosediment with the intermediate filament, but remained in the supernatant.

Putative Spred EVH-1 binding partners with proline-rich sequences

Replacement of the EVH-1 of Spred-1 with that of the WASP protein abolished the

inhibitory activity of Spred-1 in terms of ERK inhibition, suggesting that the EVH-1 domain of Spred-1 may interact with a specific target required for suppression of the MAP-kinase pathway (Wakioka et al, 2001).

Among the targets required for the inhibition of MAP-kinase activity are the components of the Ras-Raf signaling pathways. Indeed, Spred-2 has been shown, by co-immunoprecipitation, to interact constitutively with membrane-anchored farnesylated Ras protein. This interaction could be mediated by the Spred EVH-1 domain and a PRS present in the H-Ras protein. At the C-terminal hypervariable region of the H-Ras protein, just in front of the farnesylation site, a highly conserved (between mouse and human) proline-rich sequence which is composed of three prolines residues (2+1) flanking two acidic residues (in bold): PPDESGP might be the motif interacting with Spred EVH-1 domain. Peptide scan-based binding experiments between Spred-2 EVH-1 domain and H-Ras C-terminal proline rich sequence have been performed (Fig. 26). Spot intensities reflect the EVH-1 binding affinity of each peptide and should reveal a direct interaction of the Spred-2 EVH-1 domain and the C-terminal hypervariable region of H-Ras.

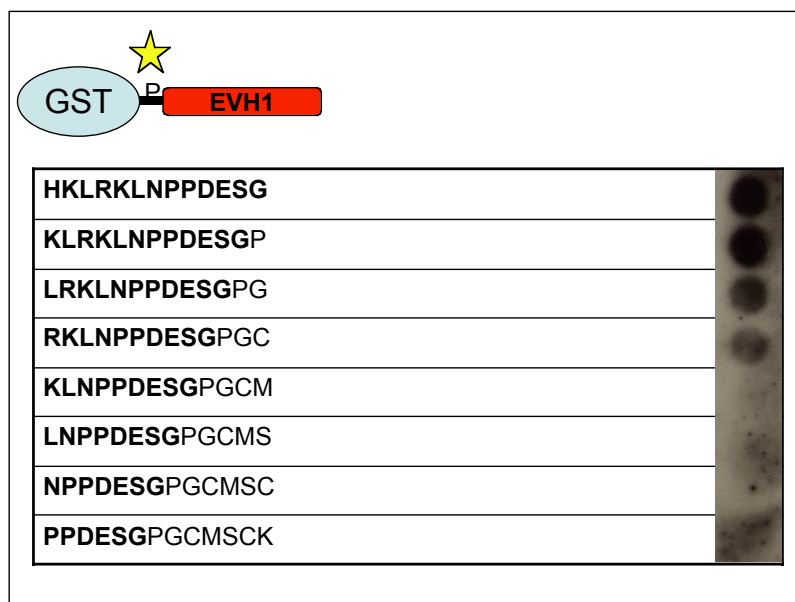


Figure 26: Overlay with ^{32}P radiolabelled GST-EVH-1 domain of spotted peptides derived for the H-Ras C-terminal hypervariable region.

The peptide “HKLRKLNPPDESG” from H-Ras (residues 166-178) displays a strong affinity for the Spred-2 EVH-1 domain. Any removal of the N-terminal residues leads to loss of binding capacity.

In order to further characterise the binding sequence, single residue substitution analyses of the Spred-2 EVH-1 binding PRS peptide: “HKLRKLNPPDESG” from H-Ras (H-Ras residues 166-178) were performed. Peptide residues were substituted one by one for all natural amino acid alternatives and assayed for binding to the Spred-2 EVH-1 domain (Fig. 27, panel A). The wild type peptide in the left column was spotted as a control.

The substitution of the three positively charged residues of the PRS of H-Ras (K2, R4, K5) led to dramatic decrease of signal intensity showing a lost of binding capacity. Furthermore, the substitution of the two negatively charged residues of the PRS of H-Ras (D10, E11) by any of the naturally occurring residues leads to a dramatic increase of signal intensity.

As well, the introduction of positively charged residues at any position led to a gain in binding affinity of the corresponding peptides for the EVH-1 domain.

These data highly suggested a lack of specificity of the assay. A large part of the observed signals seemed to be given by unspecific electrostatic interactions occurring between the ³²P GST-EVH-1 domain and the positively charged residues present in the PRS sequence of H-Ras. Because of the clear problem of lack of specificity, only very little conclusions could be drawn from these assays.

In order to circumvent the incorporation of negatively charged phosphate groups (which may play a role in these unspecific interactions) in the probe used in the overlay, a non-phosphorylated GST-EVH-1 probe was used. This alternative method allowed a slight gain of specificity of the assay (Fig. 27, panel B) but a substantial background remained and made the interpretation of the results difficult.

The two proline residues seemed to be important for the interaction between the H-Ras peptide and the EVH-1 domain. The substitution of the N7 neighbouring the proline duet with an aspartate led to a gain of binding capacity of the corresponding peptide to the Spred-2 EVH-1 domain. The substitution of the L6 residue to a proline or to a tryptophane led to an increase in binding affinity.

The three positively charged residues (K2, R4, K5) enclosed in the PRS sequence of H-Ras appeared to be essential for the binding in this assay.

With help of these preliminary substitution analyses, binding conditions have to be further optimised in order to gain specificity and obtain reliable results.

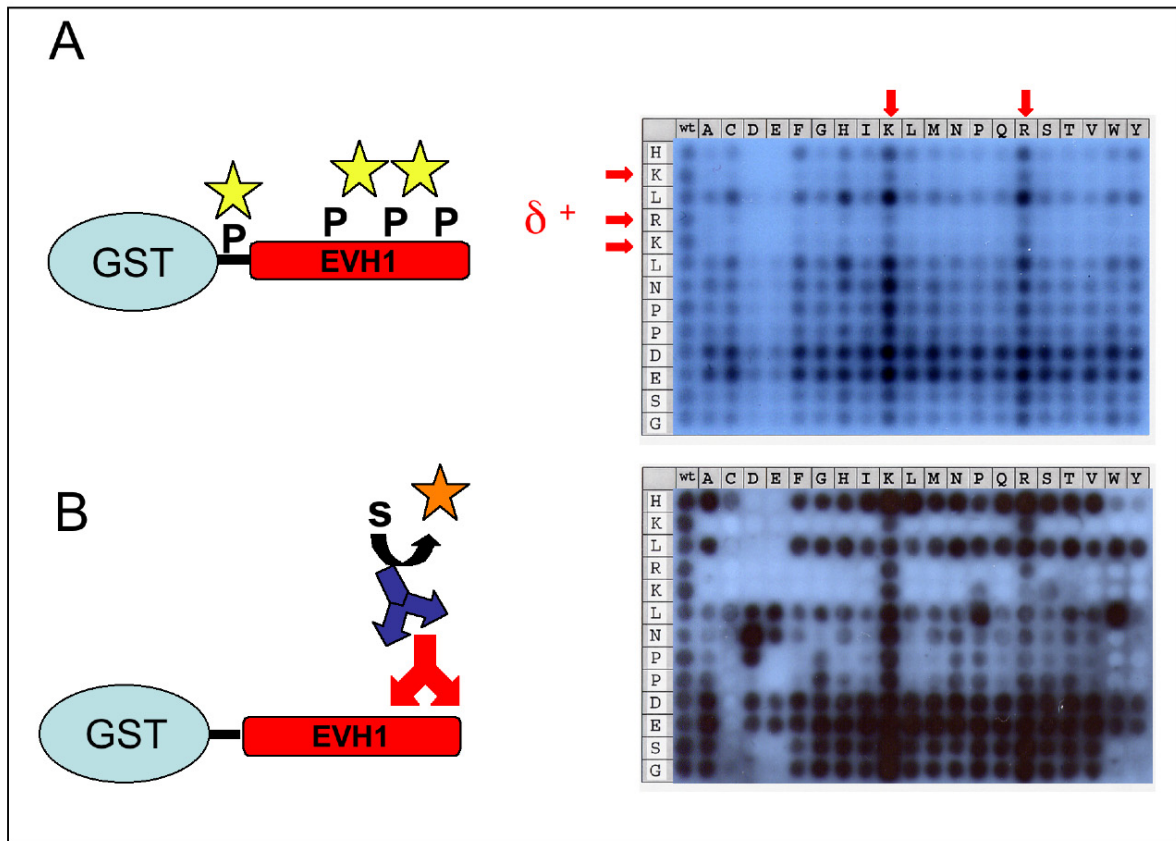


Figure 27: Single residue substitution analysis of H-Ras peptide.

(A): The overlay was performed with a ^{32}P radiolabelled GST-EVH-1. The red arrows show the influence of positively charged residues.

(B): The overlay was performed with an unlabelled non-phosphorylated GST-EVH-1. After stripping the same membrane (as in A), it was incubated with the native GST-EVH-1. The detection was then performed with the affinity purified anti-EVH-1 antibody (described above) and a secondary anti-rabbit HRP conjugated antibody.

Discussion

Differential expression of Spred-1 and -2 in mice

In the present study, differential expression, localisation, and developmental regulation of Spred-1 and Spred-2 proteins in a variety of murine and human tissues and cell types have been investigated. The present study demonstrated that the distribution of the two investigated Spred proteins is different in most tissues tested. Strong Spred-1 expression was found in adult brain and in fetal tissues, whereas high levels of Spred-2 were detected in several adult tissues, predominantly in glandular tissues but also in lung, liver and testis. This study provides strong evidence for a striking dichotomy in the tissue distribution of the two Spred family members.

Prominent Spred-1 immunoreactivity was detected in mouse brain only, but not in mouse kidney. In contrast, Kato and co-workers reported the expression of Spred-1 mRNA in brain and in kidney (Kato R. et al, 2003). This discrepancy may be due to a tight regulation of translation of the Spred-1 mRNA in this tissues or due to other regulatory mechanisms.

Additionally, Hashimoto and co-workers analysed Spred-1 and Spred-2 RNAs in rat lung from the onset of branching morphogenesis to adulthood (Hashimoto et al, 2002). They reported a lower expression of Spred-1 mRNA in adult lung than in fetal lung. As well, they detected high levels of Spred-2 mRNA in fetal lung, an observation which is not in line with our protein expression data and which may also be explained by differential regulation of translation of the Spred-2 mRNA and also by a higher turnover of the Spred-2 messenger RNA in fetal tissues.

A developmental regulation of Spred-2 expression profile during development was as well observed in rat heart. The amount of the myocyte-specific Spred-2 protein is not detectable after birth, then increases suddenly to reach a maximal level at day 20 and then decreases (Fig. 11).

Spred and Sprouty proteins are evolutionary conserved. To date, three isoforms of Spred proteins and four of Sprouty proteins have been identified in mammals, whereas only one isoform of each protein has been identified in *Drosophila*. The fine tuning of the signal transduction pathways is necessary for development and the control of complex organ patterning. Thus, Spred and Sprouty may regulate the

Ras/MAP-kinase pathway differentially in response to different stimuli in different tissues and organs in mammals.

The considerable variations in the middle region of the various mammalian Spred proteins and, in parallel, the high conservation of their SPR and their EVH-1 domains allow functional specificity and fidelity.

Spred-2 expression suggests a role in secretory pathways

The flattened cells of the *stratum granulosum* of the human skin were intensively stained with the specific anti-Spred-2 antibody. These cells contain keratohyalin and lamellar granules undergoing exocytosis; their content, the lipid-rich secretory product coalesces to form a continuous multilayered coating of the cell membranes responsible for the epidermal permeability barrier. As well, a process comparable to exocytosis of the secretory products of glandular cells is observed during the acrosome reaction, during which the outer acrosomal membrane fuses at multiple sites with the overlapping plasma membrane, creating openings through which the enzyme-rich contents of the acrosome escape. The tissue and organell-specific expression of Spred-2 and its typical vesicular staining pattern prompted us to investigate the putative involvement of Spred-2 in vesicle transport. We could show that Spred-2 specifically co-localises with the Rab11 GTPase, involved in the exocytic transport and required for TGN to plasma membrane transport (Chen et al, 1998). Together with the strong immunoreactivity of Spred-2 in the polarized glandular cells and in subcellular secretory vesicles, we speculate that Spred-2 exerts a specific function in the secretory pathway, for example in vesicle transport and/or in exocytosis.

Cavalli et al demonstrated the existence of a cross-talk between membrane traffic regulation and the MAPK signal transduction pathway. Rab5-mediated endocytotic trafficking was shown to be regulated by activated p38-MAP-kinase which stimulates the GDI/Rab complex formation (Cavalli et al, 2001). Spred proteins have recently been described as potent negative regulators of MAP-kinase-signaling through direct interaction of the SPR domain of Spred with Raf-1 (Sasaki et al, 2003). Our findings now suggest a potential role for Spred-2 in the control of trafficking events, where Spred-2 would be a possible mediator between Rab GTPase and the MAP-kinase pathway.

Distribution of Spred-2 in the decidua: a role in trophoblast invasiveness

During the first trimester of pregnancy, the trophoblast cells undergo a temporal and spatial differentiation towards an invasive phenotype (Loke and King, 1995; Norwitz et al, 2001).

The implantation proceeds due to the regulated trophoblast migration. Growth factors and cytokines are of crucial importance in the regulation of invasion and differentiation of human placental trophoblast cells.

Noteworthy, the expression pattern of Spred-2 in the decidua is very similar to the expression pattern of another EVH-1 containing protein: VASP (Kayisli et al, 2002).

The strongest Spred-2 and VASP immunoreactivities were observed in the first trimester of gestation. Such an expression profile is linked to the invasive trophoblast phenotype. Indeed, the extravillous trophoblast populations, including the extravillous cells of the anchoring villi, the cell column, interstitial trophoblasts, endovascular trophoblasts and placental bed giant cells exhibited strong Spred-2 and VASP immunoreactivities, whereas syncytiotrophoblasts were clearly negative and the villous cytotrophoblasts were weakly stained.

The observations concerning the strong Spred-2 and VASP immunoreactivity in invasive trophoblast suggested that the expression of the two EVH-1 containing proteins may be associated with trophoblastic cell motility and play a critical role in the infiltration of maternal tissues by fetal trophoblasts during the first trimester in the process of implantation.

Two structurally distinct groups of human Spred proteins generated by extensive alternative splicing

The novel Spred gene family comprises three human genes, three mouse genes and one fly homologous gene. As observed within the Homer family (Soloviev et al, 2000), two structurally distinct groups of human Spred proteins generated by alternative splicing have been reported here (Fig. 28).

The two domains of Spred which have been mostly conserved between fly and mammals are the EVH-1 and the SPR. The encoded large protein isoforms ("a" forms) of Spred-1, Spred-2, Spred-3 comprise the two highly conserved functional

domains: the N-terminal EVH-1 and the C-terminal SPR. Furthermore, Spred-1 and Spred-2 large variants share high homology within a third important functional domain located in the intermediate region: the c-KBD, which has been reported to interact in case of Spred-1 and -2 with the tyrosine kinase receptor, c-Kit and c-Fms (Wakioka, et al, 2001).

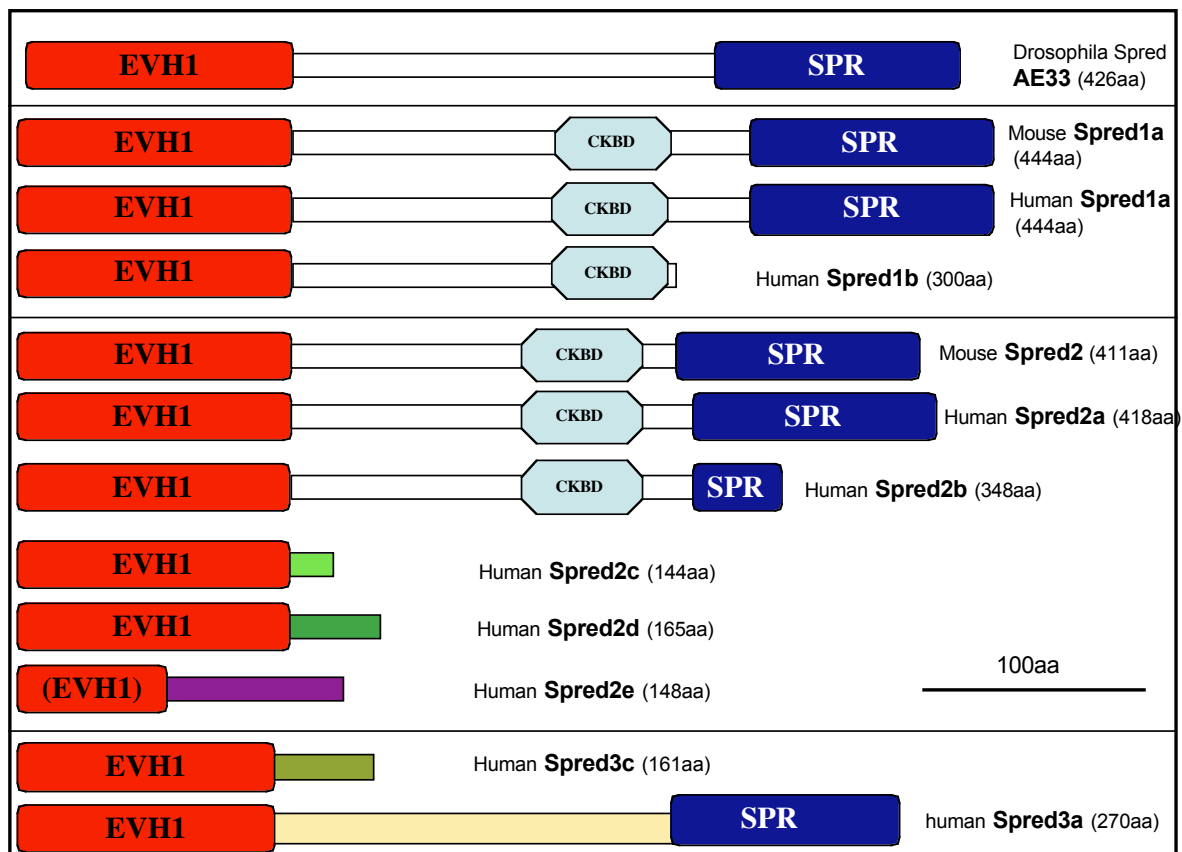


Figure 28: Members of the Spred family.

The EVH-1 domain is depicted in red, the SPR in blue, and the C-Kit binding domain in light blue.

I reported that the Spred-1, Spred-2 and Spred-3 mRNAs could undergo alternative splicing to produce Spred forms differing substantially in their C-terminus. All the naturally occurring human Spred protein variants could be divided into two structurally distinct groups of short and long Spred proteins. Short Spred proteins include Spred-2c, Spred-2d, Spred-2e, Spred-3c and long Spred proteins include Spred-2a, Spred-2b, Spred-1a, Spred-1b, Spred-3a.

Until now *spred1*, *spred2*, and *spred3* have been shown to code for only one large protein form in mammals (Kato et al, 2003; Wakioka et al, 2001). Our results suggest that the members of the Spred family share a general organisational or regulatory principle in common, evidenced by both short and long forms of each of the proteins,

with the missing C-terminal c-KBD, preventing the interaction with the receptor tyrosine kinase of the short forms.

My results extend the Spred protein family from a group of three proteins to a much wider family of 12 proteins, produced from three human genes, three mouse genes and the *Drosophila* orthologue gene by means of alternative splicing (Fig. 28).

The generation of short and long forms, which is differentially controlled, allows probably regulation of functional properties. In order to address some of the open questions about molecular mechanisms that underlie Spred's functions, five novel splicing variants of the human *spred-2* gene were cloned and their functional characterisation has been initiated in epithelial cells.

Being aware of the importance of the cellular localisation in respect to function, I studied the subcellular localisation of the Spred-2 protein variants in mammalian cells.

Spred-2a localisation and function

Spred-2a is an intracellular protein localised at the inner layer of the plasma membrane where it can act as a regulator of the Ras pathway and colocalised with Rab11-associated vesicles where it may control the vesicular trafficking. Spred-2 was computationally predicted as displaying a transmembrane segment within its C-terminal cysteine-rich region called SPR (Bruehl, 2002). I demonstrated experimentally that the highly hydrophobic segment within its SPR is not a transmembrane domain but likely a membrane association domain (Bruehl, 2002). The findings concerning the membrane localisation were as well reported by Wakioka et al (2001). Like Sprouty (Cashi et al, 1999), Spred-2a is an intracellular protein acting on cytoplasmic signal transduction pathways rather than on the extracellular part of various RTKs. Importantly, Ras signaling occurs in complexes associated with the inner face of the plasma membrane (Stokoe et al, 1994).

The Ras pathway is activated at least in part by bridging together the signaling components into a complex at the plasma membrane in association with the tyrosine phosphorylated cytoplasmic tail of the receptor (Leevers et al, 1994). It is therefore important that regulators like Sprouty and Spred are also tightly associated with the inner face of the plasma membrane.

The short Spred-2 proteins

The small variants generated by alternative splicing of the *spred2* gene: Spred-2c, -2d form, do not localise to the membrane. They are mostly composed of the EVH-1 domains and a short C-terminal tail; they lack the SPR thought to be responsible for membrane localisation and the domain within the intermediate region interacting directly with the RTK. The small derivatives of the *spred2* gene essentially exhibit a nuclear localisation.

These 2 endogenous variants seem to be specifically detected at the nuclear rim and within some subnuclear structures, which could be either speckles or coiled bodies. However, the 2d forms displayed dot-like, mostly intranuclear inhomogeneous aggregates in transiently transfected overexpressing epithelial cells. Either the non-physiological expression level of the transiently overexpressed protein in eukaryotic cell or an unfunctional protein originating from the irregular mRNA could explain the formation of aggregates.

Indeed, the cloned cDNA fragment of Spred-2d could derive from an incompletely processed messenger RNA. Spred-2d transcripts comprise an exon (called 3a), which could be the intronic sequence between exons 3 and 4. With a probe specific for this messenger, the RNase protection assay showed only low levels of this transcript in human brain. These results cannot rule out the possibility that the cloned Spred-2d cDNA is a pre-messenger RNA of the Spred-2c comprising a contaminating genomic sequence as the DNase treatment performed on the extracted total RNA can never be complete.

However, an argument favouring the existence of Spred-2d is that the 2 products Spred-2d and Spred-2c are highly related in matter of size and domain organisation. Interestingly, the small C-terminal tail of Spred-2c and Spred-2d encoded by the exons 4 and 3a, respectively, are very similar. These observations suggest that the Spred-2d product may have a functional relevance in being the derivative of a real fully processed splicing product of the human *spred2* gene. Homologous amino-acid sequences encoded by different (neighbouring) exons could be a way to insure the production of protein regions of potential functional importance. The small homologous C-terminal regions of 20 aa (for Spred-2c) and 41 aa (for Spred-2d), could be a localisation signal since these two products display a similar pattern in terms of subcellular localisation. It would be interesting to visualise the localisation of the EVH-1 domain and to test whether the C-Terminal tail could target a protein to

the nucleus, especially to the subnuclear structures.

Because these variants do not seem to be present at the membrane under stimulated conditions and they do not have the RTK interacting motif (c-KBD), it is very unlikely that they display some dominant negative effects interfering with the functions of the larger Spred derivatives by mediating the inhibition of the RTK signaling. However, they could interact with Spred-2 EVH-1 binding partners in case they would be located closely in the cell.

The Spred-2e variant cloned from mature human placenta lacks the SPR, the c-KBD and half of the EVH-1 domain. The transcript seems to be present in human brain and weakly in human heart as seen in the RNase protection assays. The truncated EVH-1 is not expected to fold properly.

As shown by indirect immunofluorescence microscopy, the Spred-2e product piled up in aggregates. From the known structures of the EVH-1 domains (reviewed by Ball et al, 2002), the first 69 amino-acid residues of the Spred-2 EVH-1 domain are expected to fold in three β -sheets, which may accumulate in aggregates.

When the pCMV-Spred-2e construct was expressed transiently in PtK2 cells, it produced low levels of Spred-2e protein whereas the pCMV-Spred2a or -2b plasmid generated high amounts of proteins under the same conditions. This strongly suggests a rapid turnover of the Spred-2e protein in epithelial culture of cells. Furthermore, this product appeared to be toxic for the cells since a lot of dead cells were observed after transfection of the epithelial monolayer. This variant could be a pathological hypomorphic derivative exhibiting loss of function.

The function of the cysteine-rich domain

Role of the SPR in membrane targeting

The findings concerning the subcellular localisation of the “a” form of Spred-2 are very similar to the previously reported data regarding the subcellular distribution of the Sprouty proteins. Cashi et al. (1999) showed by biochemical analyses that *Drosophila* Sprouty is associated with the inner surface of the membrane due to its cysteine rich domain. This domain, which is the most highly conserved region between mammals and fly Sprouty (Impagnatiello et al, 2001), is highly related to the SPR present at the C-terminal domain of large Spred proteins.

The membrane targeting function of such domains is likely conserved. Indeed, the

subcellular localisation of a deletion mutant lacking the SPR is dramatically different from the localisation of the full-length protein. The deletion of this C-terminal region of mouse Spred-2 and mouse Spred-1 has been shown to disrupt its localisation at the membrane (Wakioka et al, 2001). The specific localisation pattern of Spred-2 was dependent on the integrity of the SPR domain. This finding is consistent with the subcellular localisation of Spred-2b protein, a splice variant mutated in the SPR. I demonstrated that Spred-2b, displaying a truncated SPR, does not localise at the plasma membrane or within the vesicles but is distributed evenly throughout the cytoplasm and also showed a nuclear localisation. The first 41 amino acids of the SPR present at the C-terminus of Spred-2b, are then not sufficient to ensure membrane localisation. According to these findings, one could conclude that the integrity of this domain is required and essential for proper membrane and vesicular localisation. The C-terminal region of human Spred-2 protein encoding the SPR was sufficient to mediate its specific vesicular and membrane localisation.

Furthermore, Impagnatiello et al (2001) demonstrated that murine Sprouty 1 and 2 were membrane anchored by palmitoylation. The internal cysteine residues can be modified via labile thioester bonds by palmitoylation (Veit et al, 1998). The Sprouty residues susceptible to be modified by palmitoylation are likely located in the cysteine-rich domain of Sprouty. In the C-terminal region, Spred-1 and 2 (like Sprouty) most likely harbor a palmitoylation motif, which could provide a mean by which they can be anchored to vesicular membranes (Impagnatiello et al, 2001).

As 71% of the cysteine residues in the highly homologous C-terminal parts between Sprouty and Spred are conserved, it would be interesting to investigate whether Spred associates to the membrane by the same molecular mechanism.

Role of the cysteine-rich domain in growth factors induced ERK activation

Yigzaw et al (2001) investigated the role of the C-terminal cysteine-rich region (residues 178-194 of the human Sprouty2 protein) in mediating its biological activity, i.e. the ability to modulate cell migration in response to growth factors and proliferation in response to serum. The deletion of the region in the C-terminus, which has been shown to disrupt its localisation to membrane ruffles (Lim et al, 2000), obliterates the biological actions of the proteins.

Similar deletion experiments have been performed with the SPR domain of Spred-2.

The SPR domain of Spred, responsible for membrane targeting of Spred, is expected to be necessary for proper Spred function.

I showed that the deletion of the SPR obliterates the inhibiting function of Spred-2 on ERK signaling (monitored in HEK 293 cells by serum- or EGF- induced ERK phosphorylation)(Fig. 23).

Similar results have been published recently. Nobuhisa et al (2004) studied the function of each domain by using deletion mutants. A SPR lacking mutant could not inhibit the production of CD45⁺ cells in aorta-gonad-mesonephros culture in contrast to the full-length Spred-2. The SCF-induced ERK phosphorylation was suppressed by Spred-2 full-length but not by a mutant lacking the SPR domain (Nobuhisa et al, 2004). These data indicated that the C-terminal region of Spred-2 was required for the interaction with c-Kit and for the efficient suppression of SCF-induced ERK-2 phosphorylation. Their data suggest that the SPR domain of Spred-2 plays a critical role in the suppression of hematopoietic cell development in aorta-gonad-mesonephros cultures.

In a previous study, they showed that the SPR was sufficient for the suppression of ERK activation induced by VEGF in 293 cells (Sasaki et al, 2003). Therefore, EGF, VEGF, and SCF may have a similar activation mechanism for MAPK kinase. Indeed, Wakioki et al. (2001) showed that the EVH-1 and SPR were essential for the suppression of the activation of MAP-kinase in two independent differentiation systems.

Wakioka et al. (2001) used as functional assay the differentiation of PC12 cells induced by NGF stimulation and dependent on MAP-kinase activity. In this model, Spred counterparts inhibited the NGF-induced differentiation of PC12 cells, which was visualised by neurites outgrowth. The genetically engineered truncated derivative lacking the SPR domains did not prevent the differentiation induced by NGF. The C-terminal deletion mutant augmented NGF-induced neurites outgrowth in PC12 cells suggesting that this mutant may work as a dominant negative form against endogenous Spred proteins. I cloned a naturally occurring Spred-2 transcript lacking part of the exon 8, which codes for the variant Spred-2b, which is structurally very similar to this truncated mutant used in their model. So this “natural” form missing a large part of the SPR was not able to inhibit the EGF-induced ERK activation. A role of Spred-2b in modulating the signaling cascade by balancing the regulation of MAP-kinase activity could be speculated.

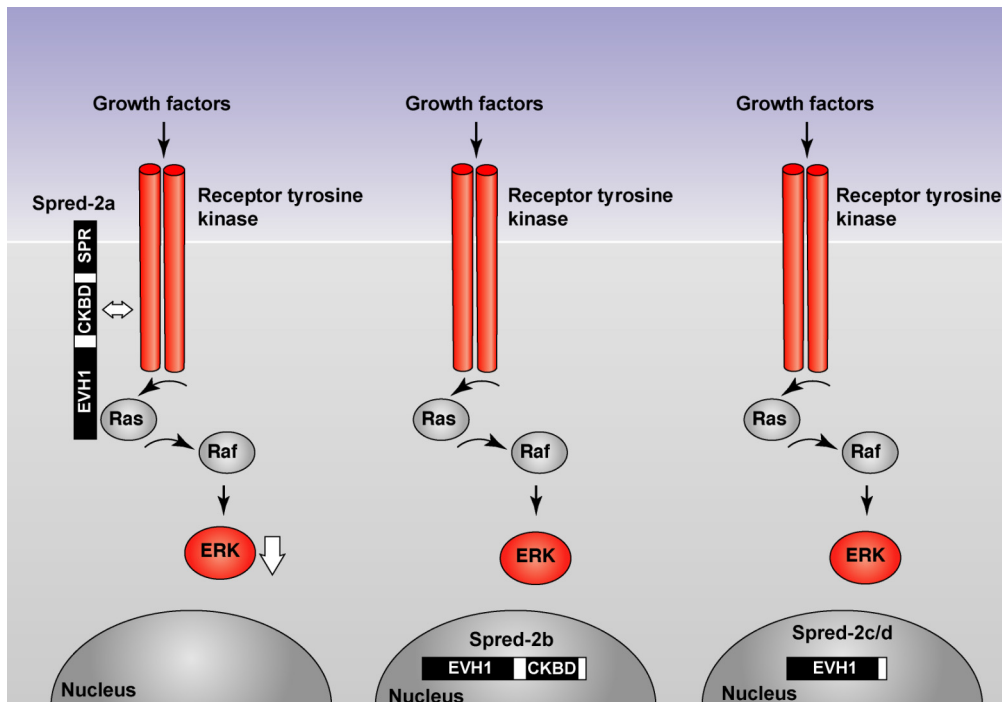


Figure 29: Spred-2 proteins and the inhibition of ERK activation after RTK stimulation. Spred-2a can inhibit the activation of ERK upon growth factor stimulation. Spred-2b, a splice variant, lacks a large part of the SPR-domain and localises mostly to the nucleus. This variant is enabled to inhibit ERK activation upon EGF stimulation although it could interact with the RTK thanks to its c-KB domain. The splice variants Spred-2c/-2d, are not able to inhibit ERK activation under the same conditions because they localise to the nucleus and have no c-KB domain interacting to the RTK.

Among the SPR-lacking derivatives generated by alternative splicing of the human *spred* genes, the variants Spred-2b and Spred-1b (“b” forms) with an intact intermediate region comprising the c-Kit binding domain are supposed to be able to interact with the intracellular part of the receptor tyrosine kinase and compete for the binding with the large “a” form. This functional role of the “b” forms as dominant negative regulators of the protein-protein interaction in the membrane macromolecular complex mediated by Spred-1a/-2a could be possible if the “b” form would localise to the plasma membrane. But our immunofluorescence experiments revealed that most of the Spred-2b proteins localised to the nucleus. It is then very unlikely that an increased level of the “b” form could disrupt the interaction at the membrane and could lead to the redistribution of the Ras signaling components (Fig. 29).

The alternative splicing may be responsible for the generation of truncated derivatives localising in different compartment in order to balance the MAP-kinase signaling regulation.

A new subclass of EVH-1 domains

The interactions of EVH-1 domains with their specific ligands diverge in order to fulfill specialised functions in different cellular contexts whilst maintaining the common ability to bind proline rich sequences (PRS) (Ball et al, 2002).

A substitution in the putative binding pocket

Analyses of multiple sequence alignments comparing EVH-1 domains from different families reveal some signatures characterising the Spred EVH-1.

Comparison of the putative Spred EVH-1 binding site with the so-called aromatic triad found in class I EVH1 domains (Y16+W23+F79, VASP numbering) reveals a substitution of the first aromatic residue to a basic side chain residue (Y16R).

A substitution of the first aromatic residue to an aliphatic residue was as well observed for class II EVH-1 domains of Homer proteins.

Such a substitution in the recognition site results in charge changes and shape changes of the binding cleft and, therefore, ligand-docking mechanisms are different. This divergence is at the basis of specificity control. The Spred EVH-1 triad R24, W31, F89 (hsSpred-1 numbering) constitute the putative binding pocket of the third class of EVH-1 domains.

Structural information extracted from resolved EVH-1/PRS complexes

To date three-dimensional structures of four EVH-1 domains in complex with their proline-rich sequences have been solved (Fedorov et al, 1999; Predora et al, 1999; Ball et al, 2000; Barzik et al, 2001). The structural data suggest that the EVH-1 evolved from the versatile PH folding scaffold.

In class I and class II EVH-1 domains, the invariant W23 (hsVASP numbering) has been reported to be a crucial residue for ligand docking and correct folding (Ball et al, 2002). This residue is conserved among Spred EVH-1 domains.

The structure reveals that W23 side chain position between F79 (conserved among class I and II EVH-1) and Y16 (conserved within class I EVH-1, hsVASP numbering) form an exposed hydrophobic sticky platform with the correct geometry to dock the polyproline II-based structure common to PRS ligands. Substitution within the recognition site implies that some very different contacts are made in class I and II and new class interactions. In both class I and II EVH-1 domains, conserved F79

forms an hydrophobic cleft between its own side chain and that of the W23 angled approximately to 90° to each other into which the pyrrolidine ring of the proline packs efficiently (Ball et al, 2002).

From this observation and from the information extracted from the EVH-1 alignment, I suggest that the proline-rich sequence of the putative new class of ligand would contain a proline at this position and possibly an acidic residue in proximity to the proline core (because of the arginine in the triad).

Knowing that full-length Spred-2 interacts constitutively with Ras (Wakioka et al, 2001) and knowing that Ras contains a PRS motif surrounded with acidic residues within its c-terminal hypervariable region, Ras could be a candidate ligand for the EVH-1 domain of Spred-2. In order to check this hypothesis, preliminary overlay experiments with the EVH-1 domain of Spred-2 and with the H-Ras PRS motif in order to clearly define the epitopes and their substitution tolerance were initiated and showed a certain affinity between these two motifs.

Other small GTPases like Rap1 contains a PRS motif surrounded with acidic residues which could be a putative ligand for the Spred-2 EVH-1. This sequence EQELPPSPPSAPR from Rap1 was as well tested and gave a prominent signal (data not shown).

The small GTPase Rab11 associated with perinuclear transport vesicles (immunoreactive for Spred-2), comprise within its C-terminal primary sequence a proline-rich sequence surrounded by negatively charged residues, which may be as well putative binding targets for Spred-2 EVH-1 (DESPG residues 188-192 and PPTTD residues 201-205, hsRab11 numbering). The hypothesis that Rab11 GTPase may represent a candidate for direct interaction with the new class of EVH-1 domain of Spred should be now seriously considered and further investigated.

On-going resolution of the Spred-2 EVH-1 structure by NMR will give further insights into the interaction of this new type of EVH-1 domain with its specific target. The ¹H, ¹⁵N resonance assignment of the human Spred-2 EVH-1 domain has been recently reported (Zimmermann et al, 2004). These data will allow a comparison of Spred -2 EVH-1 domain with structurally well-characterised EVH-1 domains (Ball et al, 2000).

Concluding remarks

In summary, we could show that - on the protein level - Spred-1 and Spred-2 are expressed differentially and that the expression pattern changes during the development of the mammalian organism. Furthermore, Spred-2 protein was found to be predominantly expressed in glandular, epithelial tissues and in cells which are involved in endo- and exocytotic pathways. Together with the co-localisation of Spred-2 with Rab11, this suggests a role for Spred-2 in regulation of GTPase- and/or MAP-kinase dependent secretory pathways, which remains to be clarified in detail.

Furthermore, the existence of short and long splicing variants of Spred 1, 2 and 3 reveals a common principle of organisation and splicing pattern in the Spred family. Therefore, the heterogeneity and the diversity of spliced variants may be even greater than described here.

The fine tuning of the function of the Spred family may be achieved by varying the ratio of the Spred-1, -2, -3 mRNAs in different tissues. The variation introduced by alternative splicing of Spred mRNA provides a molecular basis for the regulation of the translation of Spred proteins.

Further studies on the expression levels of the individual Spreds and their binding affinity to interacting proteins will be needed to elucidate the specific functional significance of each of the individual proteins in signal transduction pathways and regulation of vesicle transport. Identification of direct interaction partners and gene ablation may help to unravel the signaling cascades affected by Spred.

References

- Amann KJ, Pollard TD (2001) The Arp2/3 complex nucleates actin filament branches from the sides of pre-existing filaments. *Nat Cell Biol* 3 : 306-10.
- Bachmann C, Fischer L, Walter U, Reinhard M (1999) The EVH2 domain of the vasodilator-stimulated phosphoprotein mediates tetramerization, F-actin binding, and actin bundle formation. *J Biol Chem* 274 : 23549-57.
- Bai RY, Koester C, Ouyang T, Hahn SA, Hammerschmidt M, Peschel C, Duyster J (2002) SMIF, a Smad4-interacting protein that functions as a co-activator in TGF beta signaling. *Nat Cell Biol* 4 : 181-90.
- Ball LJ, Jarchau T, Oschkinat H and Walter U (2002) EVH1 domains: structure, function and interactions. *FEBS Lett* 513 : 45-52.
- Ball LJ, Kuhne R, Hoffmann B, Hafner A, Schmieder P, Volkmer-Engert R, Hof M, Wahl M, Schneider-Mergener J, Walter U, Oschkinat H, Jarchau T (2000) Dual epitope recognition by the VASP EVH1 domain modulates polyproline ligand specificity and binding affinity. *EMBO J* 19 : 4903-14.
- Barzik M, Schubert WD, Carl U, Wehland J, Heinz DW (2000) Crystallization and preliminary X-ray analysis of the EVH1 domain of Vesl-2b. *Acta Crystallogr D Biol Crystallogr* 56 : 930-2.
- Beneken J, Tu JC, Xiao B, Nuriya M, Yuan JP, Worley PF, Leahy DJ (2000) Structure of the Homer EVH1 domain-peptide complex reveals a new twist in polyproline recognition. *Neuron* 26 : 143-54.
- Brakeman PR, Lanahan AA, O'Brien R, Roche K, Barnes CA, Huganir RL, Worley PF (1997) Homer: a protein that selectively binds metabotropic glutamate receptors. *Nature* 386 : 284-8.
- Brindle NP, Holt MR, Davies JE, Price CJ, Critchley DR (1996) The focal-adhesion vasodilator-stimulated phosphoprotein (VASP) binds to the proline-rich domain in vinculin. *Biochem J* 318 : 753-7.
- Bruel CM (2002) Molecular Characterisation of the human *Spred2* protein. Bayerische Julius-Maximilians-Universität Würzburg, Fakultät für Biologie, Progress Report.
- Callebaut I (2002) An EVH1/WH1 domain as a key actor in TGFbeta signaling. *FEBS Lett* 2002 519 : 178-80.
- Callebaut I, Cossart P, Dehoux P (1998) EVH1/WH1 domains of VASP and WASP proteins belong to a large family including Ran-binding domains of the RanBP1 family. *FEBS Lett* 441 : 181-5.
- Casci T, Vinos J, Freeman M (1999) Sprouty, an intracellular inhibitor of Ras signaling. *Cell* 96 : 655-65.

Cavalli V, Vilbois F, Corti M, Marcote MJ, Tamura K, Karin M, Arkinstall S, Gruenberg J (2001) The stress-induced MAP kinase p38 regulates endocytic trafficking via the GDI : Rab5 Complex. *Mol Cell* 7 : 421-432.

Chakraborty T, Ebel F, Domann E, Niebuhr K, Gerstel B, Pistor S, Temm-Grove CJ, Jockusch BM, Reinhard M, Walter U, et al. (1995) A focal adhesion factor directly linking intracellularly motile *Listeria monocytogenes* and *Listeria ivanovii* to the actin-based cytoskeleton of mammalian cells. *EMBO J* 14 : 1314-21.

Chen W, Feng Y, Chen D, Wandinger-Ness A (1998) Rab11 is required for trans-golgi network-to-plasma membrane transport and a preferential target for GDP dissociation inhibitor. *Mol Biol Cell* 9 : 3241-57.

De Maximy AA, Nakatake Y, Moncada S, Itoh N, Thiery JP and Bellusci S (1999) Cloning and expression pattern of a mouse homologue of drosophila sprouty in the mouse embryo. *Mech Dev* 81 : 213-6.

DeMille MM, Kimmel BE and Rubin GM (1996) A *Drosophila* gene regulated by rough and glass shows similarity to ena and VASP. *Gene* 183 : 103-8.

Drees B, Friederich E, Fradelizi J, Louvard D, Beckerle MC, Golsteyn RM (2000) Characterisation of the interaction between zyxin and members of the Ena/vasodilator-stimulated phosphoprotein family of proteins. *J Biol Chem* 275 : 22503-11.

Eigenthaler M, Engelhardt S, Schinke B, Kobsar A, Schmitteckert E, Gambaryan S, Engelhardt CM, Krenn V, Eliava M, Jarchau T, Lohse MJ, Walter U, Hein L (2003) Disruption of cardiac Ena-VASP protein localisation in intercalated disks causes dilated cardiomyopathy. *Am J Physiol Heart Circ Physiol* 285 : 2471-81.

Engelhardt CM, Bundschu K, Messerschmitt M, Renné T, Walter U, Reinhard M, and Schuh K (2004) Expression and subcellular localisation of Spred Proteins in mouse and human tissues. *Histochem Cell Biol* (accepted for publication).

Fedorov AA, Fedorov E, Gertler F, Almo SC (1999): Structure of EVH1, a novel proline-rich ligand-binding module involved in cytoskeletal dynamics and neural function. *Nat Struct Biol* 6 : 661-5.

Fradelizi J, Noireaux V, Plastino J, Menichi B, Louvard D, Sykes C, Golsteyn RM, Friederich E (2001) ActA and human zyxin harbour Arp2/3-independent actin-polymerization activity. *Nat Cell Biol* 3 : 699-707.

Freeman M, Kimmel BE, Rubin GM (1992) Identifying targets of the rough homeobox gene of *Drosophila*: evidence that rhomboid functions in eye development. *Development*. 116 : 335-46.

Galbiati F, Razani B, Lisanti MP (2001) Emerging Themes in Lipids Rafts and Caveolae. *Cell* 106 : 403-411.

Gambaryan S, Hauser W, Kobsar A, Glazova M, Walter U (2001) Distribution, cellular localisation, and postnatal development of VASP and Mena expression in mouse tissues. *Histochem Cell Biol* 116 : 535-43.

Gambaryan S, Hausler C, Markert T, Pohler D, Jarchau T, Walter U, Haase W, Kurtz A, Lohmann SM (1996) Expression of type II cGMP-dependent protein kinase in rat kidney is regulated by dehydration and correlated with renin gene expression. *J Clin Invest* 98 : 662-70.

García Arguinzonis MI, Galler AB, Walter U, Reinhard M, Simm A (2002) Increased spreading, Rac/p21-activated kinase (PAK) activity, and compromised cell motility in cells deficient in vasodilator-stimulated phosphoprotein (VASP). *J Biol Chem* 277 : 45604-10.

Gross I, Bassit B, Benezra M, Licht JD (2001) Mammalian sprouty proteins inhibit cell growth and differentiation by preventing ras activation. *J Biol Chem* 276 : 46460-8.

Hacohen N, Kramer S, Sutherland D, Hiromi Y and Krasnow MA (1998) sprouty encodes a novel antagonist of FGF signaling that patterns apical branching of the *Drosophila* airways. *Cell* 92 : 253-63.

Haffner C, Jarchau T, Reinhard M, Hoppe J, Lohmann SM, Walter U (1995) Molecular cloning, structural analysis and functional expression of the proline-rich focal adhesion and microfilament-associated protein VASP. *EMBO J* 14 : 19-27.

Halbrugge M, Walter U (1989) Purification of a vasodilator-regulated phosphoprotein from human platelets. *Eur J Biochem* 185 : 41-50.

Harlan JE, Hajduk PJ, Yoon HS, Fesik SW (1994) Pleckstrin homology domains bind to phosphatidylinositol-4,5-bisphosphate. *Nature* 371 :168-70.

Hartmann E, Rapoport TA, Lodish HF (1989) Predicting the orientation of eukaryotic membrane-spanning proteins. *Proc Natl Acad Sci U S A* 86 : 5786-90.

Hashimoto S, Nakano H, Singh G, and Katyal S (2002) Expression of Spred and Sprouty in developing rat lung. *Mech Dev* 119 : 303-9.

Hauser W, Knobloch KP, Eigenthaler M, Gambaryan S, Krenn V, Geiger J, Glazova M, Rohde E, Horak I, Walter U, Zimmer M. (1999) Megakaryocyte hyperplasia and enhanced agonist-induced platelet activation in vasodilator-stimulated phosphoprotein knockout mice. *Proc Natl Acad Sci U S A*. 96 : 8120-5.

Impagnatiello MA, Weitzer S, Gannon G, Compagni A, Cotten M, Christofori G (2001) Mammalian sprouty-1 and -2 are membrane-anchored phosphoprotein inhibitors of growth factor signaling in endothelial cells. *J Cell Biol* 152 : 1087-98.

Jarchau T, Hausler C, Markert T, Pohler D, Vanderkerckhove J, De Jonge HR, Lohmann SM, Walter U (1994) Cloning, expression, and in situ localisation of rat intestinal cGMP-dependent protein kinase II. *Proc Natl Acad Sci U S A* 91 : 9426-30.

Kato A, Ozawa F, Saitoh Y, Fukazawa Y, Sugiyama H, Inokuchi K (1998) Novel members of the Ves1/Homer family of PDZ proteins that bind metabotropic glutamate receptors. *J Biol Chem* 273 : 23969-75.

Kato A, Ozawa F, Saitoh Y, Hirai K, Inokuchi K (1997) Ves1, a gene encoding VASP/Ena family related protein, is upregulated during seizure, long-term potentiation and synaptogenesis. *FEBS Lett* 412 : 183-9.

Kato R, Nonami A, Taketomi T, Wakioka T, Kuroiwa A, Matsuda Y and Yoshimura A (2003) Molecular cloning of mammalian Spred-3 which suppresses tyrosine kinase-mediated ERK activation. *Biochem Biophys Res Commun* 302 : 767-72.

Kramer S, Okabe M, Hacohen N, Krasnow MA and Hiromi Y (1999) Sprouty: a common antagonist of FGF and EGF signaling pathways in *Drosophila*. *Development* 126 : 2515-25.

Kayisli UA, Selam B, Demir R, Arici A (2002) Expression of vasodilator-stimulated phosphoprotein in human placenta: possible implications in trophoblast invasion. *Mol Hum Reprod* 8 : 88-94.

Kozak M (1991) An analysis of vertebrate mRNA sequences: intimations of translational control. *J Cell Biol* 115 : 887-903.

Laemmli UK (1970) Cleavage of structural proteins during the assembly of the head of bacteriophage T4. *Nature* 227 : 680-5

Leevers SJ, Paterson HF, Marshall CJ (1994) Requirement for Ras in Raf activation is overcome by targeting Raf to the plasma membrane. *Nature* 369 : 411-4.

Lim J, Wong ES, Ong SH, Yusoff P, Low BC and Guy GR (2000) Sprouty proteins are targeted to membrane ruffles upon growth factor receptor tyrosine kinase activation. Identification of a novel translocation domain. *J Biol Chem* 275 : 32837-45.

Lim J, Yusoff P, Wong ES, Chandramouli S, Lao DH, Fong CW and Guy GR (2002) The cysteine-rich sprouty translocation domain targets mitogen-activated protein kinase inhibitory proteins to phosphatidylinositol 4,5-bisphosphate in plasma membranes. *Mol Cell Biol* 22 : 7953-66.

Loke Y.W and A. King (1995) Human implantation, cell biology and immunology. Cambridge university press.

Machesky LM and Way M (1998) Actin branches out. *Nature* 394 : 125-6.

Messerschmitt M (1998) Klonierung und Charakterisierung einer neuen humanen EVH-1 (Ena/VASP Homologie 1)-Domäne. Bayerische Julius-Maximilians-Universität Würzburg, Fakultät für Biologie, Diplomarbeit.

Minowada G, Jarvis LA, Chi CL, Neubuser A, Sun X, Hacohen N, Krasnow MA and Martin GR (1999) Vertebrate Sprouty genes are induced by FGF signaling and can cause chondrodysplasia when overexpressed. *Development* 126 : 4465-75.

Miyoshi K, Wakioka T, Nishinakamura H, Kamio M, Yang L, Inoue M, Hasegawa M, Yonemitsu Y, Komiya S, Yoshimura A (2004) The Sprouty-related protein, Spred, inhibits cell motility, metastasis, and Rho-mediated actin reorganization. *Oncogene* 23 : 5567-76.

Nagai K, Thogersen HC (1987) Synthesis and sequence-specific proteolysis of hybrid proteins produced in *Escherichia coli*. *Methods Enzymol* 153 : 461-81.

Naisbitt S, Kim E, Tu JC, Xiao B, Sala C, Valtschanoff J, Weinberg RJ, Worley PF, Sheng M (1999) Shank, a novel family of postsynaptic density proteins that binds to

the NMDA receptor/PSD-95/GKAP complex and cortactin. *Neuron* 23 : 569-82.

Niebuhr K, Ebel F, Frank R, Reinhard M, Domann E, Carl UD, Walter U, Gertler FB, Wehland J and Chakraborty T (1997) A novel proline-rich motif present in ActA of *Listeria monocytogenes* and cytoskeletal proteins is the ligand for the EVH1 domain, a protein module present in the Ena/VASP family. *Embo J* 16 : 5433-44.

Nobuhisa I, Kato R, Inoue H, Takizawa M, Okita K, Yoshimura A, Taga T (2004) Spred-2 Suppresses Aorta-Gonad-Mesonephros Hematopoiesis by Inhibiting MAP Kinase Activation. *J Exp Med* 199 : 737-42.

Norwitz ER, Schust DJ, Fisher SJ (2001) Implantation and the survival of early pregnancy. *N Engl J Med* 345 : 1400-1408.

Novick P, Zerial M (1997) The diversity of Rab proteins in vesicle transport. *Curr Opin Cell Biol* 9 : 496-504.

Ono Y, Fujii T, Igarashi K, Kuno T, Tanaka C, Kikkawa U, Nishizuka Y (1989) Phorbol ester binding to protein kinase C requires a cysteine-rich zinc-finger-like sequence. *Proc Natl Acad Sci U S A* 86 : 4868-71.

Prehoda KE, Lee DJ, Lim WA (1999) Structure of the enabled/VASP homology 1 domain-peptide complex: a key component in the spatial control of actin assembly. *Cell* 97 : 471-80.

Reich A, Sapir A and Shilo B (1999) Sprouty is a general inhibitor of receptor tyrosine kinase signaling. *Development* 126 : 4139-47.

Reinhard M, Giehl K, Abel K, Haffner C, Jarchau T, Hoppe V, Jockusch BM and Walter U (1995) The proline-rich focal adhesion and microfilament protein VASP is a ligand for profilins. *Embo J* 14 : 1583-9.

Reinhard M, Halbrugge M, Scheer U, Wiegand C, Jockusch BM, Walter U (1992) The 46/50 kDa phosphoprotein VASP purified from human platelets is a novel protein associated with actin filaments and focal contacts. *EMBO J* 11 : 2063-70.

Reinhard M, Jarchau T, Walter U (2001) Actin-based motility: stop and go with Ena/VASP proteins. *Trends Biochem Sci* 26 : 243-9.

Reinhard M, Rudiger M, Jockusch BM and Walter U (1996) VASP interaction with vinculin: a recurring theme of interactions with proline-rich motifs. *FEBS Lett* 399 : 103-107.

Reinhard M, Zumbunn J, Jaquemar D, Kuhn M, Walter U, Trueb B (1999) An alpha-actinin binding site of zyxin is essential for subcellular zyxin localisation and alpha-actinin recruitment. *J Biol Chem* 274 : 13410-8.

Renfranz PJ and Beckerle MC (2002) Doing (F/L)PPPPs: EVH1 domains and their proline-rich partners in cell polarity and migration. *Curr Opin Cell Biol* 14 : 88-103.

Samarin S, Romero S, Kocks C, Didry D, Pantaloni D, Carlier MF (2003) How VASP enhances actin-based motility. *J Cell Biol* 163 : 131-42.

Sasaki A, Taketomi T, Kato R, Saeki K, Nonami A, Sasaki M, Kuriyama M, Saito N, Shibuya M and Yoshimura A (2003) Mammalian Sprouty4 suppresses Ras-independent ERK activation by binding to Raf1. *Nat Cell Biol* 5 : 427-32.

Sasaki A, Taketomi T, Wakioka T, Kato R and Yoshimura A (2001) Identification of a dominant negative mutant of Sprouty that potentiates fibroblast growth factor- but not epidermal growth factor-induced ERK activation. *J Biol Chem* 276 : 36804-8.

Schuh K, Cartwright EJ, Jankevics E, Bundschu K, Liebermann J, Williams JC, Armesilla AL, Emerson M, Oceandy D, Knobloch KP, Neyses L (2004) Plasma membrane Ca²⁺ ATPase 4 is required for sperm motility and male fertility. *J Biol Chem* 279 : 28220-6.

Skoble J, Auerbuch V, Goley ED, Welch MD, Portnoy DA (2001) Pivotal role of VASP in Arp2/3 complex-mediated actin nucleation, actin branch-formation, and *Listeria monocytogenes* motility. *J Cell Biol* 155 : 89-100.

Soloviev MM, Ciruela F, Chan WY, McIlhinney RAJ (2000) Molecular characterisation of two structurally distinct groups of human Homers, generated by extensive alternative splicing. *J Mol Biol* 295 : 1185-1200.

Sönnichsen B, De Renzis S, Nielsen E, Rietdorf J, Zerial M (2000) Distinct membrane domains on endosomes in the recycling pathway visualized by multicolor imaging of Rab4, Rab5, and Rab11. *J Cell Biol* 149 : 901-14.

Stokoe D, Macdonald SG, Cadwallader K, Symons M, Hancock JF (1994) Activation of Raf as a result of recruitment to the plasma membrane. *Science* 264 : 1463-7.

Tefft JD, Lee M, Smith S, Leinwand M, Zhao J, Bringas P, Jr., Crowe DL and Warburton D (1999) Conserved function of mSpry-2, a murine homolog of *Drosophila* sprouty, which negatively modulates respiratory organogenesis. *Curr Biol* 9 : 219-22.

Treisman JE, Rubin GM (1996) Targets of glass regulation in the *Drosophila* eye disc. *Mech Dev* 56 : 17-24.

Tu JC, Xiao B, Naisbitt S, Yuan JP, Petralia RS, Brakeman P, Doan A, Aakalu VK, Lanahan AA, Sheng M, Worley PF (1999) Coupling of mGluR/Homer and PSD-95 complexes by the Shank family of postsynaptic density proteins. *Neuron* 23 : 583-92.

Ullrich O, Reinsch S, Urbe S, Zerial M, Parton RG (1996) Rab11 regulates recycling through the pericentriolar recycling endosome. *J Cell Biol* 135 : 913-24.

Urbé S, Huber LA, Zerial M, Tooze SA, Parton RG (1993) Rab11, a small GTPase associated with both constitutive and regulated secretory pathways in PC12 cells. *FEBS Lett* 334 : 175-82.

Veit M, Schmidt MF (1998) Membrane targeting via protein palmitoylation. *Methods Mol Biol* 88 : 227-39.

Wakioka T, Sasaki A, Kato R, Shouda T, Matsumoto A, Miyoshi K, Tsuneoka M, Komiya S, Baron R and Yoshimura A (2001) Spred is a Sprouty-related suppressor of Ras signaling. *Nature* 412 : 647-51.

Walter U, Eigenthaler M, Geiger J, Reinhard M (1993) Role of cyclic nucleotide-dependent protein kinases and their common substrate VASP in the regulation of human platelets 344 : 237-49.

Yigzaw Y, Cartin L, Pierre S, Scholich K, Patel TB (2001) The C terminus of sprouty is important for modulation of cellular migration and proliferation. *J Biol Chem* 276 : 22742-7.

Zigmond SH (2000) How WASP regulates actin polymerization. *J Cell Biol* 150 : 117-20.

Zimmermann J, Jarchau T, Walter U, Oschkinat H, Ball LJ (2004) ¹H, ¹³C and ¹⁵N resonance assignment of the human Spred2 EVH1 domain. *J Biomol NMR* 29 : 435-6.

Abbreviations

aa:	amino acid
BSA:	bovine serum albumin
c-KBD:	c-Kit binding domain
DAG:	Diacylglycerol
<i>dm:</i>	<i>Drosophila melanogaster</i>
ECL:	enhanced chemiluminescence
<i>E.coli:</i>	<i>Escherichia coli</i>
EDTA:	ethylenediamine tetraacetic acid
EGF:	epithelial growth factor
Ena:	Enabled
EST:	expressed sequence tags
EVH-1:	enabled/vasodilatator-stimulated phosphoprotein homology 1
Evl:	enabled/ vasodilatator-stimulated phosphoprotein-like protein
Fig.:	figure
GDI:	guanylnucleotide dissociation inhibitor
GSH:	glutathione
GST:	glutathione-s-transferase
Ig:	immunoglobulins
IP3:	inositol-1,4,5-triphosphate
HRP:	horse-radish peroxidase
<i>hs:</i>	<i>Homo sapiens</i>
MALDI-MS:	matrix-assisted laser desorption ionization mass spectrometry
MAP-kinase:	mitogen-activated protein-kinase
Mena:	mammalian Enabled
mRNA:	messenger ribonucleic acid
NGF:	nerve growth factor
ORF:	open reading frame

PCR:	polymerase chain reaction
PDGF:	platelet-derived growth factor
PH:	pleckstrin homology
PIP2:	phosphatidylinositol 4,5-bisphosphate
PSD:	post-source decay
PP-II:	polyproline II conformation
PRR:	proline-rich region
PRS:	proline-rich sequence
PTB:	phosphotyrosine binding domain
SCF:	stem cell factor
SDS-PAGE:	sodium dodecyl sulfate - polyacrylamide gel electrophoresis
SH3:	Src homology domain 3
Spred:	sprouty-related protein with an EVH-1 domain
SPR:	sprouty domain
STS:	sequence tagged site
TGF- β :	transforming growth factor- β
TGN:	Trans-Golgi network
RACE:	rapid amplification of cDNA ends
RTK:	receptor tyrosine kinase
RT-PCR:	reverse transcription- polymerase chain reaction
VASP:	vasodilator-stimulated phosphoprotein
VSV-G:	vesicular stomatitis virus (VSV) glycoprotein
WASP:	Wiskott-Aldrich syndrome protein
WH1:	Wiskott-Aldrich syndrome protein homology 1
WIP:	WASP interacting protein.

Acknowledgements

Ganz besonders möchte ich mich bei Herrn Prof. Dr. Ulrich Walter bedanken. Ich danke ihm für sein Engagement und seine sehr persönliche Unterstützung meiner Arbeit.

Herrn Dr. Kai Schuh sei ganz herzlich für seine Hilfe gedankt, insbesondere für die hervorragende Zusammenarbeit im Labor und seinen Einsatz bei der Betreuung meiner Arbeit.

Bei Frau Dr. Karin Bundschu möchte ich mich insbesondere für die sehr gute Zusammenarbeit, ihre motivierende Art und gemeinsame Diskussionen bedanken.

Thanks a lot to PD Dr. Suzanne Lohmann for very interesting discussions and conversations.

Bei Herrn Prof. Dr. G. Krohne möchte ich mich ganz herzlich für die Betreuung der vorliegenden Arbeit bedanken.

Dr. Thomas Renné is sincerely acknowledged for fruitful scientific discussions and good ideas.

Dr. Stepan Gambaryan has been a great help with the immunohistochemistry work and was always there to discuss scientific problems, thank you very much Stepan!

Herzlich bedanken möchte ich mich zudem bei Dr. Matthias Reinhardt, der die vorliegende Arbeit zu Beginn betreut hat.

I would like to thanks specially Lilo Fisher for her excellent technical assistance.

I am thankful to Ursulla Keller who helped me with the RNase protection analyses.

Dr. Ulrike Kammerer is acknowledged for her help with providing the placenta and decidua sections and with the identification of the cell types.

Dr. Thomas Jarchau is acknowledged for discussing the EVH-1 structure and the putative ligands.

The V5 people especially Elfi, Petra, Inge, Jörg, Monika, Leif, Nora, Naresh, Barbara, Laura are acknowledged for contributing to make V5 despite the building situation a pleasant place to work.

Last but not least I would like to specially thank the PhD students from the clinical Biochemie, Maisa, Barsom, Annette, Jochen, Mick, Vanessa and as well from the MSZ: Dima, Suzana, Jan, Bruce, Jörg, Marc for the nice time in and outside the lab.

Un grand Merci à ma mère pour m' avoir encouragée tout au long de mes études.

A toi Stefan, mille Mercis pour m' avoir apporté soutien, courage et foi.

Declaration

I hereby declare that the submitted dissertation was completed by myself and no other; and I have not used any sources or materials other than those enclosed.

Moreover, I declare that the following dissertation has not been submitted further in this form or any other form and has been used for obtaining any other equivalent qualification in any other organisation.

Additionally, other than this degree I have not applied or will attempt to apply for any other degree or qualification in relation to this work.

Würzburg,

Curriculum vitae

Catherine Marie Engelhardt

Personal details

Maiden name: Bruel
 Address: Eichendorffstraße 4, 97072 Wuerzburg
 Date and place of Birth: 19th of February 1976, Aurillac (France)
 Nationality: French
 Marital status: Married to Dr. Stefan Engelhardt

Education

From 04 / 2003	University of Wuerzburg	Medical school
10 / 1999 - 2004		Institute for Clinical Biochemistry and Pathobiochemistry PhD Program
1998 - 1999	University of Aarhus (DK)	Institute for Molecular and Structural Biology University Advanced Research Course in Biotechnology
1994 - 1998	University of Montpellier (FR)	Faculty of Science Degrees in Biochemistry ("Licence et Maîtrise de Biochimie")
1994 - 1993	High school of Aurillac (FR)	A-level: Mathematics and Natural Sciences ("Diplôme du Baccalauréat, série D")

Research experience

Institute of Clinical Biochemistry and Pathobiochemistry, University of Würzburg:

Date: From October 1999
Research project: Identification and characterisation of the Spred protein family
Supervisors: Prof. Dr. U. Walter, Dr. K. Schuh, Dr. M. Reinhard.

Institute for Molecular and Structural Biology, University of Aarhus (Denmark):

Date: February 1998 - July 1999
Frame: One year Research Stipendium from the Danish Medical Research Council
 Six months European Exchange Program SOCRATES
Research project: Recognition features of human β 2-glycoprotein to endocytotic receptors
Supervisors: Dr. M. Etzerodt, Dr. H.C. Thøgersen

Publications

Eigenthaler M, Engelhardt S, Schinke B, Kobsar A, Schmitteckert E, Gambaryan S, **Engelhardt CM**, Krenn V, Eliava M, Jarchau T, Lohse MJ, Walter U, Hein L (2003) Disruption of cardiac Ena-VASP protein localisation in intercalated disks causes dilated cardiomyopathy. *Am J Physiol Heart Circ Physiol* 285:2471-81.

Engelhardt CM, Bundschu K, Messerschmitt M, Renné T, Walter U, Reinhard R, and Schuh K (2004) Expression and subcellular localisation of Spred Proteins in mouse and human tissues. *Histochem Cell Biol* (accepted for publication).